SinBerBEST
Singapore-Berkeley Building Efficiency and Sustainability in the Tropics

SinBerBEST Technology Energy Assessment Results

Carlos Duarte, Paul Raftery*, Stefano Schiavon

Center for the Built Environment, University of California Berkeley
**** Corresponding author: p.raftery@berkeley.edu***

April 2015

Executive Summary

This report describes the creation of a benchmark large (28,000 m^2) office building in Singapore and the energy savings assessment of a selected range of technologies developed by SinBerBEST. The benchmark building meets the Green Mark (GM) version 4.0 requirements at the Certified level that have been in effect since 2010, when the SinBerBEST project began. We defined the characteristics of the benchmark building through an iterative review process involving both the Singaporean Building Construction Authority (BCA) and Beca, one of the largest professional services consultancies in the Asia Pacific, to ensure that the model parameters were realistic in the Singaporean context. At each stage of this process, we created a whole building energy model in EnergyPlus so that we could review and compare to existing literature. One additional outcome of this process was that we identified knowledge gaps regarding the Singaporean building stock. For example, there is insufficient publicly available information regarding measured plug loads, and designers may be using higher than necessary values to account for these unknowns. Recent efforts such as the BCA building energy benchmarking report (2014) are an excellent contribution to knowledge regarding the Singaporean building stock, and could conceivably be extended in future to gather this information in a randomly selected sample of the surveyed buildings.

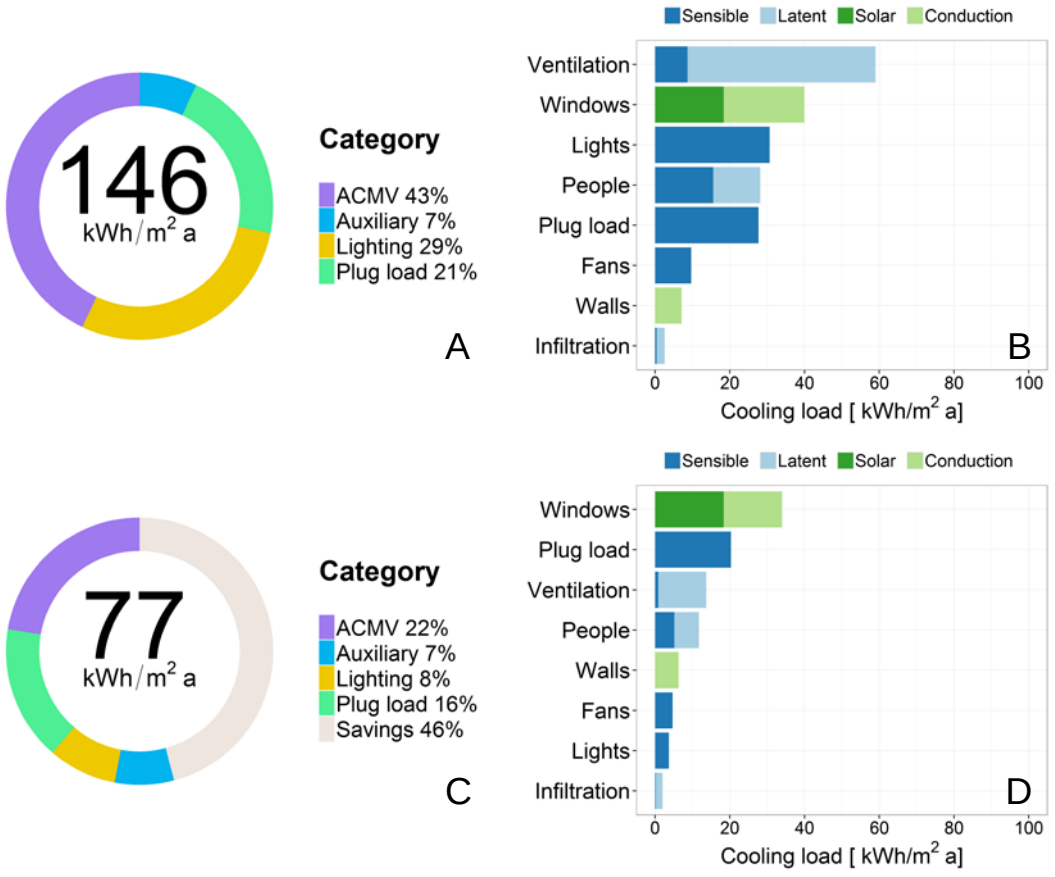

Figure i: (A) Annual Energy Use Intensity (EUI) broken into four main categories and (B) total cooling load by source during occupied hours for the benchmark building. (C) Annual EUI and (D) total cooling load breakdown by source for a building that implemented a selected number of SinBerBEST technologies (occupant localization, improved lighting and control, and increased indoor temperature setpoints).

The final model yields energy consumption results at a level of detail that is otherwise difficult and cost prohibitive to obtain from physical measurements. This level of details allows us to identify the key aspects on which to focus in order to improve energy performance. The energy model allows us to quantify the impact of various technologies on whole building energy consumption in a robust manner, accounting for temporal variation in performance and the interaction effects of different solutions. For example, an improved lighting system may provide lighting energy savings as well as savings due to the reduction in heat gains that the air conditioning and mechanical ventilation (ACMV) system must remove from the building. Figure i A shows the resulting end use distribution and a total annual energy consumption of 146 kWh/m^2·a. The auxiliary category includes sources such as exterior lighting, mechanical ventilation in car park floors, miscellaneous domestic water pumps, and lifts. The total EUI value is within the range of what we expected given data from BCA on GM certified buildings and 2014 benchmarking report on the Singaporean building stock. Note that this benchmark model is most usefully compared to other similar sized office buildings as Green Mark v4.0 has a mandatory chiller efficiency requirement based on size that is independent of certification level[1].

The results show that the ACMV system is the major energy consumer, and is responsible for 43% of the total annual electricity consumption. A more in depth analysis of the cooling loads that the ACMV system must handle shows that ventilation requirements are the larger driver of energy consumption (see Figure i B). This is due to the high moisture content of outside air in Singapore and the associated latent load, which can be up to 85% of the total ventilation load. Figure i B illustrates this by breaking down the cooling loads during occupied hours into eight categories. It is clear from these results that the technologies with the greatest potential for energy savings are those that address ventilation related loads, either by reducing ventilation rates based on occupancy detection, or by providing a more efficient means of dehumidifying air, or by increasing indoor setpoints.

Window assemblies are the second most significant source of cooling load. Given the tendency to design predominantly glass facades in modern office buildings in Singapore, appropriate external shading designs and energy-efficient window assemblies have significant energy savings potential. Technologies that focus on opaque exterior walls have less potential for savings in commercial buildings. The correct balance between window area, shading, and glass types for different orientations of the building will help lower cooling loads, while still providing access to daylight and views to the outside that are beneficial to occupants.

Lights and plug loads consume 29% and 21%, respectively, of the overall building energy consumption. These two categories account for 50% of the direct annual energy consumption in the benchmark building. This means that these two categories offer a large impact on reducing the energy needs of a building. For instance, by using efficient artificial lighting systems like LED lights or the ability to control plug load base on real occupancy.

We used the energy model to evaluate all SinBerBEST technologies in detail within the following constraints: that it was feasible to evaluate within a benchmark model of this type (without modifying the source code of the simulation software); and that the technology and results were sufficiently developed to provide data for evaluation at the time of assessment. This yielded six technologies:

[1] The requirement is for cooling loads greater than 500 refrigeration tons, which translates to approximately 15,000 m^2 of office space (or larger) using rules of thumb common to the building industry in Singapore.

improved lighting and controls; increased temperature setpoints with air movement; occupant localization; titanium dioxide coating; ultra-lightweight cement composites (ULCC); and translucent concrete (TC) panels. We restrict our analysis to retrofit scenarios (except for concrete technologies) due to the highest potential that these solutions have in Singapore. Therefore, we do not resize the ACMV system with the corresponding technologies' impact on cooling load reductions. Resizing would also have an effect on reducing initial capital cost and increasing the energy efficiency. We modified the primary benchmark with a concrete exterior wall construction to implement the latter three technologies and analyze their potential energy savings.

Figure i (C) and (D) shows the impact of using improved lighting and controls, increased temperature setpoints, and occupant localization solutions. Overall, the results show 46% savings in total annual energy consumption. This demonstrates SinBerBEST technologies may lead to significant energy savings. Increased temperature setpoints is relatively simple to implement in the existing building stock. It could only require a change in building control and maybe in the cooling coil; it may be inexpensive to implement. Improved lighting and controls are also relative simple to implement but can come at higher cost due to need for new hardware and labor. Indoor occupant localization systems are still in the research phase and more time is needed to make their way into the building market. However, demand control ventilation is a technology available to reduce ventilation energy costs but carbon dioxide sensors have been cited to have issues with measurement consistency.

Overall, SinBerBEST technologies can drastically reduce energy use in existing and new buildings.

Table of Contents

List of Figures

List of Tables

Acronyms

ACH.....air changes per hour
ACMV .....air conditioning and mechanical ventilation
AHU .....air-handling units
ASHRAE .....American Society of Heating, Refrigerating and Air-Conditioning Engineers
BCA.....Building Construction Authority
BESS.....Building Energy Submission System
BREEM.....Building Research Establishment Environmental Assessment Methodology
COP.....coefficient of performance
DCV.....demand control ventilation
DOE .....Department of Energy
EEI.....energy efficiency index
ETTV .....envelope thermal transfer value
EUI.....energy use intensity
GFA.....gross floor area
GM.....Green Mark
IMCSD.....Inter-Ministerial Committee on Sustainable Development
LEED .....Leadership in Energy and Environmental Design
LPD .....lighting power densities
NTU .....Nanyang Technological University
NUS .....National University of Singapore
RT .....refrigeration tons
SAT .....supply air temperature
SinBerBEST .....Singapore Berkeley Building Efficiency and Sustainability in the Tropics
TC .....translucent concrete
UC Berkeley.....University of California, Berkeley
ULCC.....ultra-lightweight cement composites
VAV.....variable-air-volume
VFD.....variable frequency drive
WWR .....window-to-wall

1 Introduction

Buildings account for 40% of global primary energy consumption and 30% of global annual greenhouse emissions (UNEP 2007). For Singapore, this is even higher at about 50% (EMA 2015). This has led the Inter-Ministerial Committee on Sustainable Development (IMCSD) to set goals to have a sustainable building stock in Singapore for years to come. IMCSD established that 80% of Singapore's building stock achieve Green Mark Scheme certification and a 35% reduction in energy use intensities from 2005 levels by 2030 (IMCSD 2015). Singapore Berkeley Building Efficiency and Sustainability in the Tropics (SinBerBEST) was established to provide research that will help reach these targets. SinBerBEST is an interdisciplinary group of researchers from UC Berkeley, Nanyang Technological University (NTU), and the National University of Singapore (NUS) who come together to make an impact with broadly applicable research leading to the innovation of energy efficient and sustainable technologies for buildings located in the tropics, as well as for economic development.

Given that SinBerBEST researchers come from different backgrounds and have a diverse range of skills, they will likely have different approaches in assessing the energy impact of their respective technologies on the commercial building stock. Whole building energy simulation is one method to provide standardization while still retaining the flexibility to evaluate a range of topics and technologies. It has been used extensively by governments worldwide in developing building standards, such as at the state ("Title 24-California Code of Regulations, Part 6: Building Energy Efficiency Standards for Residential and Nonresidential Buildings" 2012) and federal level (ASHRAE 2013b) in the USA, and in the European Union (European Parliament, n.d.). However, developing these models can be time consuming and inputs can be difficult to define properly as many depend strongly on common design practices in a given location. Therefore, we established an iterative process with Singapore Building and Construction Authority (BCA) and Beca, a mechanical engineering firm with experience in designing buildings in the Asian-Pacific climates, to develop a representative whole building energy model. We relied on Singapore's building codes, standards, and Beca's expertise to help define parameter inputs and reasonable assumptions that are relevant in a Singaporean context. The model represents characteristics and operation of a typical large commercial office building in Singapore that complies with requirements set in BCA's Green Mark (GM) Scheme version 4.0 at Certified Level (BCA 2010a).

The main purpose of this whole building energy model is to provide a reference for SinBerBEST researchers to estimate the potential energy savings for a particular technology, and to easily compare to other research results. Additionally, other stakeholders can use the model as a starting point in their energy simulation projects. It is important to note that this model is one possible reference model that the three involved parties came to an agreement upon as representative for Singapore given the information available. The absence of detailed design information about the population of Singaporean large commercial office buildings and the expected diversity of designs within that population, means that many other reference models would also be valid choices. We created the model for use with EnergyPlus version 8.1 (see Chapter 4 for a detailed description) and this paper describes the process, assumptions, and results of developing that model and using it to assess a variety of technologies. We restrict most of the potential saving analysis to the retrofit of existing buildings.

2 Methods

We reviewed current building codes, standards, and performed an extensive literature review pertinent to Singapore to start the iterative process illustrated in Figure 1 (SPRING Singapore 2006a; SPRING Singapore 2009a; SPRING Singapore 2009b; SPRING Singapore 2006b; BCA 2010a). These documents led to information about the design of buildings in Singapore. It also allowed us to learn legislative changes to the Building Control Act that will affect building design, as they contain efficiency requirements. For example, new construction and major retrofits after April 2008 and greater than 2,000 m^2 needs to achieve a minimum of Green Mark (GM) Certified. Another example is that existing buildings undergoing a cooling system retrofit had to meet minimum GM cooling system standards and have their cooling systems subjected to audits every three years starting from September 2012. Eventually an existing building will need to have its largest energy consuming system meet minimum GM criteria.

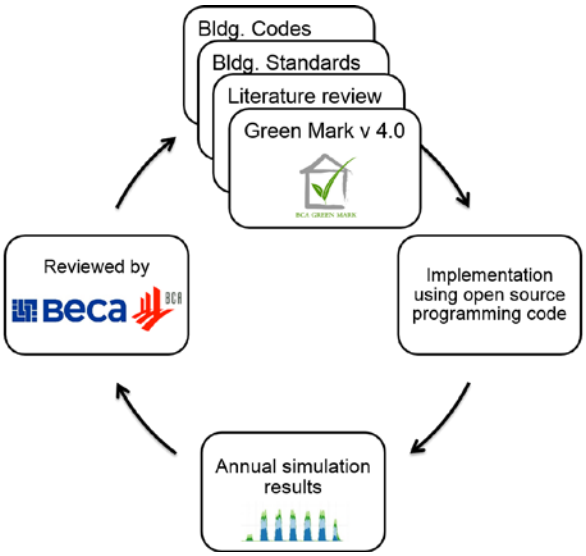

Figure 1: Overview of process to create whole building energy model.

As a result, we chose GM version 4.0 for the benchmark model. GM version 4.0 became effective in December 2010, at the beginning of the SinBerBEST project. It prescribed the minimum performance requirements for cooling systems in existing buildings and raised the energy efficiency standard by 10% for new construction and major retrofits from the previous version 3.0 (BCA 2010a; BCA 2010b). The GM rating is somehow similar the Leadership in Energy and Environmental Design (LEED) rating system established in the US by the US Green Building Council and Building Research Establishment Environmental Assessment Methodology (BREEM) established by BRE Global Limited in the United Kingdom (U.S. Green Building Council 2010; BREEAM 2014). In choosing GM version 4.0, we have minimized the possibility of counting mandatory energy efficiency measures as energy savings. The benchmark model will also be relevant for Singapore's future pursuits to a sustainable building stock.

We took the US Department of Energy's (DOE) large commercial office building with ASHRAE 90.1-2010 for Miami's climate as the starting point for Singapore's benchmark building energy model (Thornton et al. 2011; DOE 2012). We met with BCA and Beca on a weekly basis (typically) to decide on the design days, geometry, size, construction, design loads, and mechanical systems. We performed modifications based on these meetings, after which both BCA and Beca regularly reviewed the results. If results appeared to be not correct from any one party's perspective, we sought documents to further inform decisions related to the relevant building parameters. The parties reviewed further adjustments once

again in an iterative process, which we completed eight times until all parties agreed to a common benchmark model. We modified the model using open source software and packages to make the work repeatable and easy to change, as decisions were sometimes not final. For instance, when results were not as expected and we needed to find alternative solutions. The following sections describe the final model description yielded by this process, along with the parameters and software used to simulate the model.

2.1 Weather data

The weather in Singapore is characterized by hot and humid conditions. The ASHRAE weather file named SINGAPORE - SGP IWEC Data WMO#=486980 was used to simulate these characteristics, which BCA approves for use in energy modeling (BCA 2010a). ASHRAE weather files are compiled from historical weather data to represent a typical year (Yu Joe et al. 2014). Figure 2 demonstrates the extreme, but relatively consistent Singaporean climate. The daily average for outside dry bulb temperature, dew point temperature, and relative humidity found in the weather file are 27.5 °C, 24.3 °C, and 83.6%, respectively.

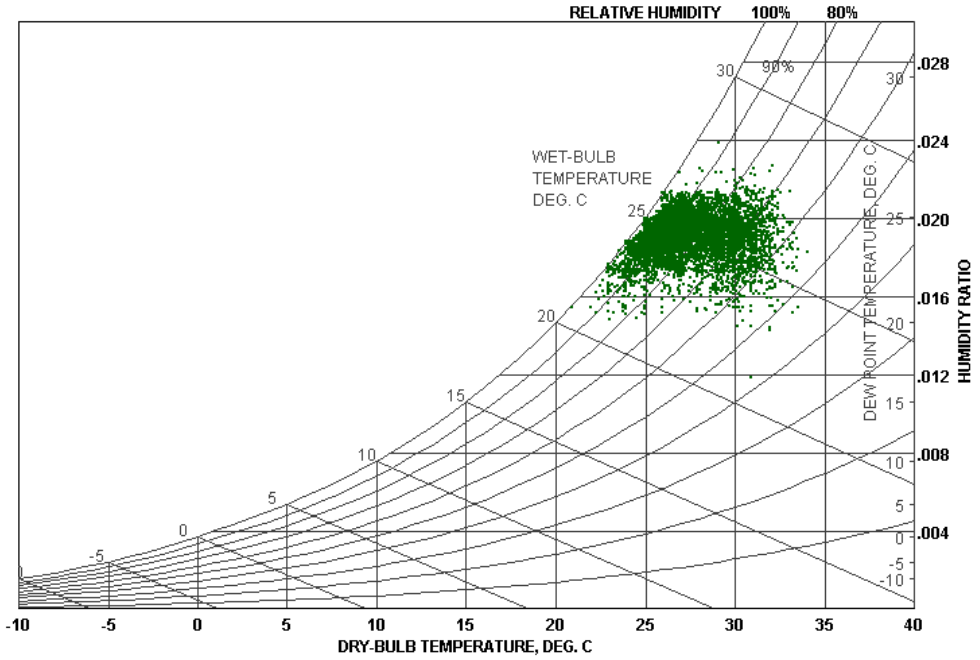

Figure 2: Hourly data from a typical meteorological year (TMY) for Singapore on a psychrometric chart.

The cooling design day dry bulb temperature for Singapore is 33.3 °C with a design wet bulb temperature of 27.8 °C. We defined six design days throughout the year to account for solar variation in a year. We used the 21th day for months February, April, June, August, October, and December, which will prevent zones from being undersized due to orientation and sun position on the design day.

2.2 Building description

The 28,000 m^2 building model is 20 floors with each square floor plate being 1,400 m^2. Floors 1-3 are modeled as carparks with the rest, floors 4-20, modeled as office floors. Every office floor is divided into seven thermal zones: four on the perimeter, one core, one staircase, and one restroom. Table 1 shows the total area for each zone type. Perimeter zones have a depth of 4.6 m. Floors 4-20 are open plan

offices and we did not explicitly model internal partitions. Instead, we defined internal mass objects to account for thermal mass effects in the interior zones. Wood material properties were used to define the interior mass of offices (Raftery et al. 2014). The total exposed surface area of interior mass for core and perimeter zones are 1,684 and 324 m^2, respectively. We also set most inside zone boundaries to an EnergyPlus material (infrared_wall in Table 2) that transforms solar radiation energy (shortwave radiation) that is incident on the surface to longwave radiation. It allows core zones to engage in the longwave radiation exchange with perimeter zones. The exceptions are in the restroom and staircase zones where brick material properties are used to define wall constructions based on Beca's experience in Singaporean buildings.

The building envelope is an all glazed facade with 59% window-to-wall (WWR) ratio for floors 4-20. Floor-to-floor height is 4 m including a 1.2 m return plenum. We applied selective window treatments based on facade orientation to ensure compliance with GM minimum envelope thermal transfer value (ETTV). North and South facade windows are tinted single pane glazing while East and West facade windows are clear double glazed windows. Argon gas fills the void between the two glass panes. The facade includes 0.6 m horizontal projection shading for all orientations for a projection factor of 0.22 again, based on Beca's experience in Singapore. We used methods described in BCA's "Code on envelope thermal performance for buildings" to calculate the ETTV (BCA, n.d.). The ETTV resulted in 50 W/m^2; GM's minimum for certification. Figure 3 shows a visualization of the energy model. Each floor in the model is not explicitly defined as we used a zone multiplier for the middle floor to recreate the other 14 floors. This reduces unnecessary complexity of the geometry and simulation time. The exposed surface areas between the gaps where the other floors would have been seen visually in Figure 3 are defined as adiabatic surfaces.

Table 1: Benchmark model zone area

Zone type	Area [m^2]
Core	689.2
Perimeter	150.2
Restroom	50
Stairs	60
Carpark perimeter	1,220
Carpark core	180

Carpark floors also have perimeter and core zones, with a 4 m floor-to-floor height. We took this approach because we assumed perimeter zones to be naturally ventilated while the core zone had a fixed speed fan exhaust system as this is typical in Singapore. Carpark perimeter zones have a depth of 12 m. The combination of having mechanically and naturally ventilated carparks floors will have insignificant effects on the overall energy consumption of the building due to the size of the mechanical system.

Table 2 and Table 3 show the overall U-values and layers for each construction assembly used in the benchmark model. We kept the same naming convention from the benchmark model for convenient reference to the model input file. The tables list layers in the construction assemblies starting from the outermost layer and ending with the layer facing into the zone. The Appendix shows the details of the physical properties for each material.

Table 2: Opaque construction assemblies used in benchmark model with layers listed from outside to inside of zone

Construction name	U-value [W/m²·K]	Layers
Exterior_Wall		Glass_6mm Air_Gap_150mm
	0.4	Aluminum_Shadow_Box_3mm
		Semi_Rigid_Insulation_75mm
Roof		Cement_Sand_Screed_50mm
	0.6	Exp_Polystyrene_50mm
		Concrete_200mm
Infrared_Wall	NA	IRTMaterial
Floor	3.5	Concrete_100mm Carpet
Ceiling	3.5	Carpet Concrete_100mm
Drop_Ceiling	3.8	Ceiling_Tile_15mm
Brick_Wall	8.1	Covered_Brick_100mm
InteriorFurnishings	NA	Wood_150mm
Car_Park_Wall	9.6	Concrete_150mm
Car_Park_Floor	7.2	Concrete_200mm

Table 3: Fenestration construction assemblies used in benchmark model with layers listed from outside to inside of zone

Construction name	U-value [W/m²·K]	SHGC	Visible transmittance	Layers
SinglePaneWindow	5.7	0.5	0.3	Ref_D_Tint_6mm
DoublePaneWindow				Ref_B_Clear_Lo_6mm
	2.2	0.2	0.2	Argon_13mm
				Clear_6mm

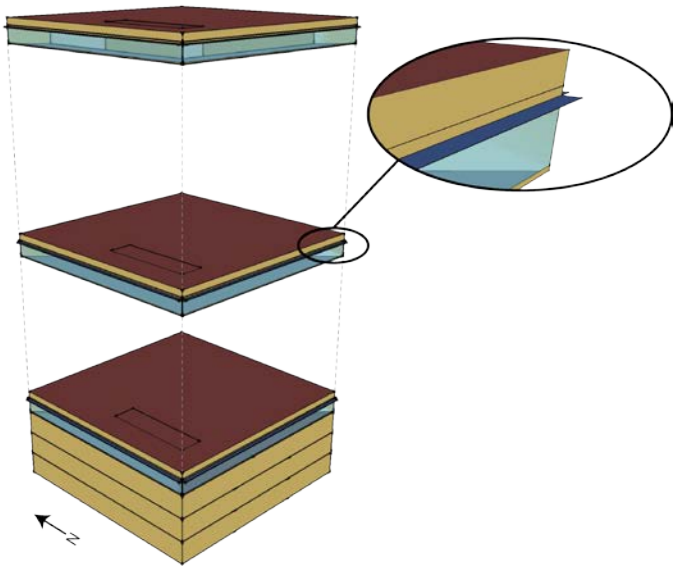

Figure 3: Singapore benchmark building model with close-up on horizontal overhangs.

2.3 Indoor design conditions

Singapore standard SS 553:2009 *Code of Practice for Air-conditioning and mechanical ventilation in buildings* dictates that operative temperature shall be maintained between 24 °C and 26 °C in occupied zones (SPRING Singapore 2009a). Given the selected glazing and shading parameters we set the core and perimeter zone mean air temperature setpoints to 24 °C and 23 °C respectively to ensure that operative temperature conditions remained within these bounds. The perimeter zones' temperature setpoint is lower because those zones experience solar loads and the operative temperature requirements are not met without reducing the dry bulb temperature. Air-conditioning and mechanical ventilation (ACMV) system does not directly control relative humidity at the zone level. As is typical in Singapore, the air handler modifies humidity at the system level through the supply air temperature setpoint and chilled water plant parameters. We observed zone outputs to confirm relative humidity was below 65% during occupied hours, however it is often significantly below this upper limit as discussed later.

2.4 Schedules and internal design loads

2.4.1 Occupancy

The building model operates on typical hours for a commercial office building. We assume occupancy hours on weekdays from 8:00 to 18:00, 8:00 to 13:00 on Saturdays, and closed on Sundays and public holidays. Singapore observes 11 public holidays every year, which we have also incorporated into the annual simulation. Figure 4 shows the schedule for occupancy, in which we used continuous lines though these diversity factors are discrete at each hour. Schedules for occupancy and the following loads mentioned below are used to show fractional use from the design value at each time step. For people, we assume office spaces to have a design density of 10 m^2/person, yielding a peak building occupancy of 2,380 people. Singapore has a significantly higher density of people in offices than the United States, where 15 m^2/person is more common. The activity for people in this model is "moderately active office work" referenced from ASHRAE Handbook Fundamentals (ASHRAE 2013a). At this activity level people have a combined sensible and latent heat output of 130 W/person (ASHRAE 2013a).

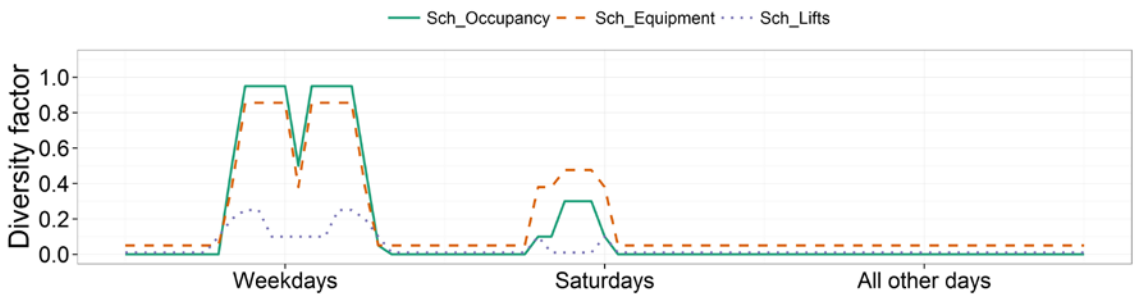

Figure 4: Office occupancy, equipment, and lift schedules in benchmark model for three different week day types (excluding design days).

2.4.2 Lighting

We obtained the baseline lighting power from Singapore standard SS 530:2006 *Code of practice for energy efficient standard for building services and equipment* (SPRING Singapore 2006a). Table 4 shows lighting power densities (LPD) with schedules shown graphically in Figure 5. LPD is the total lighting

power demand of a zone divided by the area of the zone. Lights in the office, staircase, restroom, and carpark spaces were modeled as recessed lighting with radiant and visible fractions of 0.37 and 0.18, respectively. We did not implement automated daylighting and occupancy controls in the benchmark model, as these are not yet commonplace in Singapore.

We did not show the exterior and facade lighting schedules because they are all on or off based on a set time, which is typical practice for Singapore. Exterior lights activate from 19:00 to 7:00 and facade lights illuminate from 19:00 to 24:00. We calculated power demands for exterior lights from the assumption that they illuminate an area of 800 m^2. We took 5% of the total demand from lights in office, staircase, restroom, and carpark spaces to calculate façade lighting.

Table 4: Design lighting loads defined for different areas of benchmark building.

Lighting load type	Power
Office	15 W/m^2
Staircase	6 W/m^2
Restroom	10 W/m^2
Carpark	5 W/m^2
Exterior	4 kW
Facade	17.85 kW

Figure 5: Lighting power demand schedules in benchmark model for three different week day types.

2.4.3 Equipment

We selected a design level of 14 W/m^2 for office equipment like computers, monitors, printers, and other miscellaneous equipment. This is lower than what is referenced in GM documents for energy models (16 W/m^2) and which is based on an ASHRAE 1989 standard (ASHRAE 1989). However, we determined 14 W/m^2 to be a more reasonable design level value through consensus with BCA and Beca. Office equipment has become more energy efficient by occupants using LCD monitors versus CRT monitors or opting to use laptops instead of full size desktop computers. However, this figure is still significantly higher than in the US due to far higher occupant densities found in Singapore. Figure 4 shows the schedules used for office equipment.

We aggregated other building equipment into a few modeling objects in the benchmark building model to avoid excessive complexity in the model related to components about which we had almost no information other than anecdotal evidence or engineering estimates and rules-of-thumb. Pumps used for domestic water and drainage operate 24 hours a day at an averaged power demand of just under 3 kW. Mechanical ventilation for the mechanical room and electrical room was calculated in a similar fashion. In these rooms, we assumed a supply and exhaust air fan that operate on the same schedule as

in the cooling system shown in Figure 6. The mechanical and electrical rooms have a design power consumption of 12 kW and 16 kW respectively. The electrical room ventilation system is set to operate continuously throughout the day, but at only at 75% of the peak load. The higher peak demand is because we also assume the room to be temperature controlled. The Appendix describes the details on assumptions and calculations for the aggregated rated power for the systems described above.

We also accounted for energy consumed by lifts in the energy building model. We assumed six lifts with motors rated at 45 kW each; from the assumption that each lift has the capacity for 24 people and a rated speed of 4 m/s. Figure 4 shows the lift schedule.

2.4.4 Ventilation and infiltration rates

Ventilation rates in the model comply with Singapore standard SS 553 (SPRING Singapore 2009a); at the larger flow rate of 5.5 L/s per person or 0.6 L/s m^2. The air system provides outdoor ventilation air to dilute pollutants found inside buildings. This selected value will be the minimum flow rate at which ventilation rate during occupied hours. Figure 6 shows the schedule for ventilation air. An important note is that the minimum outdoor airflow rate will not vary with occupancy because the benchmark model does not use demand control ventilation (DCV), as it is not common in Singapore.

We modeled infiltration rates for perimeter zones assuming a peak infiltration rate of 0.2 air changes per hour (ACH). We assumed that the building is slightly pressurized during occupied hours and therefore the maximum infiltration will be observed in the model when the ventilation system is off in the building and only a quarter fraction when the ventilation system is on during occupied hours. This is based on the approach used in the US Department of Energy's (DOE) large commercial office building. Figure 6 shows the schedule for infiltration.

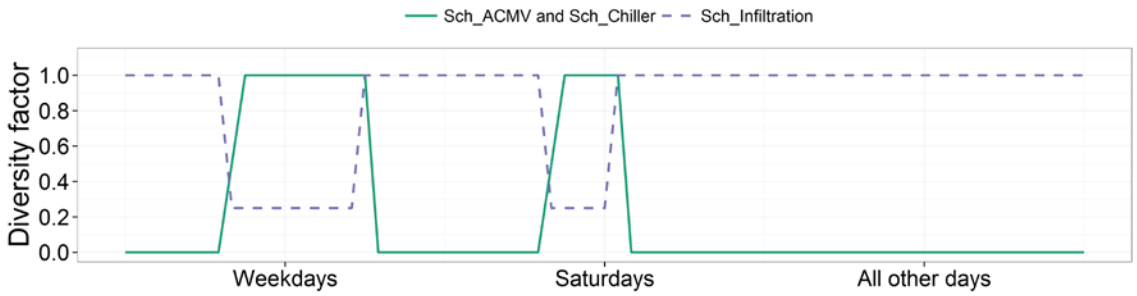

Figure 6: Ventilation and infiltration schedules in benchmark model for three different week day types.

2.5 Mechanical systems and operation

The ACMV system in the benchmark model is available for operation from 7:30 to 18:00 during the weekdays and from 8:00 to 13:00 during Saturdays. It is shut off on all other day types. Figure 6 shows the ACMV schedule. The cooling system is a water-cooled chilled water plant serving air-handling units (AHU) at each floor. AHUs then serve variable-air-volume (VAV) terminals with no reheat at the zone level, which is a mandatory design feature in Singapore VAV terminals supply perimeter and core zones.

The variable speed chilled water primary only system is composed of two chillers with a rated capacity of 1,400 kW (398 refrigeration tons (RT)) each and two variable speed pumps rated at 16.9 kW each. Chillers operate on lead-lag system. When the lead chiller reaches full capacity, the lag chiller will start to operate along with the lead chiller to match the loads in the building. Performance curves for chillers

used in the Singapore benchmark model are based on a generic centrifugal chiller from DOE's benchmark models. We compared the part load ratio curve of the generic chiller to the performance curve of a real chiller that is commonly used in Singapore (Trane chiller model TCVHE 400 RT). The two curves resulted in a low coefficient of variation at 2.76%. For this reason, we chose to use the generic chiller. Another reason was that two other curves needed by EnergyPlus would have to be derived from experimental data that was not readily available, and which is often difficult to obtain.

The sizing for the heat rejection system is based on the ability to remove heat 1.25 times the capacity of the chillers. We used a Kuken cooling tower model SKB-645 as a reference to obtain properties for the heat rejection system. The two cooling towers are rated at 1,758 kW (500 RT) each and two constant volume pumps rated at 17.2 kW each. The cooling towers' fans have a total fan power of 33 kW at the design water flow rate. Table 5 and Table 6 shows additional design properties for the two systems mentioned above.

Table 5: Design properties for chillers in benchmark model.

Chiller design properties	Values
Leaving chilled water temperature	6.7°C
Entering chilled water temperature	12.2°C
Leaving condenser water temperature	29.5°C
Entering condenser water temperature	35°C
Design range	5.5°C
Water flow rate	0.123 m^3/s
Rated efficiency	0.577 kW/RT

Table 6: Design properties for heat rejection in benchmark model.

Chiller design properties	Values
Inlet air wet bulb	27.7°C
Design approach	1.7°C
Design range	5.5°C
Water flow rate	0.0829 m^3/s
airflow rate	62.5 m^3/s

The benchmark model uses different types of fans to distribute air. The main AHU fans have the largest combined power draw at 177.8 kW for a max combined flow rate of 108.5 m^3/s into perimeter and core zones. EnergyPlus calculated design values based on the loads, pressure rise of 1,000 Pa, and total fan efficiency of 61% in each of the 17 office floors. We assumed fans to be a draw-through variable frequency drive (VFD) fan with the motor in the air stream. We also assumed a minimum airflow rate for fan power at 50%. This value is to prevent the fan's VFD from dropping below 30 Hz, which is a common practice in Singapore. It is worth noting that this is not common practice in the US where modern VFDs on large air handling units often run at speeds below 20% without issue. The VFD fan system curve were based on Energy Design Resources' Advanced VAV Design Guide for a plenum airfoil fan static pressure drop of 170 Pa (0.7") (Stein, Zhou, and Cheng 2007).

Fans also provide ventilation to the stairwells. We assumed a ventilation rate of 4 ACH with a pressure rise of 600 Pa and fan efficiency of 65%. Ventilation source air for each staircase comes from core zones at each respective floor. We also implemented exhaust fans in the benchmark model in two locations. We defined them in restroom zones for floors 4-20 and at each carpark's core zone. Restroom fans

exhaust air at a rate of 10 ACH with a pressure rise of 800 Pa and fan efficiency of 65%. The source air comes from neighboring zones to keep a balanced airflow system. In the carpark exhaust system, we assumed fume extraction rate of 1.2 ACH with a pressure rise of 800 Pa and fan efficiency of 65%.

All individual component efficiencies for the ACMV system are below the baseline efficiencies found in Singapore standards SS 530 and SS 553 (SPRING Singapore 2006a; SPRING Singapore 2009a). We calculated an efficiency of 0.70 kW/RT that met GM requirements. The chiller plant includes chillers, cooling towers, chiller pumps, and condenser pumps. We presented an overview of the ACMV in this section. The report in the Appendix contains further details of capacities, power, flow rates, efficiencies, and other information for each.

2.6 Green Mark points

We created the benchmark model to meet GM at Certified level requirements outlined in version 4.0 (BCA 2010a). This required a minimum of 30 points in the *Energy* section and a minimum of 20 points in the *Other Green Requirements* section. GM version 4.0 also outlined certain prescribed criteria that the building must meet in order to qualify for certification. The building model needed a calculated ETTV of 50 W/m^2 and water-cooled chilled water plant efficiency of 0.70 kW/RT or less as the total building cooling load was over 500 RT. This translates to approximately 15,000 m^2 of office space (or larger) using rules of thumb common to the building industry in Singapore. It is noteworthy that this minimum chilled water efficiency criterion represents a relatively efficient chilled water plant, particularly when compared to older or smaller systems. Thus, this benchmark model is most usefully compared to other similar sized office buildings, as the mandatory chiller efficiency requirement *is independent of certification level*.

Table 7 and Table 8 present the estimated points obtained from the two sections. We calculated some of the points based on the characteristics of the benchmark model and determined reasonable assumptions in others, especially for the *Other Green Requirements* section. The GM assessment of the benchmark model results in a total of 53 points; over the GM Certified minimum requirement.

Table 7: Green Mark v4.0 points obtained from the Energy section for benchmark model.

Section	Sub-section	Description	Points
Part 1-A	NRB 1-1	ETTV	0
	NRB 1-2 a	Water-cooled chilled-water plant	15
	NRB 1-2 c	Air distribution system	6
	NRB 1-2 d	Instrumentation for monitoring chilled water plant	1
	NRB 1-2 f	Variable speed controls for chilled water pump	0.5
		Sub-total A	**22.5**
Part 1-B	NRB 1-3 a	West facing orientation	7.5
	NRB 1-3 bi	West facing window openings	4.1
	NRB 1-3 bii	West facing shading	10
	NRB 1-3 c	West facing thermal transmittance	5
	NRB 1-3 d	Thermal transmittance on roof (heavy)	5
	NRB 1-4 b	Mechanical ventilation in non-AC areas	15
		Sub-total B	**46.6**
Part 1-C	NRB 1-6	Artificial lighting	0
	NRB 1-7	Ventilation in carparks (87.1% naturally ventilated)	3.5
	NRB 1-8	Ventilation in common areas (restroom, stairs)	1
	NRB 1-9	Lifts has sleep mode features	1
	NRB 1-10	Calculation of Energy Efficiency Index (EEI) at design load	1
		Sub-total C	**6.5**
		Sub-total A * (AC building area/total floor area)	21.5
		Sub-total B * (Non-AC building area/total floor area)	2
		Sub-total C	6.5
		Total score in Energy section	**30**

Table 8: Green Mark points obtained from Other Green Requirements section for benchmark model.

Section	Sub-section	Description	Points
Part 2: Water efficiency	NRB 2-1	Water efficient fittings (Very Good WELS rating)	8
	NRB 2-3 a	Use of non-potable water including rainwater for irrigation	1
Part 3: Environmental protection	NRB 3-1 b	Concrete Usage Index (CUI)	3
	NRB 3-2	Sustainable products	4
	NRB 3-4 d	Firms ISO 14000 certified	0.5
	NRB 3-4 e	Project team has a GM Certified member	0.5
	NRB 3-4 f	Provision of building users' guide	1
	NRB 3-4 g	Provision of recycling bins	1
	NRB 3-6	Refrigerants	1
Part 4: Indoor environmental quality	NRB 4-1	Thermal comfort	1
	NRB 4-2	Noise level	1
	NRB 4-4 a	IAQ provision	1
		Total score in Other Green Requirements Section	**23**

2.7 Modifications to the Benchmark Model

After finalizing the approved benchmark model, we further modified it to provide appropriate references for some of the technologies simulated, specifically indoor occupant localization, titanium dioxide coating, and ultralight concrete cement composite. We created five additional adjusted baseline models to give realistic comparisons of the implemented technologies. This section describes the adjusted baseline models. The original benchmark model, which has an all glass façade, will be designated as benchmark-A. We derived the second reference model from benchmark-A to provide a baseline when SinBerBEST technologies needed to take into account the building occupancy to realize energy savings. The occupancy schedule was reduced by 60% and the rest of the model remains the same as Section 2.3 describes. We designated this benchmark with reduced occupancy as benchmark-A1.

We developed a third benchmark to implement technologies that required a concrete façade building. We used a survey of Singapore buildings in the central business district provided by Chong (2012) to serve as a guideline for a reasonable concrete facade (Chong Zhun Min Adrian 2012). We selected a 150 mm reinforce concrete wall with 20 mm plaster coating on both sides, without insulation. We calculated a U-value of 5.6 W/m^2 K and we retained the same window assemblies as in benchmark-A, we reduced the WWR to meet the 50 W/m^2 ETTV criteria. This resulted in 35% WWR for the new concrete exterior walls. This is in line with the survey where the WWR lower and upper quartiles were from 35% to 50% respectively for 16 concrete buildings (Chong Zhun Min Adrian 2012). The rest of the parameters are identical to those in benchmark-A. We designated this model as benchmark-B and Table 9 describes the exterior wall layer properties.

We derived the last three reference models from benchmark-B. The additional reference models were needed to assess the energy savings potential of a SinBerBEST technology that depends on the exterior opaque surface area, which we have described in Section 3.7. The first modification was to add

daylighting controls to benchmark-B. We modified the WWR of benchmark-B three times after we added daylighting controls. The three WWRs are 0%, 10%, and 35% and we designated them as benchmark-B0, benchmark-B10, and benchmark-B35, respectively.

Table 9: Exterior opaque construction assembly used in benchmark-CC model with layers listed from outside to inside of zone

Layers	Thermal conductivity [W/m·K]	Density [kg/m^3] (Specific heat [J/kg·K])	Solar Reflectance
Cement_Sand_Plaster_20mm	0.53	1568 (991)	0.45
Concrete_150mm	1.44	2400 (832)	0.45
Cement_Sand_Plaster_20mm	0.53	1568 (991)	0.45

3 SinBerBEST Case Studies

After finalizing the benchmark models, we thoroughly reviewed and evaluated the results. We then sought building technologies that SinBerBEST researchers were developing at the time of this report, in order to implement them in the model. These technologies ranged from concept phase to relatively established technologies that are not yet common in Singapore. The chosen technologies had to have enough data to define it in the model, meaning that the details of the technology did not have to be complete but we required sufficient information to derive reasonable assumptions, or at least derive reasonable bounds for performance. We chose three building technologies to model and show potential energy savings from the all glass façade benchmark model (benchmark-A) or its respective adjusted baselines. We also present a fourth case to illustrate the impact of combining different technologies.

We chose another three technologies to model and show potential savings from the concrete façade building (benchmark-B) and its respective adjusted baselines. The following sections describe the seven comparisons.

3.1 Lighting controls and lamps

Singapore's location near the equator provides daylight from about 7:00 to 19:00 with minimal change throughout the year. SinBerBEST researchers have investigated the daylight performance of interior surface reflectance, glazing visual transmittance, light shelves, and shading control actions in office spaces (Chien and Tseng 2014). They presented daylight performance metrics like daylight autonomy, continuous daylight autonomy, and daylight autonomy max.

In this case study, we present the energy benefits from using daylighting, where applicable, in a building of this shape and size. We first modeled different lighting power densities (LPDs) to account for the different lighting technologies available today and then integrated daylighting controls at the same LPDs. The first set of simulations will show energy savings from retrofitting buildings to higher efficiency lighting. The second set of simulations will assess the additional savings from incorporating daylighting controls. We expect daylighting controls to have a bigger impact on larger LPDs. We selected 12, 7, 5 W/m^2 to compare against the benchmark model. These different LPDs can be obtained by using fluorescent T8 (12 W/m^2), fluorescent T5 (7 W/m^2), and LED (5 W/m^2) lighting technologies. We changed LED emitted radiant and visible fractions to 0 and 0.85, respectively. We assumed the remaining 15% energy is lost through LEDs' heat sink.

As different zones had different LPDs as shown in Table 4, we selected to keep the lower LPD when comparing to one of the three cases. For example, the restroom zone's LPD in the benchmark is 10 W/m^2, it remained 10 W/m^2 when we changed the office lighting to the first compared LPD of 12 W/m^2 but changed to 7 W/m^2 when comparing to the next LPD. The exterior, facade, and carpark lighting remained unchanged throughout the three different LPD levels.

We modeled daylight controls in perimeter zones only. Figure 7 shows daylighting zones with a slanted line pattern. We assumed occupants performing office related tasks that require an illuminance level of 500 lux at desk height (0.8 m), and combined daylight and electric lights to reach the required illuminance level. The 500 lux requirement comes from Singapore standard SS 531 *Code of practice for lighting of working places* (SPRING Singapore 2006b). Electric lights are dimmed continuously as more daylight is available. We did not model blind controls in any of these comparisons. The baseline for this case study is benchmark-A.

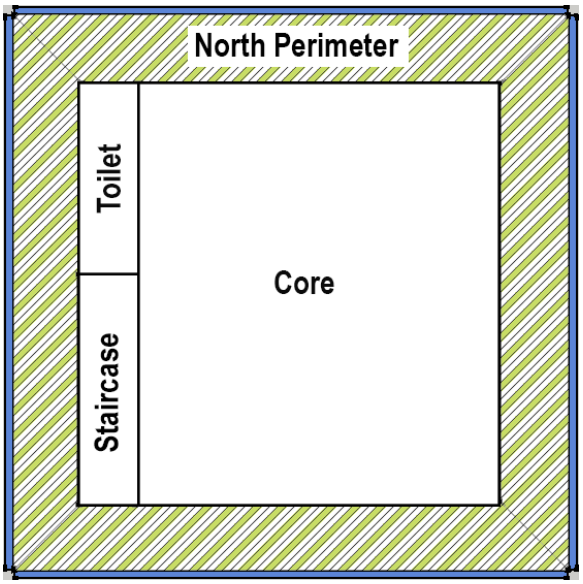

Figure 7: Daylighting controls for perimeter zones shown with yellow pattern.

3.2 Cooling setpoint increase

In the weather section above, we observed that the typical mean outdoor dry bulb temperature for Singapore is 27.5 °C with a mean relative humidity of 83.6%. These hot and humid conditions require substantial energy to dehumidify and cool to the stated indoor air criteria. Rim, Schiavon, Nazaroff (2015) shows ventilation cost reductions when indoor air setpoints are raised (Rim, Schiavon, and Nazaroff 2015). Occupant thermal comfort is still achieved through increased air velocities in the office space (Schiavon and Melikov 2008) when energy efficient fans are used (Yang et al. 2015).

Benchmark-A model can give more details of this strategy. We apply three different scenarios of this strategy and assume the same equipment sizing of the ACMV for each one. First, only the perimeter and core zone setpoints were changed. We defined the range of setpoint increase from the benchmark to be from 1 to 9 °C. Second, the indoor setpoints were changed with the same range as in the first case but the chilled water and supply air temperature (SAT) were also changed. We increased chilled water and SAT in three steps because the average zone relative humidity would not have been below 65%, a requirement from Singapore standard SS 554 *Code of practice for indoor air quality for air-conditioned buildings*, if we used a similar setpoint increases as for zones (SPRING Singapore 2009b). We defined personal fan objects in the energy model to account for the additional energy usage that result from increasing air movement for occupants (Yang et al. 2015). Personal fans were defined at 0.5 W/m^2 for any scenario equal or greater than a 3 °C zone temperature increase even though fans would not be required for this conservative zone temperature increase (Rim, Schiavon, and Nazaroff 2015). Preliminary results showed a maximum chilled water and SAT temperature increase of 4 °C and 3 °C, respectively, for the higher zone temperature setpoint increases. Table 10 shows the specific increases in setpoints. In addition, we reduced the minimum fan speed fraction from 0.5 to 0.15 in all simulations without affecting the minimum outdoor airflow rate. Motor manufacturers have recommendations on minimum VFD speeds that can be applied to their respective motors. The values generally range from 10 Hz to 20 Hz and depend on the motor installed. The 0.15 fraction represents the lower range of recommended VFD speeds commonly used in office HVAC systems in USA. The VFD fan system curve for the reduce airflow fraction is still based on Energy Design Resources' Advanced VAV Design Guide for a plenum airfoil fan static pressure drop of 170 Pa (0.7") (Stein, Zhou, and Cheng 2007). The change to the

lower fan speed minimum was motivated because elevated zone temperature setpoints will reduce cooling loads in the building, which will require lower airflow rates. If the constraint on fan speed remains at 0.5, duct static pressure will increase as airflow decreases[2]. This will have negative effects by unnecessarily increasing power consumption at the fan (due to the higher static pressure) and increasing duct air leakage. Another option to avoid these issues is to use smaller fans but we do not present this analysis as we only focus on the retrofit case.

We present the energy savings by increasing setpoints from benchmark-A. We also looked at the average relative humidity to confirm that it was still complying with Singapore standards. Relative humidity level plots will help foresee any moisture problems that an actual building might encounter with increasing setpoints.

Table 10: Setpoint increase parameters for each of the two scenarios.

	Scenario 1		Scenario 2	
Zone setpoint increase [°C]	Chilled water setpoint increase [°C]	SAT setpoint increase [°C]	Chilled water setpoint increase [°C]	SAT setpoint increase [°C]
1	0	0	0	0
2	0	0	0	0
3	0	0	3	2
4	0	0	3	2
5	0	0	3	2
6	0	0	3	2
7	0	0	4	3
8	0	0	4	3
9	0	0	4	3

3.3 Occupant localization

Knowing where people are in a building is another technology with the potential to have a significant impact on energy consumption in the built environment. Spaces can reduce their energy consumption by turning off lights and equipment, reducing ventilation flow rates, and increasing setpoint temperatures when not in use. SinBerBEST researchers have been investigating several methods to accomplish this (Chen et al. 2015; Shuo et al. 2015; Zou et al. 2015; Jin, Zou, et al. 2014; Jin, Jin, et al. 2014).

To implement occupant localization in the benchmark-A model, we reduced diversity factors in lighting and office equipment schedules and set demand control ventilation in the building. Lighting schedule reductions were based on studies performed by Halvarsson (2012). Halvarsson found that the ratio between the number of occupied zones to the total number of zones found in a typical office floor was on average 40%. He counted a zone as occupied when there was at least one person in the zone, and thus, the total number of people in a building can be far lower than 40% from the design occupant density. These data are not available for Singapore and it would be valuable to collect them. To reduce model complexity, we implemented this by reducing occupancy and lighting schedules by 60% from the

[2] assuming pressure-independent VAV boxes common in modern office buildings with DDC controls.

benchmark values. We assume no delays between when zones become unoccupied and lights shut off or ventilation rate decreases, and so the simulation represents ideal controls.

We did not find any similar studies done for office equipment. Therefore, we determined that a 30% reduction in the office equipment schedules from the benchmark model is reasonable. The reduction would not be directly proportional as in lighting schedules because equipment like computers would still be on but could enter a low power mode when the occupant leaves. It would be impractical to completely shut down computers, but monitors, task lighting, and other small devices may be turned off when the occupant leaves. We retained the same ACMV equipment sizing as used in the benchmark model.

We compared the results from this case study to benchmark-A1. The baseline will also have a 60% reduction in occupancy schedule. The change will be small since only the heat gains from the people will change, but it gives a realistic comparison.

3.4 Combined strategies

In this case study, we bring the different strategies mentioned above into one simulation. Starting from benchmark A, we implemented LED lighting, a 3 °C zone temperature setpoint increase, 2 °C setpoint increase for chilled water and supply air temperatures, 60% reduction in lighting and occupancy, and 30% reduction in office equipment schedules. We also compared this case study to the benchmark-A1 because we assume occupant localization technology in the building.

As in all of the alternative benchmarks, we kept ACMV equipment sizing the same as the benchmark model because we want to represent a retrofit of an existing building. It is also true in the case studies mentioned above. If a case study for a new building is evaluated then we would need to resize equipment to account for reduced design cooling loads. ACMV equipment has the potential to be downsized, saving building stakeholders on initial capital costs. However, the scope of this paper is limited to retrofits of existing buildings.

3.5 Titanium dioxide coating

Titanium dioxide (TiO_2) coatings have been used in building surfaces because they have shown to have self-cleaning properties and the ability to degrade various organic and inorganic compounds (Krishnan, Zhang, Yu, et al. 2013; Krishnan, Zhang, Cheng, et al. 2013; Folli et al. 2010; Maury and De Belie 2010). The coatings use sunlight and rainwater to produce these effects. The self-cleaning property of TiO_2 is of interest in this report because it can prevent a concrete building's exterior surface from soiling. In addition, TiO_2 coatings produce surfaces on the material that can achieve higher solar reflectance values. This will reduce heat gains through the building's exterior envelope as the higher reflectance values will reflect more solar irradiance.

SinBerBEST researchers provided solar reflectance values of 0.54 for a TiO_2 coating applied to conventional concrete wall and 0.53 when the coating was applied to an ultra-lightweight cement composite (ULCC) wall. However, solar reflectance for TiO_2 coated concrete can range as high as 0.8 based on recent laboratory results from SinBerBEST researchers. We simulated both values and compared them to benchmark-B for potential energy savings. In practice, the long term average solar reflectance of exposed concrete on a building façade can vary significantly depending on a large number of factors. To account for this, we also performed a parametric study on the reflectance values that

ranged from 0 to 1 to examine the potential effects of a range of soiled, un-soiled and coated concrete surfaces.

3.6 Ultra-lightweight cement composite exterior wall

Ultra-lightweight cement composites (ULCCs) achieve their lower density and lower thermal conductivity by introducing air voids into the concrete mixture (Wu et al. 2015). Air voids have a lower density and thermal conductivity than other concrete mixture components thus lowering both values in the overall mixture. Several methods exist to introduce voids into the concrete mixtures. One method studied by SinBerBEST researchers is by using cenospheres (Wu et al. 2015). These are very small (10 to 400 μm) hollow spheres that are a byproduct of coal combustion (Wandell 1996) and are available at low cost. The lower values have potential benefits in several aspects of the building industry; however, this report only investigates the benefits from an energy consumption perspective. Therefore, we modified the exterior wall of benchmark-B to represent a ULCC wall. We kept the same overall thickness of the wall as in the benchmark-B for simplicity, and the overall U-value for this construction assembly was 2.1 W/m^2·K. Table 11 shows the relevant properties of the ULCC layers.

Table 11: Exterior opaque construction assembly with ULCC wall with layers listed from outside to inside of zone

Layers	Thermal conductivity [W/m·K]	Density [kg/m^3] (Specific heat [J/kg·K])	Solar Reflectance
ULCC_Concrete_170mm	0.39	1306 (832)	0.42
Cement_Sand_Plaster_20mm	0.53	1568 (991)	0.45

3.7 Translucent concrete panels

Translucent concrete (TC) panels have been developed to provide daylight into buildings through embedded optic fibers that run through a concrete wall construction (Aashish Ahuja, Casquero-Modrego, and Mosalam 2015). The application of TC panels will ideally be in a room that has limited window area in order to provide the maximum benefits. These benefits can include reduced envelope cooling loads and energy consumed by artificial lighting.

We made several assumptions and simplifications in order to model this technology. We assumed that a daylighting control system will be needed in order to dim artificial lighting. Therefore, this technology will be compared against benchmarks that include daylighting controls for select WWRs. Daylighting sensors were only defined in perimeter zones at desk height (0.8 m). We defined TC panels in the rest of exterior opaque surfaces except where surfaces corresponded to plenum space as shown in Figure 8. In Figure 8, the yellow area represents the area where we assumed TC panels were installed. There are optimal configurations for both windows and TC panels to achieve higher quality of daylight into spaces but in this simulation we assume a uniform distribution of available light through windows and TC panels. The same 500 lux requirement from Singapore standard SS 531 still applies (SPRING Singapore 2006b).

We used a ray tracing model provided by SinBerBEST researchers to model how much light transmission went through one optical fiber of 0.01 m diameter (A. Ahuja, Mosalam, and Zohdi 2014). We then multiplied this value as needed to arrive at the desired optic fiber concentration on TC panel surfaces. The total available lumens provided by the optic fibers were then subtracted from the artificial lighting

to arrive at a reduced lighting schedule when daylight was available. Lastly, solar cooling loads through the optic fibers were not taken into account but can have a significant effect in thermal dynamics in the room (Aashish Ahuja, Casquero-Modrego, and Mosalam 2015). Thermal conductivity was adjusted using methods described by Ahuja et al. (2015) and their assumed properties for optic fibers (Aashish Ahuja, Casquero-Modrego, and Mosalam 2015).

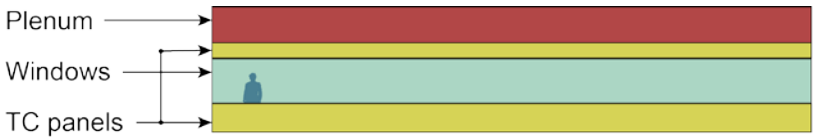

Figure 8: Schematic of TC panels and windows placement for an exterior wall in benchmark-B model for simulation purposes. TC panels are not defined for plenum zones represented in red. TC panels are defined in perimeter zones where windows were not previously defined as represented in yellow.

The total surface area of windows will significantly affect the savings potential of TC panels. If more windows exist for the room then most of the light will be provided by the window and TC panels will have little effect. Hence, we simulated different scenarios by varying the WWR of benchmark-B and varying the optic fiber surface concentration. The three selected WWRs are the current benchmark-B WWR 35%, 10% and 0%. We then changed the optic fiber concentration for each of the three scenarios from 0%, 1%, 3%, 5%, and 10%. Benchmark-B35, benchmark-B10, and benchmark-B0 were references for TC panels when the WWRs was 35%, 10%, and 0%, respectively.

3.8 Insulation

We found in the survey by Chong (2012) that only two buildings out of the 16 total concrete buildings used insulation in the walls. This is only a sample of the building stock but is an indication that insulation is rarely used in buildings in Singapore at the time of that survey. Insulation can help reduce heat gains through the building envelope, improve thermal comfort and reduce the cooling load that the ACMV must extract. Building designers may have overlooked the benefits from insulation due to the relatively small temperature difference between the indoor and outdoor environment in the Singaporean climate. However, conductive heat transfer due to incident solar radiation is significant, particularly on east and west facades. This heat transfer does not depend on the temperature difference between the indoor and outdoor environment but on solar radiation. In this simulation, we implement a 50 mm rigid insulation between the interior side of the wall and plaster. The thermal conductivity of the insulation is 0.035 W/m·K. The change is applied to benchmark-B, and reduces the exterior wall U-value to 0.62 $W/m^2 \cdot K$.

3.9 Summary

We have created two main benchmark models, one with an all glass façade and one with a concrete envelope with reduced WWR. The only difference between the two benchmarks is the construction of the envelope. Thereafter, we performed additional modifications to the main benchmarks to give realistic comparisons to some of the technologies we have described in the above sections.

Table 12 shows a summary of the different SinBerBEST case studies with the respective baselines that we used to compare them. In Section 5, we will first discuss the results of benchmark-A with its applicable technologies followed by benchmark-B with its applicable technologies.

Table 12: Summary of simulated SinBerBEST technologies and their respective referenced baselines.

SinBerBEST technology	Baseline used for comparison	Comments on baseline
Lighting controls and lamps	Benchmark-A	-
Cooling setpoint increase	Benchmark-A	-
Occupant localization	Benchmark-A1	Derived from benchmark-A. Reduced occupancy schedule by 40%.
Combined strategies	Benchmark-A1	-
Titanium dioxide coating	Benchmark-B	Derived from benchmark-A. Replaced all glass façade with concrete façade and 35% WWR.
Ultra-lightweight concrete panels	Benchmark-B	-
TC panels on 35% WWR	Benchmark-B35	Derived from benchmark-B with daylighting controls implemented.
TC panels on 10% WWR	Benchmark-B10	Derived from benchmark-B. Reduced WWR to 10% and implemented daylight controls.
TC panels on 0% WWR	Benchmark-B0	Derived from benchmark-B but reduced WWR to 0% and implemented daylight controls.
Insulation	Benchmark-B	-

4 Software

We used the EnergyPlus simulation engine version 8.10.009 to perform all simulations presented in this report. EnergyPlus offers modular and structured code that has a range of flexibilities to model many different scenarios found in buildings (Crawley et al. 2008). It performs deterministic simulations and calculates loads using the ASHRAE heat balance method. We modified the initial EnergyPlus input file using an open source programming language called Python version 2.7.10 in conjunction with a Python package called eppy version 0.4.6.4a (*Python 2.7.10* (version 2.7.10) 2015; Santosh Philip 2015). We processed raw EnergyPlus outputs using R, a statistical computing and graphics software version 3.1.2, using RStudio version 0.99.467 ("Input Output Reference: The Encyclopedic Reference to EnergyPlus Input and Output" 2014; *R* (version 3.1.2) 2014; *RStudio* (version 0.99.467) 2015) . Processing data usually involved the addition of hourly values for a given year and calculated percentages. In some cases, we apply equations to the direct outputs of EnergyPlus and in those cases we present the equations before showing the results.

5 Results and discussion

5.1 Benchmark-A model

The BCA reported on the current energy performance of Singapore's building stock using the Building Energy Submission System (BESS) (BCA 2014). This requires building owners in Singapore to submit their buildings' energy consumption on an annual basis. According to the inaugural report, commercial office buildings have an average energy utilization index (EUI) of 253 kWh/m^2·a and a median of 218 kWh/m^2·a. The top quartile shows office buildings consume 164 kWh/m^2·a or less while buildings in the bottom quartile consumed more than 280 kWh/m^2·a. EUI represents actual energy use divided by the total gross floor area (GFA), excluding carpark area, with no other correction factors or adjustments. Hours of operation and occupant density are unknown factors that can be important to explain energy consumption and group similar buildings for proper comparison. For example, we did not include a datacenter in the benchmark model, which yields a lower EUI than one would expect in measured data from most modern office buildings. Nonetheless, these numbers provide a frame of reference to put the benchmark results into perspective.

Another energy consumption metric, energy efficiency index (EEI), provides more normalization to offer better comparisons between buildings (BCA 2010a). It takes into account vacancy rate and normalizes the buildings operating hours to 55 hours per week. Table 13 describes some results from analyzing data shared by BCA for GM certified buildings which presented EEI as an energy performance metric. Table 13 provides another frame of reference for comparing the benchmark model energy consumption results. We subset the data into two smaller sets of buildings to provide as close to a direct comparison with the benchmark model as possible. The first requires buildings that have the same GM version as in benchmark-A, and the second further requires buildings to use the same type of energy efficient water-cooled chilled water plant ACMV system as benchmark-A. The more energy efficient ACMV system is required by Green Mark certification for buildings that have cooling loads of 500 tons or more, which are likely to be seen in large buildings[3].

We expect the EEIs in Table 13 to be slightly lower than the benchmark building since the data only includes GM Gold^{Plus} and Platinum certified buildings. Note however, that we also expect all simulation results to have a lower EEI than measured data from real buildings, such as those presented in BCA's BESS report. The primary reason is that the simulation results do not account for any faults in the building – the simulation assumes that controls and operation are ideal. Faults typically increase energy consumption in an ACMV system by more than 20% and in extreme cases up to 85% depending on the climate, severity, and combination of faults (Basarkar et al. 2011; Wang and Hong 2013; Pérez-Lombard, Ortiz, and Pout 2008). Another reason is that the model does not include any unexpected or unpredictable energy consuming devices that are found in real buildings. By definition, the benchmark model only includes energy consuming devices that the authors considered relevant and commonplace for a typical office building.

Table 13: Summary of GM Gold^{Plus} and Platinum certified buildings.

Surveyed buildings	Median EEI [kWh/m^2·a]	N
Gold^{Plus} & Platinum	145	33
Gold^{Plus} & Platinum since 2010	138.5	18
Gold^{Plus} & Platinum since 2010 & > 20,000 m^2	136.3	14

[3] Those approximately 20,000m^2 or larger.

The results from the benchmark-A model yield an EUI of 146 kWh/m^2·a[4], calculated excluding the carpark area. For reference to Table 13, we also calculated the EEI of the model as 139 kWh/m^2·a according to the standard calculation methodology (BCA, n.d.). Both results are within the range of what we expect given information in the BCA benchmarking report and the other considerations noted above. We determined that an EUI value of 146 kWh/m^2·a is reasonable and representative of a large office building at the Certified level. Figure 9 shows the energy breakdown. ACMV refers to the cooling system, which includes the chillers, fans, chiller and condenser pumps, and cooling towers. The ACMV category also includes ventilation for the mechanical and electrical rooms. We treat these two types of energy consumption as fan energy. Lighting refers to lighting in office floors 4-20. It does not include carpark, facade, and exterior lighting. These other types of lighting are included in the auxiliary portion of the chart along with carpark ventilation, miscellaneous domestic water pumps, and lifts. The plug load category includes equipment use in office floors 4-20.

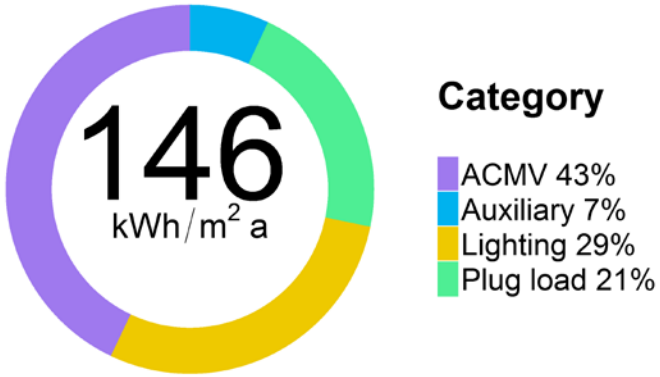

Figure 9: Annual EUI for benchmark-A building and percentages broken into four categories.

The most significant energy consumption category in benchmark-A is the ACMV system with 43% and lighting as the second largest consumer with 29%. Beca extensively reviewed the end-use energy consumption and deemed them reasonable for a large Singapore commercial office building. Further details of their review can be found in the Appendix. Figure 10 shows a further energy consumption breakdown for the ACMV system based on its main components that work together to cool. Figure 10 shows that chillers and fans are the top energy consumers from ACMV individual components.

[4] For context, if we assume faults occur in the modelled benchmark-A building according to the 20% estimate noted in other literature, this result would change to 157 kWh/m^2·a instead of 146 kWh/m^2·a.

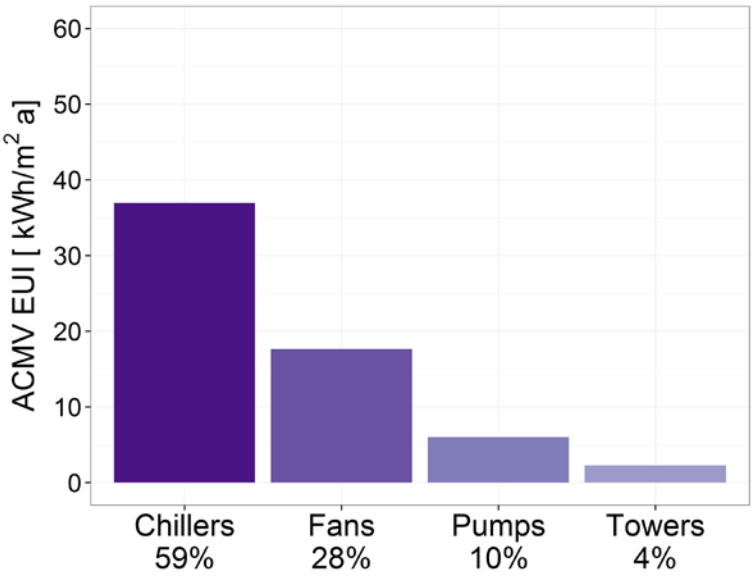

Figure 10: Energy consumption of individual components in the ACMV system for benchmark-A model.

The ACMV system is driven by the total amount of thermal energy entering a building, also known as the heat gains. In many climates, heat gains can increase or decrease ACMV energy consumption depending on the mode of the building. If the building is in heating mode then heat gains are beneficial as it reduces the heating energy required to maintain zone setpoints. On the other hand, if the building is in cooling mode heat gains becomes a cooling load for the ACMV system. Higher cooling loads in a building will result in larger cooling energy consumption for a given ACMV system. Climate is one factor that dictates the mode of the building. Given the climate in Singapore, cooling is the only mode in buildings and heat gains are now referred to as cooling loads through the rest of this report. Cooling loads enter a building through a variety of sources and mechanisms. Figure 11 shows the different cooling loads that impact the ACMV system energy consumption in the benchmark building. Since cooling loads enter the building at different rates, it is beneficial to know what process generates those cooling loads. Building stakeholders can develop methods to reduce them if they know the source and breakdown, however this is difficult to measure in a physical building. Energy simulation models such as the benchmark model provide a convenient environment in which to perform these analyses.

We obtained most of the results shown in Figure 11 directly from EnergyPlus outputs. The two exceptions are latent and sensible heat for the ventilation category. Latent energy is the amount of energy needed to remove moisture from air and sensible is the amount of energy to cause a change in temperature in air. We used Equation 1 and Equation 2 to calculate them, respectively.

$$\dot{Q}_l = L_v \dot{m}_{oat} \Delta x \quad (1)$$

$$\dot{Q}_s = C_p \dot{m}_{oat} \Delta T \quad (2)$$

where L_v is the latent heat of vaporization for water, C_p is the specific heat for air, $\dot{m}_{oat}$ is the mass flow rate for outdoor air, Δx is the difference in absolute humidity ratio between the outdoor air and return air, and ΔT is the difference in dry bulb temperature between outdoor air and return air. We performed these calculations at each particular floor and then sum for the overall building. Ventilation air heat

gains are essentially the thermal energy removed to cool and dehumidify so it would be at the same conditions as the zone air. We assume L_v and C_p to be constant for the calculations with values of 2,466 kJ/kg and 1.005 kJ/kg·K, respectively.

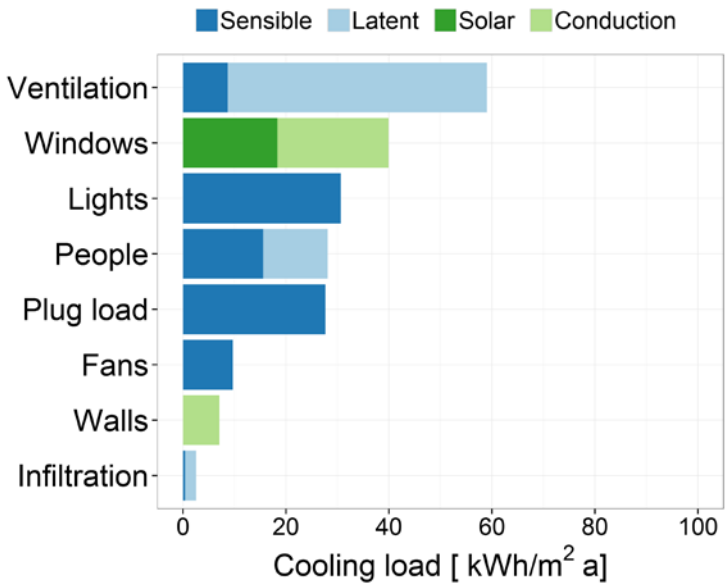

Figure 11: Total cooling load breakdown by type for occupied hours in benchmark-A model.

Figure 11 shows clearly that ventilation is the most significant cooling load source entering the building with 29% of the total. Furthermore, the ventilation bar shows dehumidification to be the predominant driving factor of energy use. The breakdown is 85% for dehumidification and 15% for sensible. The breakdown is consistent with the results of Rim et al. (2015). We present strategies that can help address the high dehumidification energy in the case studies below.

Windows are another area to focus attention. The benchmark model shows cooling loads of 40 kWh/m^2·a entering through windows. Solar and conduction thermal energies are evenly split. We selectively placed the different types of windows in the model. We defined better windows on the East and West facades because these orientations receive direct solar radiation during the morning and evenings, respectively. In other hours of the day, solar radiation comes from above the building and can be blocked through effective exterior shading. The benchmark model only uses a simple horizontal projection shading. Research for an effective integrated fenestration system is warranted to decrease heat gains through windows and still allow daylight and views that windows provide.

Cooling loads emitted from people, lights, and plug loads are similar. The fan cooling load category accounts for the temperature rise of the supply air due to motor and fan inefficiencies. Lastly, wall and infiltration are the two lowest cooling load contributors. Benchmark-A model shows very low cooling loads through wall conduction mainly due to the high WWR.

Cooling loads are due to thermal energy and shown in Figure 11. To clarify, this is not the electrical energy being consumed by the different components listed in the figure. For this reason, components like lighting, plug loads, and fans will be seen in electric energy and cooling load plots. These components have a direct contribution in the overall building energy consumption but they will also have an indirect effect on the ACMV system electric consumption through the release of thermal energy. The chillers' coefficient of performance (COP) is the reason cooling loads can be much higher

than the electrical energy consumed by the ACMV system. For instance, the benchmark chiller has a COP of 6.1 so the refrigerant can absorb 6.1 units of cooling load for every one unit of electric energy it consumes. The overall efficiency of the ACMV system decreases when we factor in the electric consumption from the other components. Figure 12 illustrated an arbitrarily selected week in the benchmark simulation and shows how cooling loads vary and how the ACMV system responds accordingly.

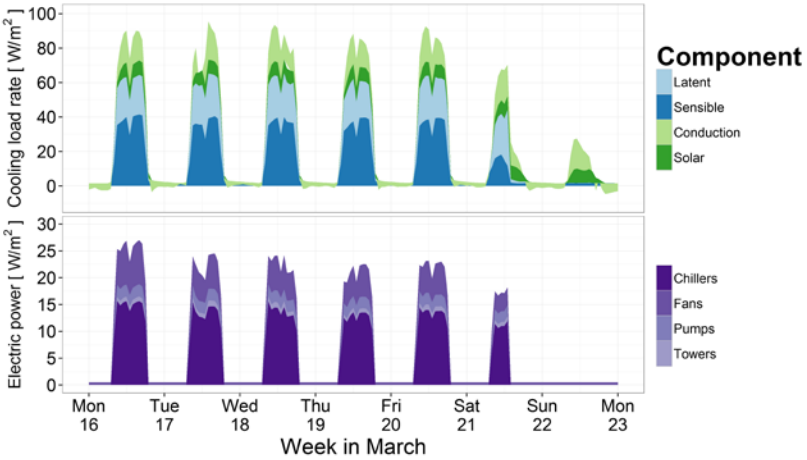

Figure 12: Heat gains and ACMV electric demand for an arbitrarily selected week in simulation of benchmark model.

Variation in the cooling loads is attributed to the variation in the climate and the variation in internal cooling loads. We define variation in internal loads through the use of schedules as mentioned in Section 2.4. Schedules reduce design internal loads in a building model for a particular timestep and we call the actual resulting load the 'effective load'. We calculated and present average effective loads in Table 14 for weekday and weekend day types. We further disaggregated effective loads into occupied and unoccupied periods. It is useful to look at the effective loads in the benchmark model and in models with energy efficiency measures to make comparisons on the effect it has on different internal loads. Table 14 shows effective loads for lights, plug loads, occupancy density, and ventilation. Categories only include internal loads from the perimeter, core, stairs, and restrooms zones.

Table 14: Effective loads in office floors for different day types and timeframes in benchmark model.

Internal loads	Weekday occupied	Weekday unoccupied	Weekend occupied	Weekend unoccupied
Lights [W/m^2]	10.6	0.9	3.8	0.9
Plug load [W/m^2]	9.4	0.6	5.6	0.6
Occupancy density [m^2/person]	13.1	0	49.3	0
Ventilation [l/s·person]	8.2	0	37.1	0

Figure 13 and Figure 14 confirms that zone air temperature and relative humidity stay within limits of the prescribed setpoints. We subsetted the data to only include occupied hours of the benchmark model. The boxplots show that the dry bulb air temperature setpoints are consistently met and that relative humidity has more variability because it is not directly controlled at the zone level; instead it is controlled at the system level through the cooling coil setpoint. The startup hour, from 7:00 to 8:00, is not consistent with normal ACMV operation and therefore, we did not include it when creating the

boxplots shown in Figure 13 and Figure 14. The startup up hour contained 336 hours in the annual simulation. Figure 13 shows only three hours above 26 °C, which is the upper limit for zone temperatures defined in Singapore standards.

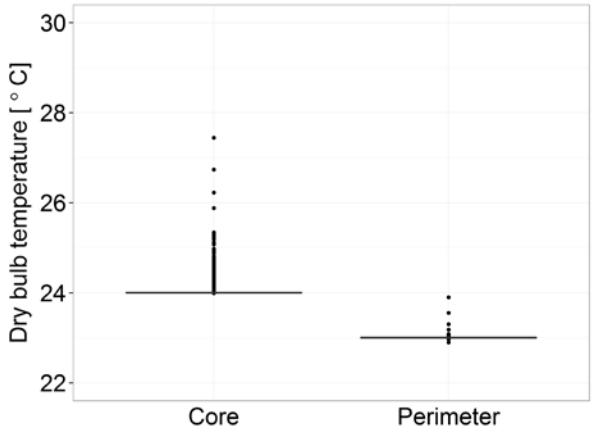

Figure 13: Core and perimeter zone dry bulb temperature for occupied hours in benchmark model.

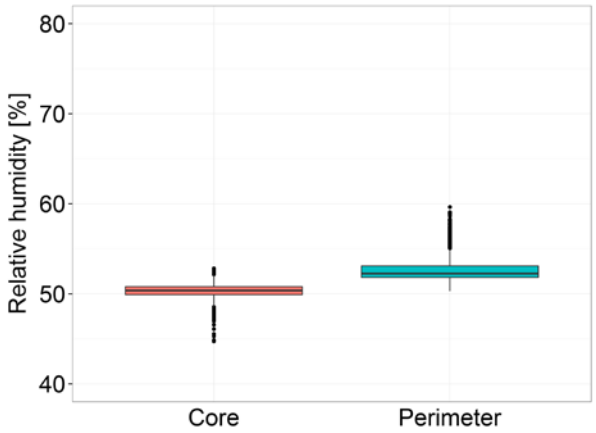

Figure 14: Core and perimeter zone relative humidity for occupied hours in benchmark model.

5.2 Lighting controls and lamps

Improved lighting primarily has a direct impact on electric consumption of the building, but it will reduce cooling loads as a secondary effect. Figure 15 shows the building's overall energy consumption as well as the ACMV energy component of the building for the different design lighting loads. Table 15 shows the resulting effective lighting loads. Figure 15 and Table 15 is data from the simulation without daylight controls defined in the model. Building stakeholders can see the potential energy savings of their lighting designs as they strive for increased energy efficiencies.

Figure 16 shows similar information as in Figure 15 but the simulation results include daylight controls in the model. Figure 16 is supplemented by Table 16 to show the resulting effective loads from lighting at the different design LPDs and daylight controls. The results from the addition of daylight control shows that additional savings from daylighting decrease as LPD in spaces also decreases. We expected these results since higher efficiency lighting like LEDs can produce the same illumination levels as fluorescent

T12 lighting but at a lower power demand. Thus, daylighting has less potential to reduce energy consumption because the total lighting demand is lower. However, building stakeholders should not base their decision to include daylighting into their building design solely on energy, especially if efficient lighting exists as daylighting has many other positive benefits on occupants (Edwards and Torcellini 2002).

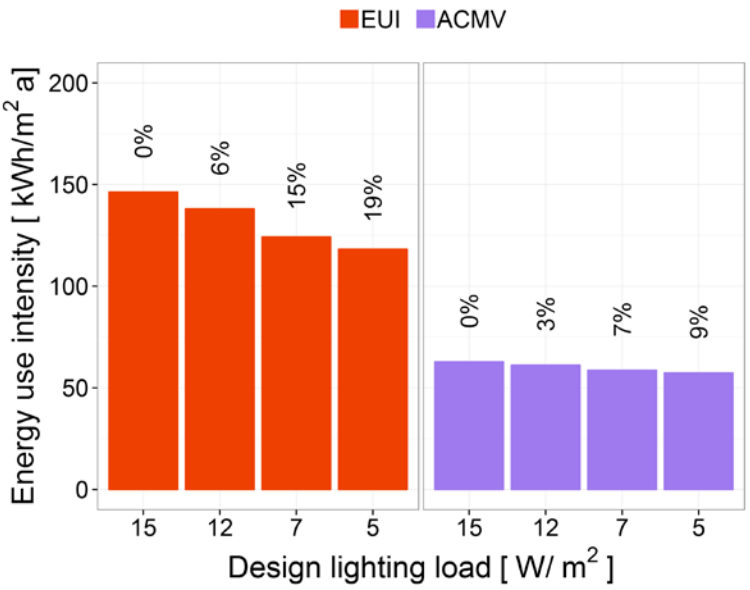

Figure 15: EUI and ACMV energy consumption with different design lighting loads and no daylight controls. The simulated results are compared to benchmark-A.

Table 15: Effective lighting loads in W/m^2 with reducing design LDPs and no daylight controls.

Design load	Weekday occupied	Weekday unoccupied	Weekend occupied	Weekend unoccupied
12	8.6	0.7	3.1	0.8
7	5.2	0.5	1.9	0.5
5	3.7	0.4	1.4	0.4

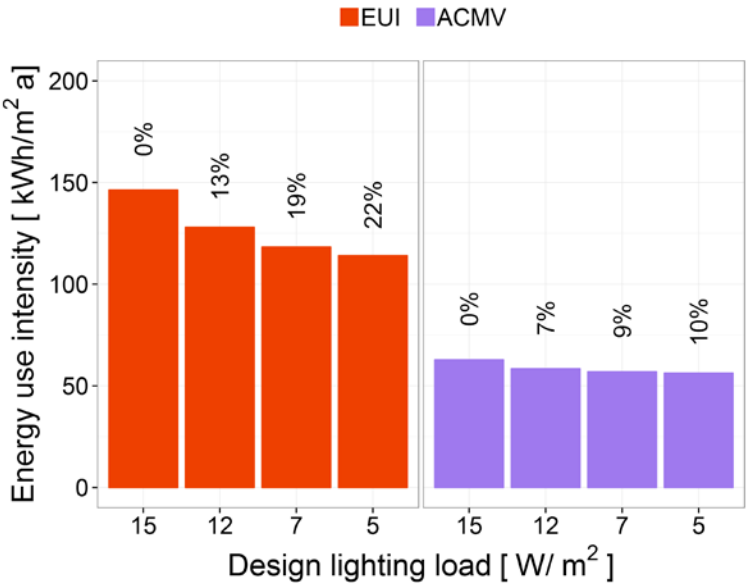

Figure 16: EUI and ACMV energy consumption with different design lighting loads and with daylight controls implemented for design loads of 12, 7, and 5 W/m^2. The simulated results are compared to benchmark-A.

Table 16: Effective lighting loads in W/m^2 with reducing design LDPs and daylight controls.

Design load	Weekday occupied	Weekday unoccupied	Weekend occupied	Weekend unoccupied
12	6.1	0.7	2.4	0.7
7	3.7	0.5	1.5	0.5
5	2.7	0.4	1.1	0.4

Figure 17 shows the distribution of the overall electricity consumption of the building model with a LPD of 5 W/m^2 and daylight controls. Improved lighting designs have the potential to reduce overall energy consumption by 22% and reduce lighting energy consumption up to 18% in a typical office building.

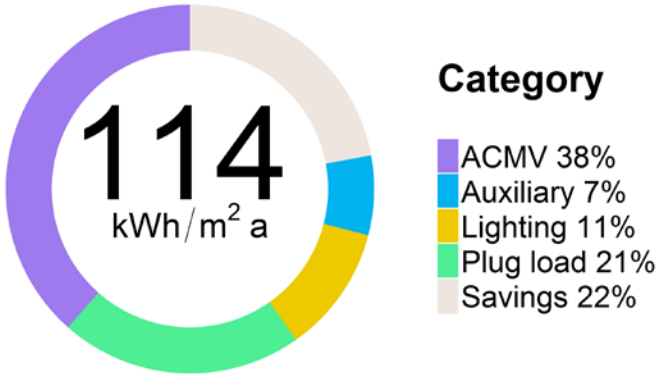

Figure 17: Annual EUI and end-use percentage for model with LPD of 5 W/m^2 and daylight controls. The simulated results are compared to benchmark-A.

5.3 Cooling setpoint increase

Increasing the room temperature setpoint has the potential to mitigate the energy intensive process to dehumidify and cool outdoor air for ventilation purposes in hot and humid climates. When coupled with increased air movement, this strategy will not have any adverse effects on thermal comfort and can even increase satisfaction among occupants (Schiavon and Melikov 2008). Schiavon et al. (2015) performed experiments where occupants in the tropics were exposed to elevated zone temperatures and air speeds. Researchers showed that people were thermally comfortable at dry bulb zone setpoints of 26 °C and 29 °C when provided with a personally controlled fan. In the building model, these two temperature setpoints would correspond to about 3 °C and 6 °C increase in temperature, respectively. The cases with an increase of 7, 8 and 9 °C are reported to explore the max potentials of this solution. As mentioned previously, we defined zone temperature setpoints in the perimeter and core zones at 23 °C and 24 °C, respectively. A 3 °C increase in zone temperatures would correspond to about 17% savings in the ACMV system in the scenarios as shown in Figure 18. Elevating zone setpoints allows building operators to relax setpoints and adjust fan speeds at the system level increasing potential savings in the building. We show relaxed setpoints at the system level in Scenario 2. Our model showed a 6 °C increase in zone setpoint has potential savings in the ACMV of up to 33% if chilled water and SAT setpoints increased by 2 °C and the minimum VFD fan speed is decreased to 0.15. We obtained these results through a brief exploration of supply air and chilled water temperature setpoints, and display these results to illustrate that significant further energy savings are possible through optimization at the system and plant level. However, a thorough optimization is outside the scope of this analysis. In regards to energy use of personal fans, the energy model results shows that the increase at the 0.5 W/m^2 level that we defined did not increase energy usage significantly e.g. 0.7% increase in overall energy consumption.

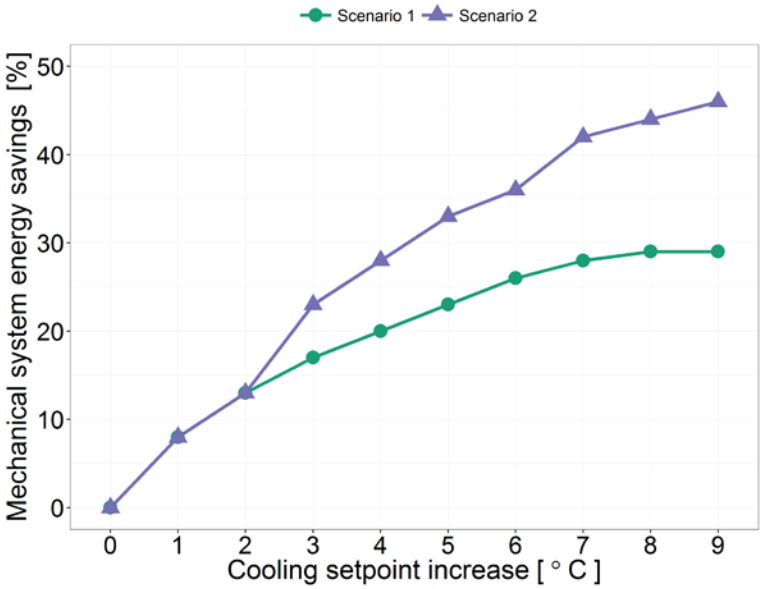

Figure 18: Potential savings in the ACMV system with increasing cooling setpoints. Scenario 1 shows the effect of zone setpoint increases only. In addition to zone setpoint increases, Scenario 2 simulates increases in chilled water and supply air temperature setpoints. Chilled water temperature setpoints increase 0 °C for zone setpoint increase of 0 to 2 °C, 3 °C for zone setpoint increase of 3 to 6 °C, and 4 °C for zone setpoint increase of 7 to 9 °C. Supply air temperature setpoints increase 0 °C for zone setpoint increase of 0 to 2 °C, 2 °C for zone setpoint increase of 3 to 6 °C, and 3 °C for zone setpoint increase of 7 to 9 °C. Both scenarios include the reduction in VFD fan speed to 0.15 from 0.5 established in the benchmark.

Dehumidification of incoming air in typical Singapore buildings takes place at the cooling coil and the supply air temperature setpoint, the airflow rate and the chilled water temperature affect the amount of moisture extracted. Therefore, as we increase chilled water temperature in the model, moisture content in the occupied zones is modified. Figure 19 shows that relative humidity decreases when we only increase zone setpoint temperatures. The relative humidity in the zones decreases with increasing setpoint because the chilled water temperature, supply air temperature, outdoor airflow rate are maintained constant. When these parameters are held constant, the cooling coil will extract latent heat to leave outgoing air at a similar absolute humidity with the different setpoint increments. Then as the supply dry bulb air temperature rises with internal sensible heat, the relative humidity will decrease because warmer air can hold more moisture than cooler air. The only increase in absolute humidity in the zones is through the latent load of people but the assumed latent load for people does not have a significant impact on the relative humidity in the zones. Relative humidity can be maintained within a similar range as in benchmark-A by modifying the supply air temperature setpoint. Changing the minimum airflow fraction has larger effects when changing setpoints towards the higher end of the range. Based on our building model, we can predict that moisture issues in zones will not occur under any of the proposed operating strategies. The average relative humidity levels for both scenarios are well below the 65% relative humidity limit required by Singapore standard SS 554. We eliminated outliers from the plots since they mostly occurred during morning startup and are similar to the one in the benchmark-A model.

Figure 20 shows the zone dry bulb temperature distribution for the different scenarios. It shows that core and perimeter zones can maintain zone temperature setpoints for the three different strategies.

For higher zone temperature setpoints, the plots show more variability but the average zone temperature is below the setpoint.

Table 17 shows that minimum outdoor airflow rates for ventilation purposes is above the requirement; the larger of either 5.5 l/s·person or 0.6 l/s·m^2. The minimum outdoor airflow in the benchmark model is based on area for perimeter and core zones. If we divide the total outdoor airflow rate by the total number of people in benchmark-A, the result will be 7.2 l/s·person. Values in Table 17 are above our calculated minimum. Weekend ventilation per person is much higher than during the weekday because the number of occupants decreases during the weekend while the total airflow rate remains the same. Figure 21 shows that the ratio between outdoor airflow and total supply air increases as the temperature setpoint increases. This is because as the temperature setpoint increases, there is a reduction in the total supply airflow needed to meet the zone setpoint but the required minimum outdoor airflow remains constant. Thus, there is a higher percentage of outdoor air in the supply air at higher zone temperature setpoints. Similar results are also shown in Figure 22 where results are from (A) benchmark-A and (B) scenario 2 at 8 °C zone temperature setpoint increase. Figure 22 (A) shows that for benchmark-A, both AHU airflow fraction and outdoor airflow to total airflow ratio have a wide range of modulation from about 0.2 to 1 for airflow fraction and 0.1 to 0.9 for outdoor airflow to total airflow ratio. This operation is expected for a fan that is sized appropriately and modulation occurs for different cooling loads throughout the day. On the other hand, when zone setpoints are increased, there is a need for reduced airflow rates through the air system. In the retrofit case, we maintain the same fan thus airflow fraction decreases. Figure 22 (B) shows that the modulation for AHU airflow fraction is decreased to 0.2-0.45 and the outdoor airflow rate contributes a greater percentage of the total airflow rate. This decreases the modulation of outdoor airflow rate to total airflow rate from 0.3 to 0.9. For the case of new construction, the fan in this situation will be oversized. Downgrading to a smaller fan will yield similar results found in the benchmark-A model while saving initial capital costs in the process.

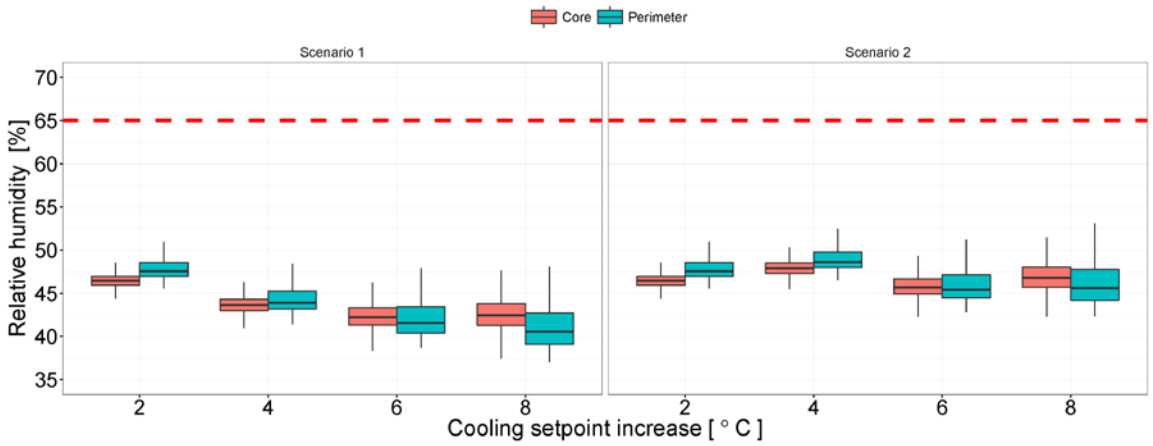

Figure 19: Boxplots of the relative humidity distribution as zone setpoints increase for the two different scenarios. The red dashed line represents the upper limit for humidity inside buildings.

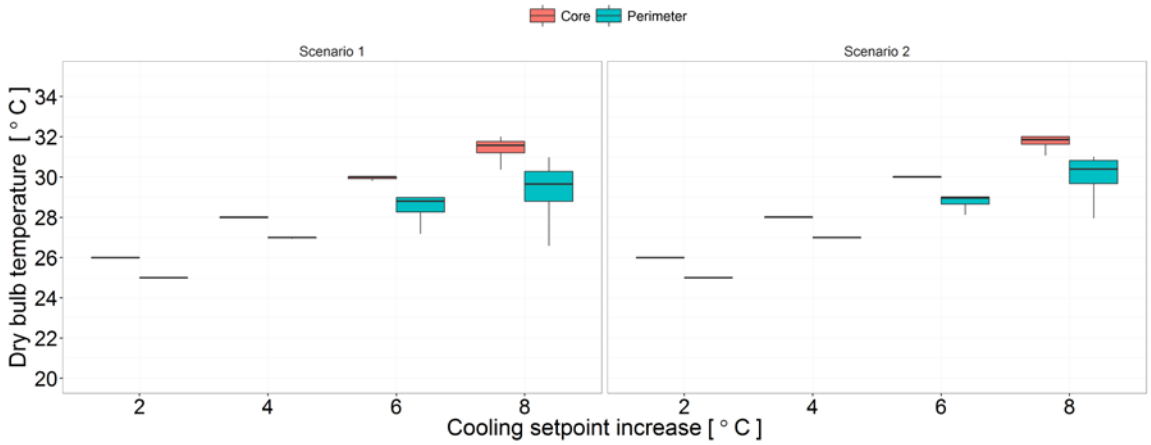

Figure 20: Boxplots of dry bulb distribution as zone setpoints increased for the two different scenarios.

Table 17: Effective ventilation rates in l/s·person with increasing zone temperatures for the two different scenarios. The total number of people divides the total ventilation airflow rate through each occupied hour timestep. The average of these values are the effective ventilation rates in the table.

	Zone Setpoint Increase [°C]	Weekday occupied [l/s·person]	Weekend occupied [l/s·person]
Scenario 1	2	8.5	40.2
	4	8.9	46
	6	9.7	53.1
	8	11.1	54.3
Scenario 2	2	8.5	40.2
	4	8.7	42.7
	6	9.2	50.4
	8	10.1	53.8

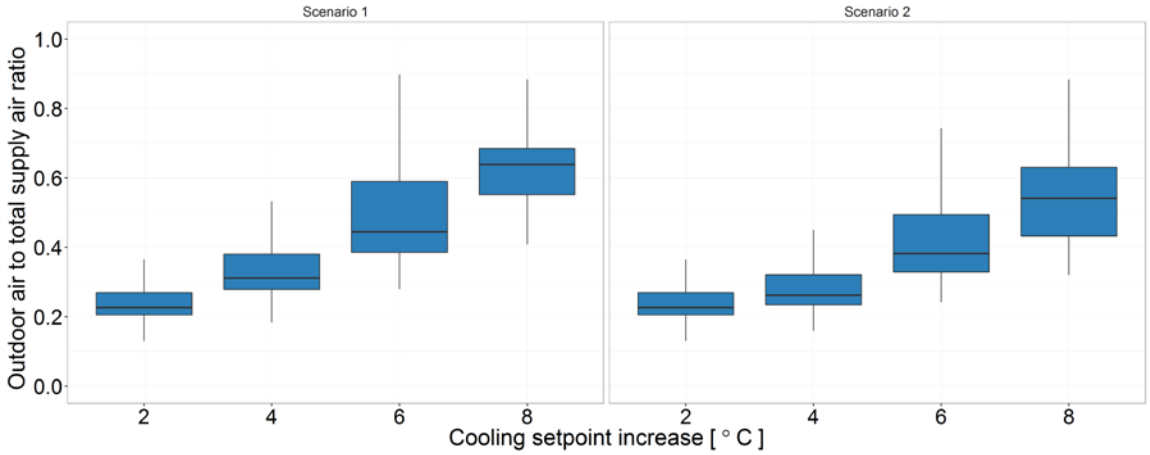

Figure 21: Boxplots of outdoor air to total supply airflow ratio for each VAV system defined in the model. The boxplots show the ratio as zone setpoints increase for the two different scenarios. The boxplots were created for each of the three office floor sections of the building model. Bottom for the first office floor (floor 4 in building model), middle for offices floors (floors 5-19), and top for the top office floor (floor 20).

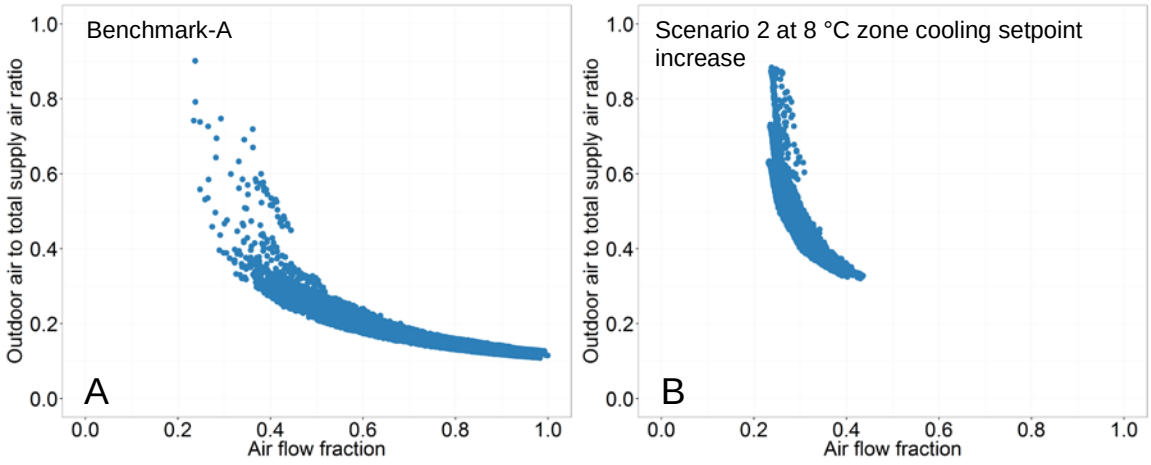

Figure 22: Outdoor airflow to total supply airflow ratio versus supply airflow fraction for all AHU systems in the building energy model. Results from (A) benchmark-A and (B) scenario 2 at 8 °C zone cooling zone temperature setpoint increase. Both scenarios include minimum VFD fan reduction to 0.15.

ACMV system energy savings can also be attributed to the reduction in cooling loads from conduction. The reason is because the conductive heat transfer rate is proportional to the temperature difference between the outside surface and the inside surface of the construction assembly. The lower the temperature difference the lower the heat transfer rate for a given assembly. Cooling loads due to solar energy transmitted through windows are unaffected since heat transfer is due to a different mechanism. Figure 23 shows the cooling load for 3 °C increase in zone, 0 °C increase in chilled water, and 0 °C

increase SAT temperature setpoints and for 6 °C increase in zone, 2 °C increase in chilled water, and 2 °C increase in SAT temperature setpoints. We aggregated the cooling load rates into ventilation, internal, and envelope sources. The ventilation category includes ventilation and infiltrations, the internal category includes plug load, lights, people, and fans, and the envelope category includes windows and walls cooling load sources. Figure 23 shows that conduction and ventilation sensible cooling loads disappear for a range of setpoint temperature increases. Sensible loads disappear due to the same concept explained above but the temperature difference is between the outdoor air and zone air.

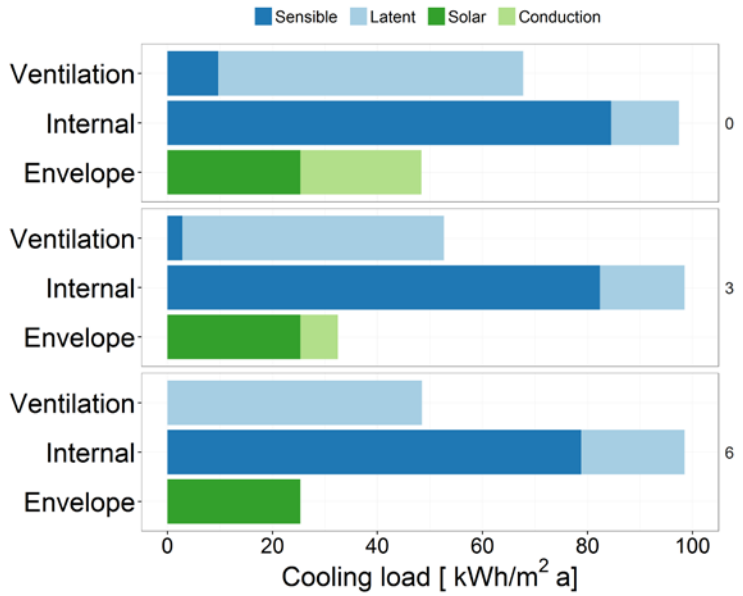

Figure 23: Total cooling load rate aggregated by type for occupied hours for 3 and 6°C increase in zone setpoints.

Figure 24 shows the overall building energy consumption distribution as temperature setpoints increases by 3 °C, 2 °C increase in SAT, and 3 °C increase in chilled water supply. This simulation differs slightly from Scenario 1 described above at 3 °C setpoint increase as it also includes the SAT and chilled water setpoint increase. The 3 °C increase in zone temperature is a conservative increase that personal fans at this level will not be required to maintain occupant comfort. Furthermore, the modification is simple to implement to existing buildings. In the case of new construction, additional savings can be realized in resizing to smaller ACMV systems. Personally controlled fans can allows an increase in temperature setpoint up to 6 °C, this would lead to a potential ACMV energy saving of 36% and a total energy savings of 15%.

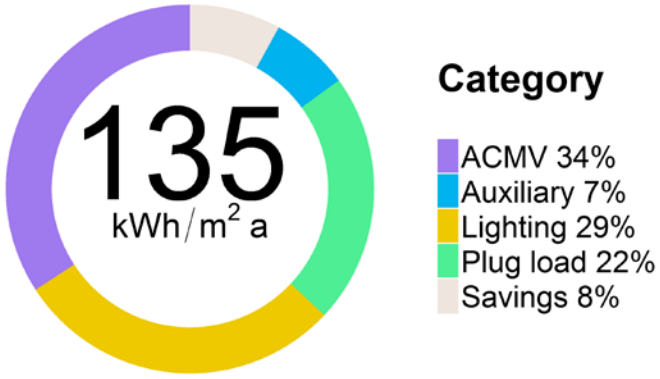

Figure 24: Overall energy consumption breakdown with 3 °C zone temperature, 2 °C SAT, and 3 °C chilled water setpoint increase. The simulated results are compared to benchmark-A.

5.4 Occupant localization

Occupant localization has the potential to influence many different systems in a building. Table 18 shows that it reduced effective loads in the model for all categories shown. This is due to the ability of occupant localization systems to cater to occupants' exact needs for the times they are in the building. Ventilation airflow rates, lights, and many plug loads can be either reduced or shut off entirely when occupants leave a room. For ventilation airflow rates, the minimum can now be based on occupancy in the building given that indoor air quality criteria indicated in Singapore standard SS 554 is being met (SPRING Singapore 2009b). Lowering systems' energy demand based on occupancy has the potential to reduce energy consumption in the ACMV system and lighting by more than 13% for each category and a total reduction of 32% when we include plug loads. These saving values are based on assumptions we gathered from research, and on idealized operation of occupancy localization systems. Overall, the total building consumption is reduced to 96 kWh/m^2·a as shown in Figure 26.

Figure 25 shows new cooling loads in the model as a result from occupant localization systems. Windows become the most significant cooling load source with plug loads ranked second. Ventilation goes from being the highest source of cooling loads to the third largest in this building; it was reduced by 73%. Even though cooling loads for people are reduced in this case study, they would be the same as in the adjusted baseline model. All other loads stay the same in the adjusted baseline as in the benchmark model.

Table 18: Effective loads in office floors for different day types and timeframes with occupant localization.

Internal loads	Weekday occupied	Weekday unoccupied	Weekend occupied	Weekend unoccupied
Lights [W/m^2]	4.4	0.5	3.8	0.9
Plug load [W/m^2]	6.6	0.5	5.6	0.6
Occupancy density [m^2/person]	32.8	0	49.3	0
Ventilation [l/s·person]	5.4	0	5.5	0

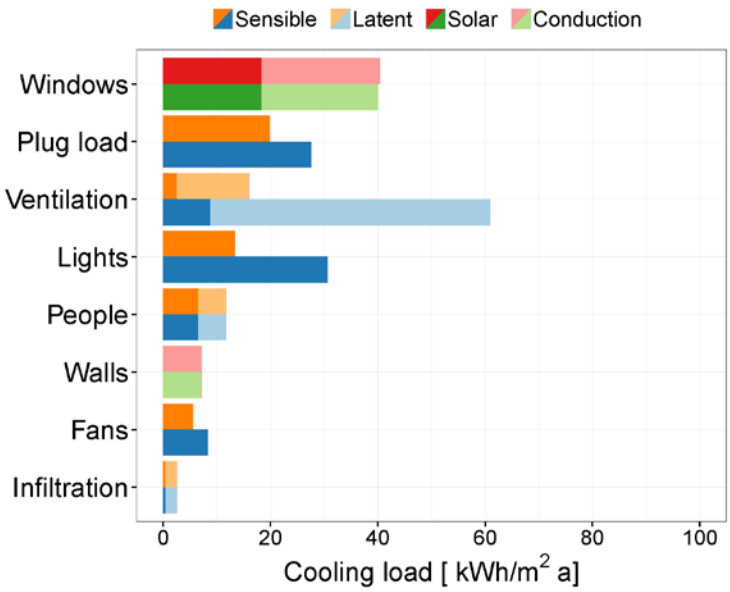

Figure 25: Total cooling load rate breakdown by type for occupied hours with occupant localization systems in orange and red colors. The occupant localization systems cooling loads are compared with benchmark-B in blue and green colors.

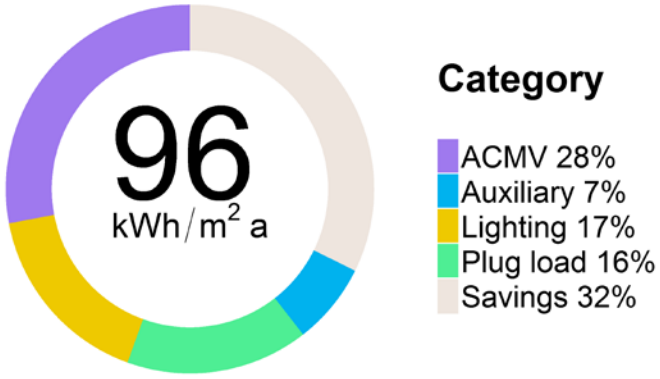

Figure 26: Annual EUI and end-use percentage for model with occupancy localization technology. The simulated results are compared to benchmark-A1.

5.5 Combined strategies

In the final case study, we implemented the different technologies described in Section 3.4 above. The combined effect of the different technologies can result in energy savings potential up to 46% in a typical renovation commercial office from Singapore. Figure 27 shows that modernized lighting systems have the largest energy consumption reduction at 21%. The ACMV system energy savings comes at a close second with 19% reduction from the adjusted baseline model. Plug loads have a 6% impact on reducing the overall energy consumption in the adjusted baseline benchmark-A1.

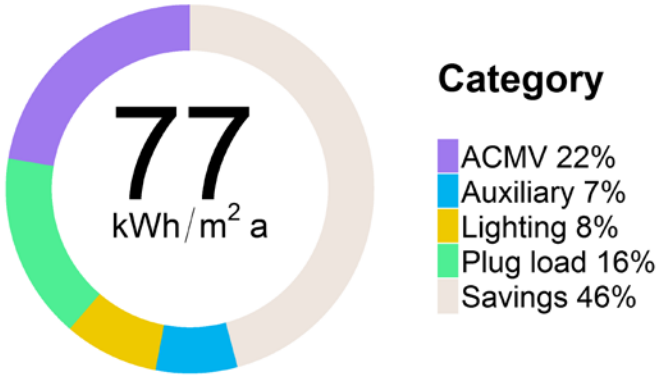

Figure 27: Annual EUI and end-use percentage for model with combined technologies. The technologies include increased setpoint temperatures, occupant localization systems, and efficient lighting systems with daylighting controls. The simulated results are compared to benchmark-A1.

The combined technologies have reduced cooling loads by 53% from the adjusted baseline. Figure 28 shows the new cooling loads as a result from the implemented technologies. Windows are the most significant cooling load source in the building model. Part of the cooling load due to conduction has been reduced for the same reasons mentioned in Section 5.3. Plug loads are ranked in second and ventilation in third. Figure 29 shows how these new cooling loads have impacted the ACMV system energy consumption on a component basis. It is interesting to see that chillers' energy consumption has decreased significantly that the energy consumption is now comparable to fans' energy consumption. Table 19 shows the effective loads in this model compared to the benchmark; the applied technologies have an effect in every category.

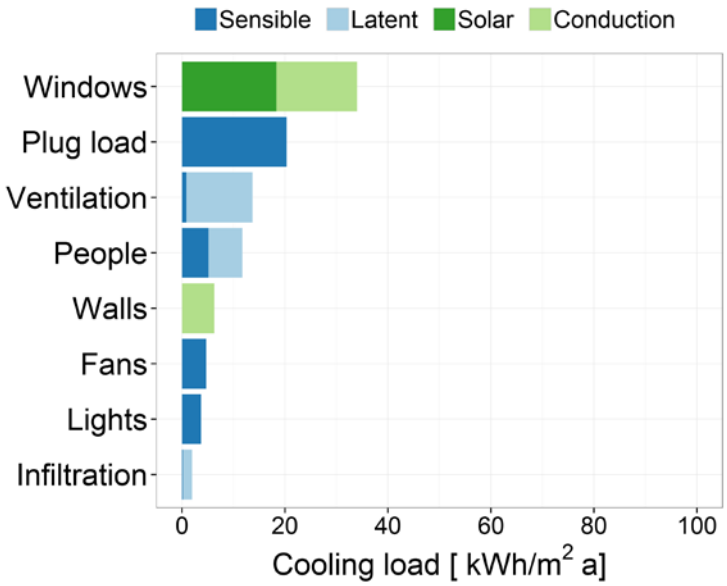

Figure 28: Total cooling load rate breakdown by type for occupied hours with combined technologies.

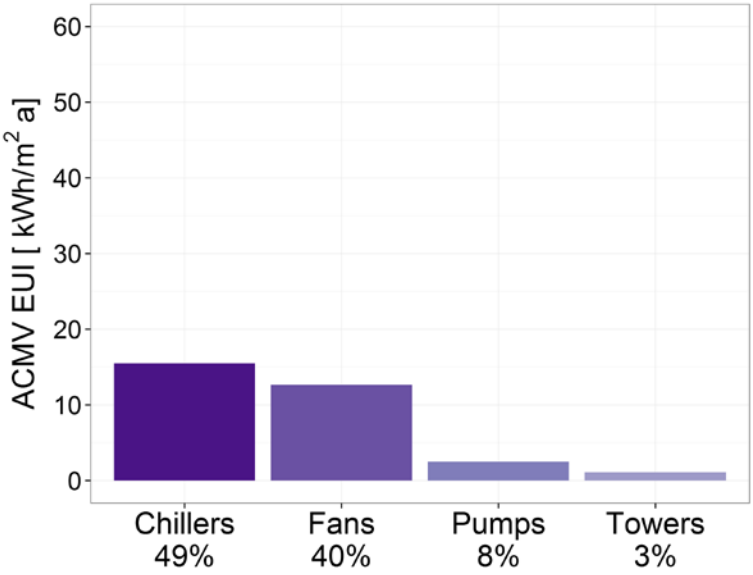

Figure 29: Energy consumption of individual components in the ACMV system with combined technologies.

Table 19: Effective loads in office floors for different day types and timeframes with combined technologies.

Internal loads	Weekday occupied	Weekday unoccupied	Weekend occupied	Weekend unoccupied
Lights [W/m^2]	1.2	0.2	1.1	0.4
Plug load [W/m^2]	6.7	0.5	5.7	0.6
Occupancy density [m^2/person]	32.8	0	49.3	0
Ventilation [l/s·person]	6.4	0	8.4	0

5.6 Benchmark-B model

We changed the benchmark-A exterior envelope to a concrete wall to derive benchmark-B as described in Section 2.7. We kept the same ETTV value as in benchmark-A by reducing the WWR to 35%. However, all other parameters remained the same. We expected to make some minor modifications to ACMV component sizing but it was not required. The ETTV showed to be an effective simplified metric to compare two different construction assemblies' building envelope cooling loads in the Singaporean climate. The ETTV equation shows an appropriate relationship between conduction and solar loads in a hot and humid climate. The total envelope cooling loads for both assemblies were very similar. The biggest difference is in the amount of each type. That is, window cooling loads decreased by 46% while wall cooling loads increased by 220% in benchmark-B. Benchmark-A's cooling loads through the envelope are 18 kWh/m^2·a for solar and 29 kWh/m^2·a for conduction. In the case of benchmark-B, solar cooling load is 9 kWh/m^2·a and 35 kWh/m^2·a for conduction. These results are reasonable since there is a higher U-value in benchmark-B and less window area for solar loads to enter through glazing. Furthermore, the small difference between the overall envelope cooling loads is due to the higher heat capacity of concrete walls. The concrete stores more energy, some of which will be transferred the indoor and outdoor environment during hours when the ACMV equipment is off. This is particularly the case for West facing zones. Figure 30 shows the cooling loads for benchmark-B and Figure 31 shows the annual energy consumption for the same benchmark.

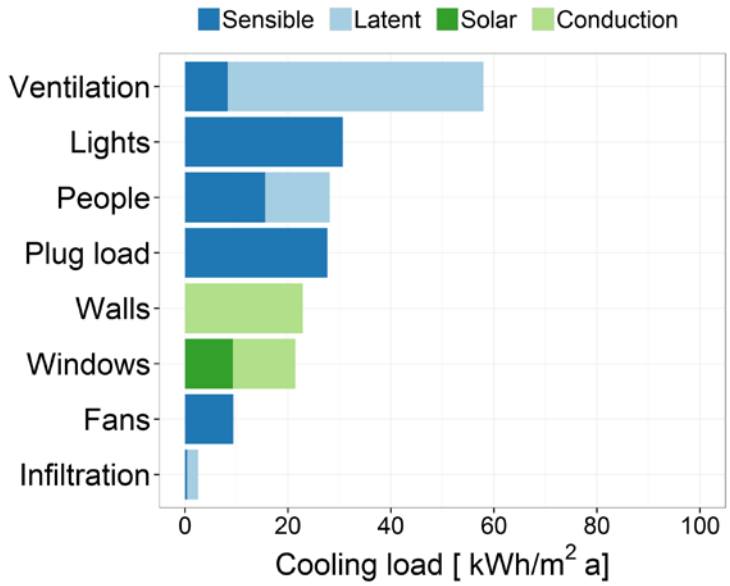

Figure 30: Cooling load breakdown by type for occupied hours in benchmark-B model.

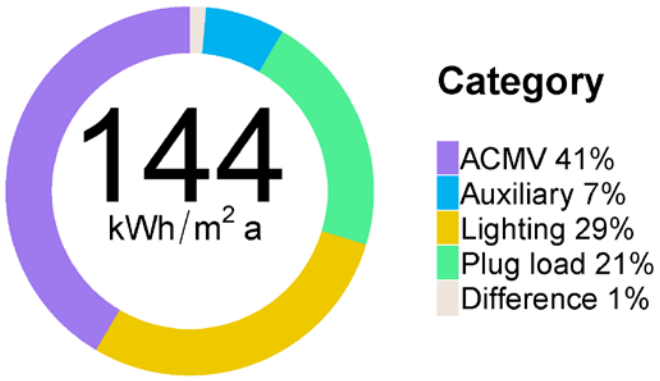

Figure 31: Annual EUI for benchmark-B and difference between benchmark-A.

For the reasons mentioned above, the sizing of ACMV components did not have to change. Figure *32* shows that energy consumption for the ACMV in benchmark-B. There is relatively little difference between Figure *32* and Figure 10 above.

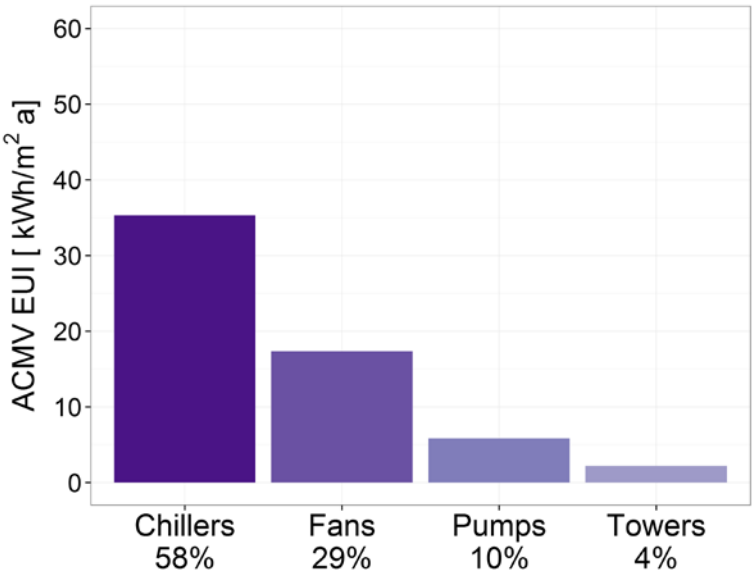

Figure *32*: Energy consumption of individual components in the ACMV system for benchmark-B model.

5.7 Titanium dioxide coating

TiO_2 coatings will reduce cooling loads through the envelope by reflecting solar heat from the exterior surfaces. Figure 33 shows the overall savings potential of having a TiO_2 coating on the concrete surface of benchmark-B. Due to rounding, the savings potential shows to be 0%. The absolute savings potential however is 12.6 MWh/a. The energy savings number is low due to a couple reasons. Firstly, the solar reflectance values as reported by SinBerBEST researchers were 0.45 and 0.54 for conventional concrete with and without the coating, respectively. This is only a 0.09 difference and according to the simulations, it does not have a significant effect on the overall energy consumption. It is important to note that these values represent concrete surfaces that have not been soiled through pollutants that buildings are exposed to. Additionally, depending on a range of conditions, solar reflectance for TiO_2 coated concrete can range as high as 0.8 based on laboratory results from SinBerBEST researchers. Thus, we performed a local sensitivity analysis on overall energy consumption and cooling loads through the envelope for the solar reflectance parameter and present the results in Figure 34. This shows that overall energy consumption changes through a range of about 4% for the various solar reflectance values occurs. The sensitivity increases when just looking at the cooling load through the envelope, where the range is about 76% of the cooling load conducted through the envelope.

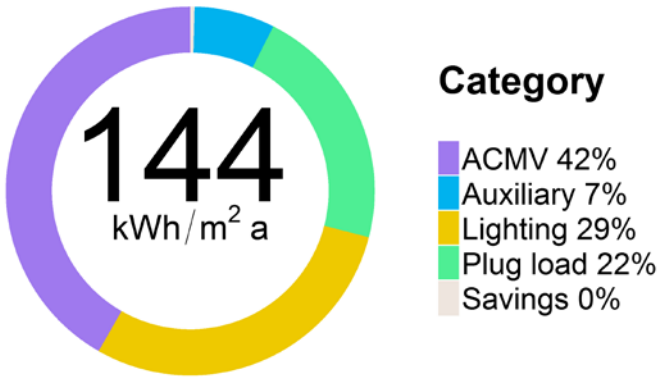

Figure 33: Annual EUI for titanium dioxide coating on conventional concrete. The simulated results are compared to benchmark-B.

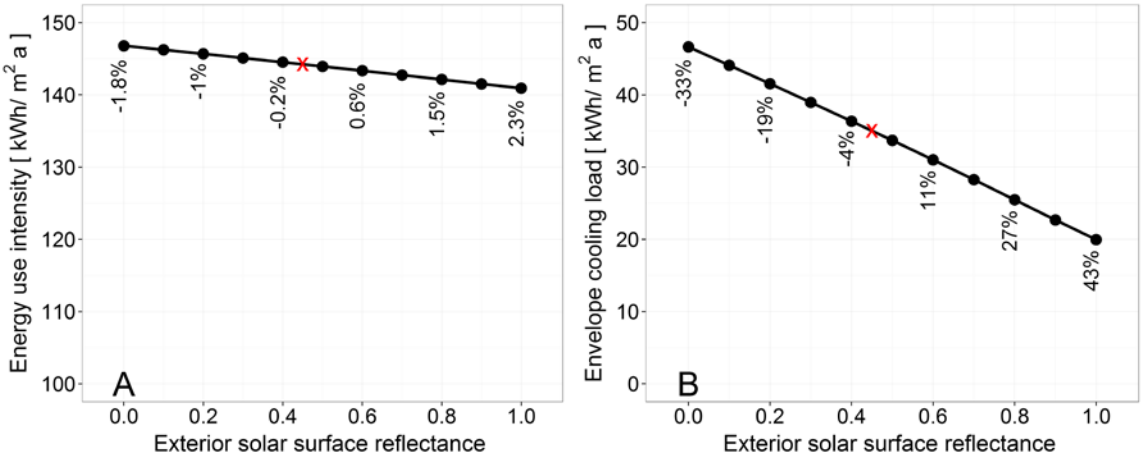

Figure 34: Overall energy consumption (A) and envelope cooling load (B) sensitivity of solar reflectance on conventional concrete exterior surfaces. The different solar reflectances represent different conditions of soiled surfaces. The red 'x' represents the values for benchmark-B.

The second reason why the energy saving potential is low is because the cooling load through the envelope is a small fraction of the total. The cooling load through opaque exterior walls is only 23 kWh/m^2·a, which represents 11% of the total, and the reduction due to the coating is 2.5 kWh/m^2·a. The cooling load through the wall is not a significant value compared to other cooling load sources for this benchmark model, and thus any reduction becomes less significant when evaluated at the whole building level (Note: the cooling load is only a part of the total energy use). This is also true for other technologies that attempt to reduce envelope cooling loads. Figure 34 shows that the envelope cooling loads is more sensitive to solar reflectance than overall energy consumption. The envelope cooling load might become significant when other cooling load sources have been managed. Meanwhile, other non-

energy benefits should be taken into account to find proper applications for this technology. Other benefits might include reduced maintain costs from cleaning an exterior façade and degrading organic and inorganic pollutant in the atmosphere.

5.8 Ultra-lightweight cement composite exterior wall

The next technology implemented in benchmark-B is ULCC exterior wall, which has a lower thermal conductivity than conventional concrete. This technology also has the potential to reduce cooling loads through walls. Figure 35 shows that, as in the case of TiO_2 coating, there is a minimal overall energy savings. We observe 0% savings potential because of rounding, thus annual energy consumption breakdown for this building model is essentially the same as in Figure 33 above. The absolute savings potential is 14.7 MWh/a which represents a 29% reduction in exterior wall cooling loads. Figure 35 shows the wall conduction cooling load comparison to benchmark-B and ULCC. In this benchmark, the exterior wall conduction will not have a significant effect on overall energy consumption but managing other cooling load sources could increase its significance. It is interesting to note that the ULCC has a lower density than conventional concrete. While this has potential structural benefits, it means that the enevelope has a lower heat capacity. The exterior wall will store less heat, and thus will release more heat when the ACMV system is operating. This effect is only noticeable for West facing zones due to the length of time between peak load conditions and the time at which the ACMV equipment switches off.

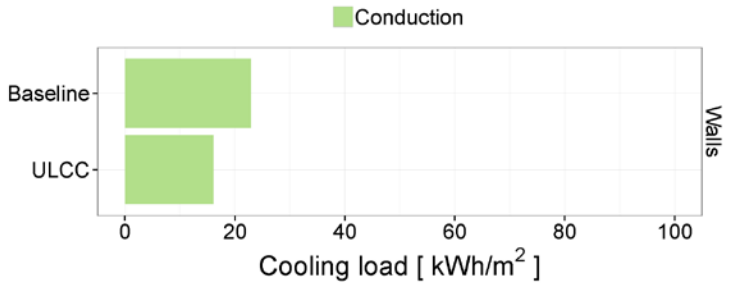

Figure 35: Comparison of exterior wall cooling load between benchmark-B and ULCC. The ULCC reduces the cooling load conducted through the exterior wall by 29%.

Combining ULCC exterior walls with TiO_2 coating also does not have a significant effect on overall energy savings potential. The combined technologies increase overall savings potential to 1%.

5.9 Translucent concrete panels

Figure 36 shows the overall energy savings potential of TC panels for three different WWR scenarios: 0%, 10% and 35%. It is important to note that the TC panels only affect zones that have an exterior wall, and thus the overall EUI results depend on the floor plan of the modeled building. Savings would increase for buildings that have a higher fraction of perimeter zone floor area (i.e. within 5 m of the exterior). Other work has assessed the isolated effect of TC panels on lighting and ACMV energy consumption within a single zone model without windows (A. Ahuja, Mosalam, and Zohdi 2015). We compared each scenario against its own respective baseline where we first implemented daylighting controls with different WWR on the envelope. As a result, Figure 37 shows the energy savings potential of implementing daylighting controls for different WWRs. As expected, overall and lighting savings potential decrease as window area decreases. The decrease in the overall energy consumption is from

the sum of the ACMV system and lighting system. The savings potential from daylighting controls alone on benchmark-B can be up to 21% as indicated by the results.

In Figure 36, we observe that as the surface area concentration of optic fibers increases, the potential savings also increase. These upward trends are a result of neglecting solar cooling loads through optic fibers. SinBerBEST researchers on this technology indicated that an optimal concentration of optic fibers exists. Beyond this optimal point, energy savings potential start to decrease because the extra solar cooling loads sets an energy penalty on the ACMV system. It is difficult to specify where the optimal point for this particular model is but in the SinBerBEST researchers' model the optimal concentration was at about 6%.

Figure 36 (C) shows the additional lighting savings potential when incorporating TC panels into the envelope design. If there is no windows in the building then results from the simulation show a 10% savings from overall lighting energy at the higher optic fiber surface concentration. As expected, the effects of TC panels decreases as window area increases. Figure 36 (C) shows savings results from using overall interior lighting in the calculation in dashed lines and only using perimeter lighting energy in solid lines. The perimeter lighting savings are larger because it only takes into account zones that are directly affected by the use of TC panels. If all the lighting can be provided by TC panels, then a theoretical maximum of 33% potential savings in overall lighting energy is shown from the simulation results. The theoretical maximum savings increases to about 90% when taking into account lighting only in perimeter zones since the only lighting use occurs for safety during unoccupied hours. We calculated this percentage value by assuming that TC panels provide all lighting needs during all occupied times in a perimeter zone with no windows (0% WWR). As in the previously described scenarios, the theoretical maximum does not take into account solar heat gains through the optic fibers. The management of solar loads will allow higher surface area concentration of optic fibers and achieve the higher lighting savings potential without adversely affecting the ACMV system.

Figure 36 shows results from using TC panels without including savings that occur from daylighting provided by windows. Therefore we included Figure 37 to show the lighting savings potential when we implement daylighting controls into benchmark-B0, B10, and B35. These results served as the baselines to calculate the additional savings for TC panels shown in Figure 36. In this case, the energy savings increased as WWR increased.

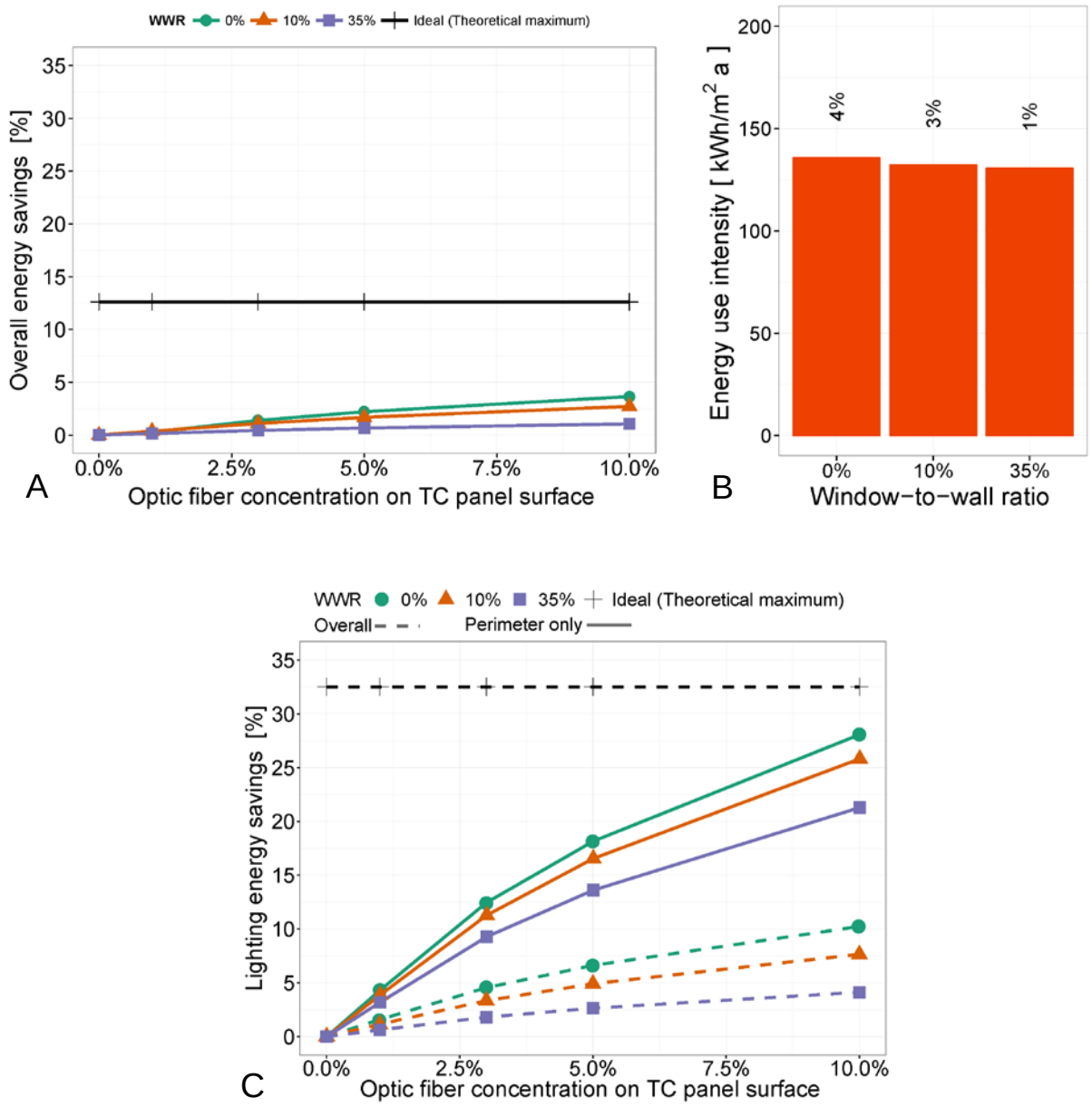

Figure 36: (A) Overall energy savings potential for three different WWR and five optic fiber surface area concentrations. The simulated results are compared to benchmark-B0, B10, and B35 for WWRs of 0%, 10%, and 35%, respectively. (B) Energy use intensity for an optic fiber concentration of 10% for 0%, 10%, and 35% WWRs. (C) Additional lighting energy savings potential by adding TC panels to exterior walls for three different WWR and five optic fiber surface area concentrations. Dashed lines show savings calculation using all interior lighting energy in building model whereas solid lines show lighting savings calculations only using perimeter zone lighting energy.

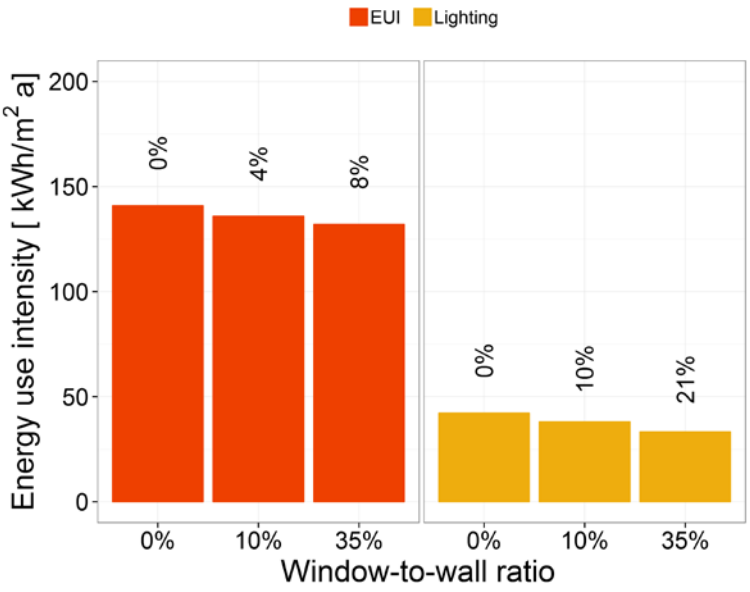

Figure 37: Overall EUI and annual lighting energy consumption and savings potential for different envelope WWR with daylighting controls. These results do not include savings potential from TC panels. The simulated results are compared to benchmark-B0, B10, and B35 for WWRs of 0%, 10%, and 35%, respectively.

5.10 Insulation

Insulation is not a SinBerBEST technology or a new technology but we wanted to show the effects of insulation. We decide to perform this simulation since we found a survey of Singapore buildings with insulation in exterior walls rarely used. We used benchmark-B to implement a 50 mm rigid insulation into the wall construction. Figure 38 shows a 1% overall energy savings potential and it comes from energy savings from the ACMV. Cooling loads through the opaque exterior walls are reduced by 20%. Figure 39 shows the comparison of this cooling load between benchmark-B and add insulation into the walls. Results show that depending on the severity of the soiled condition of the exterior walls of a building, insulation can be comparable to TiO_2 coating on the envelope. Which makes TiO_2 a more feasible option to obtain the same results as insulation in existing buildings. Insulation is harder to install once the building is built and occupied while a coating can be applied relatively easier without out interrupting the normal operation of tenants.

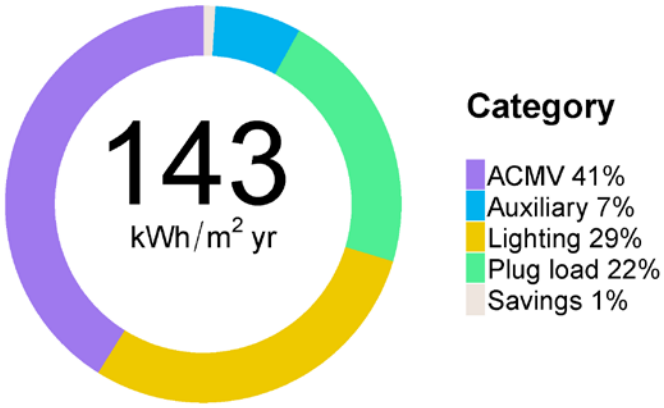

Figure 38: Annual EUI for 50 mm rigid insulation integrated into the exterior wall construction.

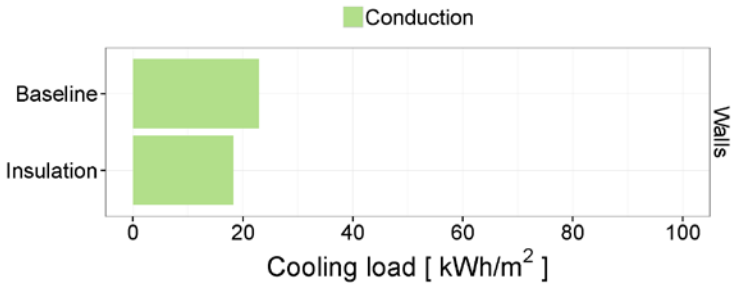

Figure 39: Comparison of exterior wall cooling load between benchmark-B and the addition of insulation. Exterior wall cooling load is reduced by 20%.

6 New energy savings solutions

Other potential energy savings solutions that we have not evaluated in this report but that arose during the model development process are supply temperature resets, humidistats, duct static pressure resets, fenestration design performance, and exterior shading. These additional solutions have the potential to further reduce direct energy consumption and sensible and latent cooling loads.

Accurate zone level humidity measurement could allow the AHU to use a supply temperature reset strategy instead of a fixed setpoint approach, which could save energy while maintaining zones at, or just below, the maximum allowable relative humidity.

We found through the development of this benchmark that controls common in the US building stock are not common for the Singaporean stock. Opportunities can occur by looking at duct static pressure resets and lowering the minimum variable frequency drive on fans, which have the potential to reduce fan energy. These control strategies and other are possible due to digital energy management systems in buildings that have become common equipment installed in modern buildings. Researchers need to take full advantage of these systems to develop clever algorithms and energy models are a platform for such investigations. This will aid decision making as to which combination of technologies and strategies will yield the greatest impact while also assessing other components of design such as indoor air quality and cost-effectiveness criteria.

Integrated energy efficient fenestration systems can aid with the reduction in cooling loads since they are the second highest cooling load in the benchmark model. Researching fenestration properties with the appropriate shading device based on orientation is worthwhile to investigate since facades on the East and West receive more direct solar radiation during sunrise and sunset, respectively. During other times, shading devices can effectively block solar radiation since the sun has a high altitude in Singapore with little variation throughout the year. Exterior shading devices can block solar radiation before it enters the building. Moreover, it prevents opaque surfaces from becoming hotter decreasing heat transfer through conduction to the interior. This integrated approach may maximize daylight availability and views to the outside, reduce glare issues, increase thermal comfort, and maintain cost effectiveness of fenestration systems.

7 Conclusion

We have created a whole building energy model to represent a typical large commercial office building in Singapore which meets Green Mark Certified Level version 4.0 energy requirements. We followed an iterative process to ensure that assumptions were reasonable for the context of a building in Singapore, and all model input values were approved by Building Construction Authority and Beca. Nevertheless, we could improve these assumptions with more detailed information about the built environment in Singapore. For example, plug loads can vary depending on the occupancy density of the building and we found very little information regarding its value for a commercial office building in Singapore. Thus, it is important to note that this is one feasible reference building created from the best available information and expertise at the time of development; however, there are many other feasible models that could be used as a benchmark.

The models allowed us to look at results pertaining to energy consumption in detail that is otherwise difficult to obtain from direct building measurements. The energy use intensity (EUI) is 146 kWh/m^2·a. Breaking down the EUI results in the air conditioning and mechanical ventilation (ACMV) system contributing 43% of the total annual electricity consumption followed by lights and plug loads at 29% and 21%, respectively. We obtained results that showed dehumidification, an energy intensive process, is the most significant source of cooling loads for the building with 29% of the total cooling loads, windows contributing 20%, and lights, people, and plug loads contributing 15% each to the total cooling loads. We show that increases in cooling setpoint and occupant localization systems are two strategies that will help mitigate ventilation cooling loads. In addition, increasing cooling setpoints is a readily available, low cost solution. It only requires alterations in the thermostat and/or building ACMV control systems along with a method to increase air movement such as using ceiling or personal fans. Efficient lighting systems integrated with daylight controls can have a significant impact in the direct energy consumption of the building. Our analysis showed that 22% of the total energy could be reduced. Plug loads can also have a significant impact by shutting down equipment when not in use.

The detailed results also showed that fenestration systems are a component that researchers should focus on. Windows provide daylighting that can help reduce electric lighting in buildings but can also introduce a major percentage of cooling loads into a fully glazed facade building in the tropics. As the efficiency of electric lighting systems increases, the value of daylighting decreases from a purely energy perspective. However, views to the outside have many other benefits to occupants that we should not underestimate. The correct balance between window-to-wall ratio, shading, and glass types for different orientations of the building will help lower cooling loads and still provide daylighting and views to the outside. Translucent concrete panels provide another source of daylighting but the effect on lighting energy is small, and diminished by higher window-to-wall ratio. TC panels would be ideal for rooms that are on the perimeter but where views to the outside are not important or possible (e.g. stairs, auditoriums). The efficiency of TC panels could improve by increasing the surface area concentration of optic fibers but solar loads through them must be managed in order to avoid taxing the cooling system.

Improving the thermal performance of opaque walls through the use titanium dioxide coating, ultra-lightweight cement composite, and insulation has a relatively little impact on energy savings because the total cooling loads through the opaque exterior were a small component of overall energy consumption to begin with. Insulation in wall construction was no exception. It had little impact on the overall energy consumption of the building. Depending on the soiled severity of the exterior surface of the envelope, insulation was comparable to TiO_2 coatings in the Singaporean climate, which also might

be easier to apply in existing buildings. In new buildings, insulation can be restricted to East and West facades since these two sides receive the highest solar radiation in Singapore.

We found through the development of this benchmark that controls common in the US building stock do not appear to be common for the Singaporean stock. For example, AHU duct static pressure set-point reset based on zone requests.

Furthermore, the process of deriving benchmark-B showed that ETTV can be an effective simplified metric to compare the heat flow through the envelope with different wall construction assemblies in a hot and humid climate. The all glass façade benchmark (benchmark-A) showed almost the same total envelope cooling loads as in the concrete façade benchmark (benchmark-B). The distribution of conduction versus solar changed but the discrepancy between the totals was because of thermal mass differences.

Finally, the building energy model allows us to assess the combined effect of three SinBerBEST technologies. We combined improved lighting and controls, increased temperature setpoints, and indoor occupant localization system to obtain the result. We saw a total energy potential savings up to 46% from the adjusted baseline model for a retrofit application. Improved lighting and controls and increased temperature setpoints are two technologies that are relative simple to implement into existing building and they are market ready. They come at different implementation costs (increased temperature setpoints can be less expensive than improved lighting and controls). In the case of indoor localization systems, the technology is still in the research phase.

Building stakeholders can perform similar simulation exercises with this freely available energy model, representing a typical large commercial office-building model in Singapore, to test innovative solutions.

8 Acknowledgements

The authors wish to thank the many contributors at both BCA and Beca who assisted in the development of the benchmark building. We would also like to that the SinBerBEST researchers for contributing valuable information about the individual technologies discussed in this report. This research was funded by the Republic of Singapore's National Research Foundation through a grant to the Berkeley Education Alliance for Research in Singapore (BEARS) for the Singapore-Berkeley Building Efficiency and Sustainability in the Tropics (SinBerBEST) Program. BEARS has been established by the University of California, Berkeley as a center for intellectual excellence in research and education in Singapore.

9 References

Ahuja, Aashish, Nuria Casquero-Modrego, and Khalid Mosalam. 2015. “Evaluation of Translucent Concrete Using ETTV-Based Approach.” In *ICBEST 2015*. Singapore: IEEE.

Ahuja, A., K. Mosalam, and T. Zohdi. 2014. “Computational Modeling of Translucent Concrete Panels.” *Journal of Architectural Engineering* 21 (2): B4014008. doi:10.1061/(ASCE)AE.1943-5568.0000167.

———. 2015. “Simulation of Innovative Solutions for Energy Efficient Building Facades.” UCB/SEMM-2015/05. Berkeley, CA: University of California, Berkeley.

ASHRAE. 1989. “ASHRAE/IES Standard 90.1-1989: Energy Efficient Design of New Buildings except Low-Rise Residential Buildings.” Atlanta, Georgia: American Society of Heating, Refrigerating and Air-Conditioning Engineers, Inc.

———. 2013a. *2013 ASHRAE Handbook: Fundamentals*. Atlanta, Georgia: ASHRAE.

———. 2013b. “ASHRAE Standard 90.1: Energy Standard for Buildings except Low-Rise Residential Buildings.” Atlanta, Georgia: American Society of Heating, Refrigerating and Air-Conditioning Engineers, Inc.

Basarkar, Mangesh, Xiufeng Pang, Liping Wang, Philip Haves, and Tianzhen Hong. 2011. “Modeling and Simulation of HVAC Faults in EnergyPlus.” In *Proceedings of Build Simulation 2011*. Sydney Australia.

BCA. 2010a. “BCA Green Mark: Certification Standard for New Buildings Version 4.0.” Building and Construction Authority. http://www.bca.gov.sg/EnvSusLegislation/others/GM_Certification_Std2010.pdf.

———. 2010b. “Circular to Professional Institutes/associations: Revised BCA Green Mark Criteria for New Buildings Version 4.0.” Building and Construction Authority. http://www.sisv.org.sg/Hottopic/e-news/Circular_GM%20Version_31%20Aug%202010%20with%20Annexes-1.pdf.

———. 2014. “BCA Building Energy Benchmarking Report 2014.” Singapore: Building and Construction Authority.

———. n.d. “Code on Envelope Thermal Performance for Buildings.” Building and Construction Authority.

———. n.d. “Energy Efficiency Index.” Building and Construction Authority. https://www.bca.gov.sg/GreenMark/others/appb.pdf.

BREEAM. 2014. “Building Research Establishment Environmental Assessment Methodology.” BRE Global Ltd. http://www.breeam.com/index.jsp.

Chen, Zhenghua, Han Zou, Hao Jiang, Qingchang Zhu, Yeng Soh, and Lihua Xie. 2015. “Fusion of WiFi, Smartphone Sensors and Landmarks Using the Kalman Filter for Indoor Localization.” *Sensors* 15 (1): 715–32. doi:10.3390/s150100715.

Chien, Szu-cheng, and King Jet Tseng. 2014. “Assessment of Climate-Based Daylight Performance in Tropical Office Buildings: A Case Study.” *International Journal of Low-Carbon Technologies*, March, ctu014. doi:10.1093/ijlct/ctu014.

Chong Zhun Min Adrian. 2012. “Evaluating the Envelope Performance of Commercial Office Buildings in Cities.” Master of Science, Singapore: National University of Singapore.

Crawley, Drury B., Jon W. Hand, Michaël Kummert, and Brent T. Griffith. 2008. “Contrasting the Capabilities of Building Energy Performance Simulation Programs.” *Building and Environment*, Part Special: Building Performance Simulation, 43 (4): 661–73. doi:10.1016/j.buildenv.2006.10.027.

DOE. 2012. “Commercial Prototype Building Models.” Department of Energy. http://www.energycodes.gov/development/commercial/90.1_models.

Edwards, L., and P. Torcellini. 2002. “A Literature Review of the Effects of Natural Light on Building Occupants.” NREL/TP-550-30769. Golden, CO: National Renewable Energy Laboratory.

EMA. 2015. “Singapore Energy Statistics 2015.” 2251-2624. Energy Market Authority. https://www.ema.gov.sg/cmsmedia/Publications_and_Statistics/Publications/SES2015_Final_website_2mb.pdf.

European Parliament. n.d. *Directive 2010/31/EU of the European Parliment and of the Council of 19 May 2010 on the Energy Performance of Buildings*. *2010/31/EU*. http://eur-lex.europa.eu/legal-content/EN/TXT/PDF/?uri=CELEX:32010L0031&from=EN.

Folli, Andrea, Isabelle Pochard, André Nonat, Ulla H. Jakobsen, Ashley M. Shepherd, and Donald E. Macphee. 2010. “Engineering Photocatalytic Cements: Understanding TiO2 Surface Chemistry to Control and Modulate Photocatalytic Performances: Engineering Photocatalytic Cements.” *Journal of the American Ceramic Society* 93 (10): 3360–69. doi:10.1111/j.1551-2916.2010.03838.x.

Halvarsson, Johan. 2012. “Occupancy Pattern in Office Buildings: Consequences for HVAC System Design and Operation.” Doctoral thesis, Trondheim: Norwegian University of Science and Technology. http://brage.bibsys.no/xmlui/bitstream/handle/11250/234598/524731_FULLTEXT01.pdf?sequence=1.

IMCSD. 2015. “Sustainable Singapore Blueprint 2015.” Ministry of the Environment and Water Resources. http://www.mewr.gov.sg/ssb/files/ssb2015.pdf.

“Input Output Reference: The Encyclopedic Reference to EnergyPlus Input and Output.” 2014. Ernest Orlando Lawrence Berkeley National Laboratory. http://apps1.eere.energy.gov/buildings/energyplus/pdfs/inputoutputreference.pdf.

Jin, Ming, Ruoxi Jin, Zhaoyi Kang, Ioannis C. Konstantakopoulos, and Costas J. Spanos. 2014. “PresenceSense: Zero-Training Algorithm for Individual Presence Detection Based on Power Monitoring.” *Buildsys Conference ’14*, November. http://escholarship.org/uc/item/4df8x2kq.

Jin, Ming, Han Zou, Kevin Weekly, Ruoxi Jia, Alexandre Bayen, and Costas J. Spanos. 2014. “Environmental Sensing by Wearable Device for Indoor Activity and Location Estimation.” *eScholarship*, December. http://escholarship.org/uc/item/75j9n849.

Krishnan, Padmaja, Min-Hong Zhang, Yuhan Cheng, Dipo Tamliang Riang, and Liya E. Yu. 2013. “Photocatalytic Degradation of SO2 Using TiO2-Containing Silicate as a Building Coating Material.” *Construction and Building Materials* 43 (June): 197–202. doi:10.1016/j.conbuildmat.2013.02.012.

Krishnan, Padmaja, Min-Hong Zhang, Liya Yu, and Huajun Feng. 2013. “Photocatalytic Degradation of Particulate Pollutants and Self-Cleaning Performance of TiO2-Containing Silicate Coating and Mortar.” *Construction and Building Materials* 44 (July): 309–16. doi:10.1016/j.conbuildmat.2013.03.009.

Maury, A., and Nele De Belie. 2010. “State of the Art of TiO 2 Containing Cementitious Materials: Self-Cleaning Properties.” *Materiales de Construcción* 60 (298): 33–50.

Pérez-Lombard, Luis, José Ortiz, and Christine Pout. 2008. “A Review on Buildings Energy Consumption Information.” *Energy and Buildings* 40 (3): 394–98. doi:10.1016/j.enbuild.2007.03.007.

Python 2.7.10 (version 2.7.10). 2015. Python Software Foundation. https://docs.python.org/2.7/#.

Raftery, Paul, Edwin Lee, Tom Webster, Tyler Hoyt, and Fred Bauman. 2014. “Effects of Furniture and Contents on Peak Cooling Load.” *Energy and Buildings* 85 (December): 445–57. doi:10.1016/j.enbuild.2014.09.081.

Rim, Donghyun, Stefano Schiavon, and William W. Nazaroff. 2015. “Energy and Cost Associated with Ventilating Office Buildings in a Tropical Climate.” *PLoS ONE* 10 (3): e0122310. doi:10.1371/journal.pone.0122310.

RStudio (version 0.99.467). 2015. RStudio. https://www.rstudio.com/.

R (version 3.1.2). 2014. The R Foundation. https://www.r-project.org/.
Santosh Philip. 2015. *Eppy* (version 0.4.6.4a). https://pypi.python.org/pypi/eppy/0.4.0.
Schiavon, Stefano, and Arsen K. Melikov. 2008. "Energy Saving and Improved Comfort by Increased Air Movement." *Energy and Buildings* 40 (10): 1954–60. doi:10.1016/j.enbuild.2008.05.001.
Schiavon, Stefano, Bin Yang, Victor W.-C Chang, and William W. Nazaroff. 2015. "Effect of Air Temperature and Personally Controlled Air Movement on Thermal Comfort for Tropically Acclimatized Persons." In *9th International Symposium On Heating, Ventilation And Air Conditioning (ISHVAC) And 3rd Conference On Building Energy And Environment (COBEE)*. Tianjin, China.
Shuo, Liu, Yin Le, Ho Weng Khuen, and Ling Keck Voon. 2015. "Improved Indoor Tracking Based on Generalized T-Distribution Noise Model." *eScholarship*, February. http://escholarship.org/uc/item/6d0837gz.
SPRING Singapore. 2006a. "Singapore Standard SS 530:2006: Code of Practice for Energy Efficiency Standard for Building Services and Equipment." Building and Construction Standards Committe.
———. 2006b. "Singapore Standard SS 531:2006 Part 1 Code of Practice for Lighting of Work Places." Building and Construction Standards Committe.
———. 2009a. "Singapore Standard SS 553:2009: Code of Practice for Air-Conditioning and Mechanical Ventilation in Buildings." Building and Construction Standards Committe.
———. 2009b. "Singapore Standard SS 554:2009: Code of Practice for Indoor Air Quality for Air-Conditioned Buildings." Building and Construction Standards Committe.
Stein, Jeff, Anna Zhou, and Hwakong Cheng. 2007. "Advance Variable Air Volume System Design Guide." Energy Design Resources. http://www.taylor-engineering.com/downloads/guides/EDR_VAV_Guide_5-2-07.pdf.
Thornton, B.A., M.I. Rosenberg, E.E. Richman, W. Wang, Y. Xie, J. Zhang, H. Cho, V.V. Mendon, R.A. Athalye, and B. Liu. 2011. "Achieving the 30% Goal: Energy and Cost Savings Analysis of ASHRAE Standard 90.1-2010." PNNL-20405. Richland, Washington: Pacific Northwest National Laboratory.
"Title 24-California Code of Regulations, Part 6: Building Energy Efficiency Standards for Residential and Nonresidential Buildings." 2012. California Energy Commision. http://www.energy.ca.gov/2012publications/CEC-400-2012-004/CEC-400-2012-004-CMF-REV2.pdf.
UNEP. 2007. "Buildings and Climate Change: Status, Challenges, and Opportunities." DTI/0916/PA. United Nations Environment Programme.
U.S. Green Building Council. 2010. "Advanced Energy Modeling For LEED:Technical Manual v1.0."
Wandell, Tracy. 1996. "Cenospheres: From Waste to Profits." *American Ceramic Society Bulletin* 75 (6). http://www.osti.gov/scitech/biblio/256843.
Wang, Liping, and Tianzhen Hong. 2013. "Modeling and Simulation of HVAC Faulty Operations and Performance Degradation due to Maintenance Issues." LBNL-6129E. Berkeley, CA: Lawrence Berkeley National Laboratory.
Wu, Yunpeng, Jun-Yan Wang, Paulo J.M. Monteiro, and Min-Hong Zhang. 2015. "Development of Ultra-Lightweight Cement Composites with Low Thermal Conductivity and High Specific Strength for Energy Efficient Buildings." *Construction and Building Materials* 87 (July): 100–112. doi:10.1016/j.conbuildmat.2015.04.004.
Yang, Bin, Stefano Schiavon, Chandra Sekhar, David Cheong, Kwok Wai Tham, and William W Nazaroff. 2015. "Cooling Efficiency of a Brushless Direct Current Stand Fan." *Building and Environment* 85 (February): 196–204. doi:10.1016/j.buildenv.2014.11.032.
Yu Joe, Huang Fenxian, Donghyun Seo, and Moncef Krarti. 2014. "Development of 3012 IWEC2 Weather Files for International Locations (RP-1477)." *ASHRAE Transactions* 120 (1): 340–55.

Zou, Han, Xiaoxuan Lu, Hao Jiang, and Lihua Xie. 2015. “A Fast and Precise Indoor Localization Algorithm Based on an Online Sequential Extreme Learning Machine.” *Sensors* 15 (1): 1804–24. doi:10.3390/s150101804.

10 Appendix

Energy Modelling Benchmark for Offices in Singapore

Prepared for

Berkeley Education Alliance for Research in Singapore Limited (BEARS)

By

Beca Carter Hollings & Ferner (S.E.Asia) Pte Ltd

July 2015

TABLE OF CONTENTS

Appendices

1 INTRODUCTION

1.1 General Description

Berkeley Education Alliance for Research in Singapore (BEARS) collaborated with Beca and Building Construction Authority (BCA) to develop a whole building energy model benchmark for a typical office building in Singapore. The benchmark model will be used to estimate energy savings potential for new Green Building Technologies that will be developed by SinBerBEST. SinBerBEST consists of an interdisciplinary group of researchers from University of California Berkeley (UCB), Nanyang Technological University (NTU), and the National University of Singapore (NUS) who come together to make an impact with broadly applicable research leading to the innovation of energy efficient and sustainable technologies for buildings located in the tropics, as well as for economic development.

The benchmark building model, developed based on publically available information and Beca's experience in the built environment industry, was a typical mid-size commercial office building located in Singapore meeting Green Mark (NRB) Version 4.0 Certified Level requirements. The benchmark office building is assumed to operate 55-hours per week and is located in the Central Business District (CBD) with no 24-hour operations. The purpose of establishing the benchmark office building was to enable researchers in SinBerBEST to assess energy savings within a standardized framework while giving early feedback to the researchers, thus encouraging focus on technologies with the highest energy saving potential.

A well-established energy modeling software, EnergyPlus (EP) was used by BEARS to input parameters and simulate the building energy consumption, together with OpenStudio which served as a result viewer. Inputs to the model, including building geometry, construction materials, operating schedules and equipment power consumption, were developed, reviewed and agreed by both BEARS and Beca.

1.2 Scope of Service

Beca, together with BCA, provided comments and recommendations on the input parameters to BEARS for the development of the benchmark building, based on past project experiences and Singapore Standards and code requirements. The inputs and outputs of the EP model were reviewed and finalized together with BEARS. This report serves as an overview of Beca's comments and analysis of the inputs and outputs. Beca's scope of works was as follows:

1. Assist in the definition of a benchmark office building for Singapore for the SinBerBEST project.
2. Review inputs to an EnergyPlus model of the benchmark office building. This will include a thorough review of the parameters related to internal loads, schedules, controls, ACMV and chilled water plant system, which are typical in Singapore.
3. Review outputs from an EnergyPlus model of the benchmark office building by BEARS to ensure that these are reasonable for Singapore.
4. Submit a report to describe the outcomes of points 1-3 above.

1.3 Exclusions

Any other works not defined in the job scope are excluded.

2 FINALIZED BUILDING DESCRIPTION

The finalized building description below is based on the discussions between BEARS, Beca and BCA to establish a typical simplified office building construction in Singapore.

The initial design of the façade Window-to-Wall Ratio (WWR) was assumed at 0.7 applied at all facades with standardized glazing SC value of 0.56 and U-value of 5 W/m^{2}K for simplicity. However, based on this proposal, the Envelope Thermal Transmittance Value (ETTV) worked out to be around 70 W/m^2 and did not meet the BCA ETTV limitation of 50 W/m^2 for Green Mark certified buildings. Hence the WWR, SC and U-value were further reviewed. By applying different glazing materials to the East and West facades and reducing the WWR, an ETTV of 49.95 W/m^2 was obtained and the building geometry was developed with this assumption.

2.1 Geometry

General:

- Total of 20 floors with 28,000m^2 floor area, no basement
- Building aspect ratio of 1 (square layout)
- 1st to 3rd storey used for carpark, 4th to 20th storey used for offices

Carpark:

- 1st to 3rd storey: Aboveground naturally ventilated carpark with 1,400m^2 per floor
- 2 zones; outer zone (within 12m of exterior wall opening) and inner zone (core zone > 12m away from exterior wall opening) per floor
- 4m floor-to-floor height

Office:

- 4th to 20th storey with GFA of 1,400m^2 per floor
- Open office layout with 50m^2 toilet and 60m^2 staircase area per floor
- Zoning per floor: 4 perimeters, 1 core, 1 staircase and 1 toilet per floor
- No internal partitions
- 4m floor-to-floor height (1.2m return plenum height)
- Drop ceiling for office and toilet
- Brick walls for staircase and toilet

Façade:

- Overall window to wall ratio (WWR) of 0.59
- North and South façade exterior walls with tinted single glazed windows
- East and West façade exterior walls with clear double glazed windows
- Horizontal projection shading of 0.6m on all sides

2.2 Construction

The following table shows the construction components of the wall, slab, floor and internal mass (which represent the wooden furniture of the office area):

	Outermost material	2nd Material	3rd Material	4th Material
Exterior wall	6mm glass	150mm air gap	3mm aluminum shadow box	75mm semi-rigid insulation
Brick wall at toilet & staircase	100mm covered brick	NA	NA	NA
Drop ceiling at office & toilet	15mm acoustic ceiling tile	NA	NA	NA
Internal mass	150mm wood	NA	NA	NA
Roof	50mm cement sand screed	50mm expanded polystyrene	200mm concrete	NA
Office floor slab	100mm concrete	Carpet	NA	NA
Carpark wall	150mm concrete	NA	NA	NA
Carpark floor	200mm concrete	NA	NA	NA

Table 1: Configurations of Constructions

The glass properties and their respective location of the windows are shown below:

Glass Properties	U-value (W/m^2K)	SHGC	Façade
Tinted single glazed window	5.72	0.467	North and South
Clear double glazed window	2.245	0.222	East and West

Table 2: Glass Properties

2.3 Construction Material Properties

The following tables show the materials specifications assumed in the model, with their respective thermal conductivity/ resistance, density and specific heat capacity. The material thermal conductivity and density values were extracted from BCA's *Code on Envelope Thermal Performance for Buildings*. The specific heat capacity values were provided by BEARS and these figures were found to be reasonable.

Material with Mass	Thermal Conductivity (W/mK)	Density (kg/m^3)	Specific Heat Capacity (J/kgK)
Aluminum shadow box	211	2672	900
Plaster	0.37	1216	1090
Concrete	1.442	2400	832
Acoustic ceiling tile	0.057	288	1339
Wood	0.125	608	1210
Expanded polystyrene	0.035	16	1210
Semi-rigid insulation	0.0335	180	840
Cement sand screed	0.533	1568	991
Glass	1.053	2500	840
Covered brick	0.807	1760	843

Table 3: Construction Material Properties with Mass

Material without Mass	Thermal Resistance (m^2K/W)
100mm air gap	0.16
150mm air gap	0.16
Carpet	0.217

Table 4: Construction Materials Properties without Mass

2.4 Lighting Loads

The following table shows the lighting loads modelled in the building for various spaces:

Lighting Load Type	Power Consumption	Operating Hours
Office lighting	15 W/m^2	Refer to **Chapter 2.7** for the respective schedules
Staircase lighting	6 W/m^2	
Toilet lighting	10 W/m^2	
Carpark lighting	5 W/m^2	
Exterior lighting	5 W/m^2	7pm to 7am daily
Facade lighting	17.85 kW	7pm to 12am daily

Table 5: Lighting Loads

The following assumptions were made for the lighting loads:

1. These lighting loads were baseline values modelled in accordance with *SS530: Code of Practice for Energy efficiency standard for building services and equipment.*
2. For simplicity, the office, staircase, toilet and carpark lightings were modelled as a typical recessed lighting with fraction radiant of 0.37 and fraction visible of 0.18. The lighting fractions radiant and visible values were obtained from *EnergyPlus Input Output Reference* manual, which referenced from *Lighting Handbook by Illuminating Engineering Society of North America.*
3. No daylighting control or occupancy control was modelled.
4. The façade lighting power budget was based on 5% of the interior spaces (Office, carpark, toilet, staircase) total lighting power.
5. The exterior walkway area was assumed to be around 800 m^2.

2.5 Equipment Loads

The following table shows the equipment loads modelled in the building:

Equipment Load Type	Power Consumption
Office equipment/plug	14 W/m^2
Lifts	270 kW
M&E plantroom MV fans	17.52 kW
Miscellaneous pumps	2.93 kW

Table 6: Equipment Loads

The miscellaneous pumps shown in Table 6 above represent the plumbing and sanitary pumps comprising the domestic water transfer and booster pumps, sump pumps and ejector pumps. The table below shows how the average hourly pump power consumption for all the pumps was obtained:

Misc Pump Type	Quantity	Rated Power (kW)	Estimated Operating Hours/Day
Domestic water transfer pump	2	5.5	3
Domestic water booster pump	2	2.2	5
Sump pump	2	2.2	0.5
Ejector pump	2	2.2	3
Average Hourly:	**2.93 kW**		

Table 7: Tabulation of Miscellaneous Pumps

Similarly, the M&E plantroom Mechanical Ventilation (MV) fans were modelled as a fixed load with the parameters shown below:

M&E Plantroom MV Fan	Quantity	Rated Power (kW)	Operating Hours/Day
Transformer room	2	4	18
LV switch room	2	4	18
Chiller plant room	2	4	Refer to **Chapter 2.7** Chiller Plant schedule
Domestic water pump room	2	4	
Average Hourly:	**17.52 kW**		

Table 8: Tabulation of M&E Plantroom MV Fans

The following assumptions were made for the equipment loads:

1. The office plug loads was based on BCA's guideline for energy modelling found in the Green Mark certification standard which stated 16 W/m^2 as a reference. However, 14 W/m^2 was assumed instead, as BEARS felt that normally the actual plug loads will be lower.

2. A total of 6 lifts, rated at 45 kW each, were assumed based the building occupancy loads. These lifts were assumed to have the capacity of 24 persons per lift and rated speed of 4 m/s. The modelled lift energy consumption per day would be based on the lift schedule.

3. Each M&E plantroom was installed with 1 no. supply air fan and 1 no. exhaust air fan.

4. The two mechanical plantroom fans operates on same schedule as the building operating hours, thus it uses the same schedule as the chiller plant for simplicity.

5. The electrical plantroom MV fans were assumed to be temperature controlled and will operate only 75% of the 24-hours operation.

6. Transformer losses were excluded in the energy model as typically the power meters are installed downstream of the transformer, thus not accounting for the transformer losses.

2.6 Mechanical Ventilation Loads

The fresh air ventilation and infiltration loads modelled for the office was based on the following assumptions:

- Fresh air ventilation rate assumed the larger of 5.5 l/s.person or 0.6 l/s.m^2
- Infiltration of 0.2 ACH at perimeter zones

Mechanical ventilation modelled for the carpark was based on the following assumptions:

- Outside zone within 12 m of exterior wall is naturally ventilated
- Core zone is ventilated assuming fume extraction rate of 1.2 ACH
- Both the outside and core zones are provided with ventilation opening equivalent to 15% of floor area
- Carpark fans with pressure rise of 800 Pa and fan efficiency of 65%

Mechanical ventilation modelled for the staircases and toilets was based on the following assumptions:

- Both zones are mechanically ventilated
- Staircase fans of 4 ACH with pressure rise of 600 Pa and fan efficiency of 65%
- Toilet fans of 10 ACH with pressure rise of 800 Pa and fan efficiency of 65%
- Due to the limitations of EP, the designed pressure rise for the middle floor toilet fans was 12 kPa. BEARS explained that EP does not apply the zone multiplier to the exhaust fan power and hence, the pressure rise had to be multiplied by 15 floors manually to achieve the total power consumption. It was noted that this increase in pressure rise will only affect the fan power consumption.

These ventilation rates were modelled in compliance with *SS553: Code of Practice for Air-conditioning and mechanical ventilation in buildings*.

2.7 Schedules

The schedules below define the operating hours for each system/ component based on four different schedules; namely Weekdays (Monday to Friday), Saturdays, Sundays (and holidays) and design days. The holidays were assumed as 11 days of public holidays for Singapore based on 2015. The one-off SG50 holiday on 7 August 2015 was excluded.

Typical office hours are assumed at 8 a.m. to 6 p.m. on weekdays, 8 a.m. to 1 p.m. on Saturdays and closed on Sundays and Public Holidays.

The schedule below was used to define the chiller plant operation. The 50% operation at 8 a.m. represents that the chiller plant starts up at 7.30 a.m.

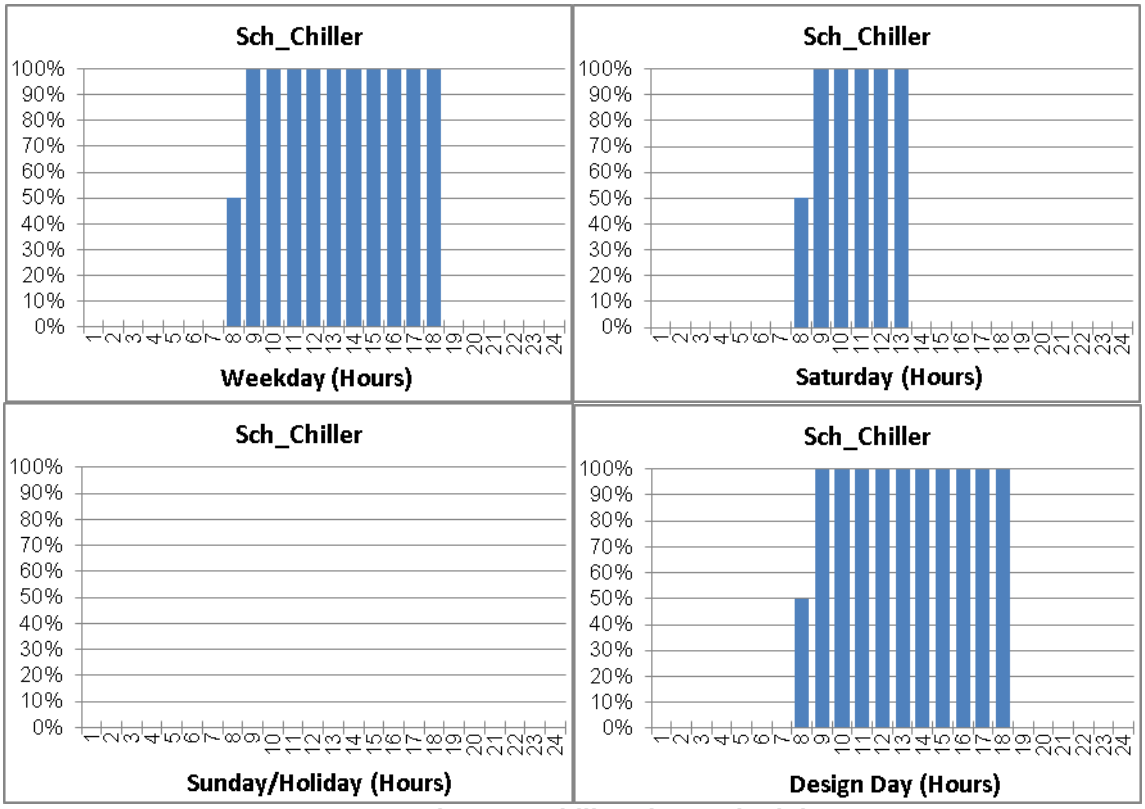

Figure 1: Chiller Plant Schedule

The schedules below were used to define the Air Handling Units (AHUs) operation. The 50% operation at 8 a.m. represents that the AHUs start up at 7.30 a.m.

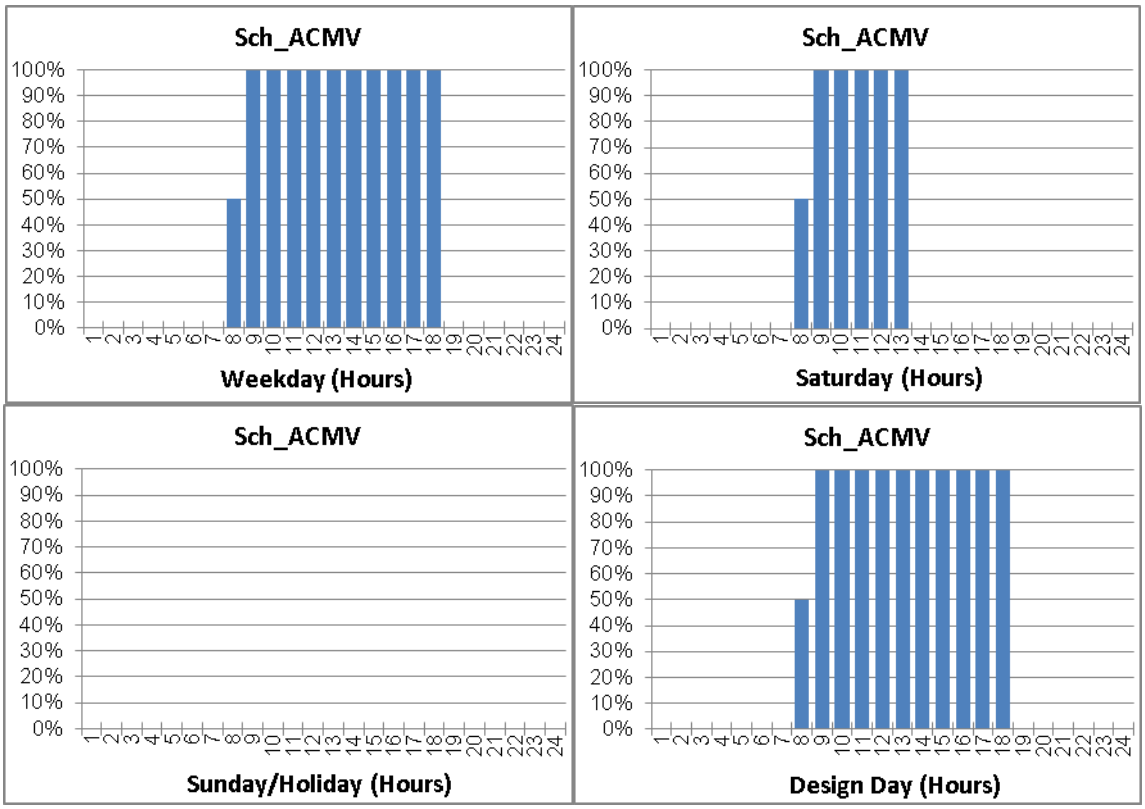

Figure 2: ACMV Schedule

Beca's initial input was for the ACMV schedules chiller plant to be in operation from 7.30 a.m. and 8 a.m. respectively. However, BEARS mentioned that EP was not able to start both systems at a different time. Hence, it was agreed that the starting time to be at 7.30 a.m. for both system schedules.

The schedules below show the occupancy loading in the office zones. The 50% occupancy load at 8 a.m. and at 6 p.m. (weekday) was assumed to account for the smooth transition of the occupants entering and leaving the building.

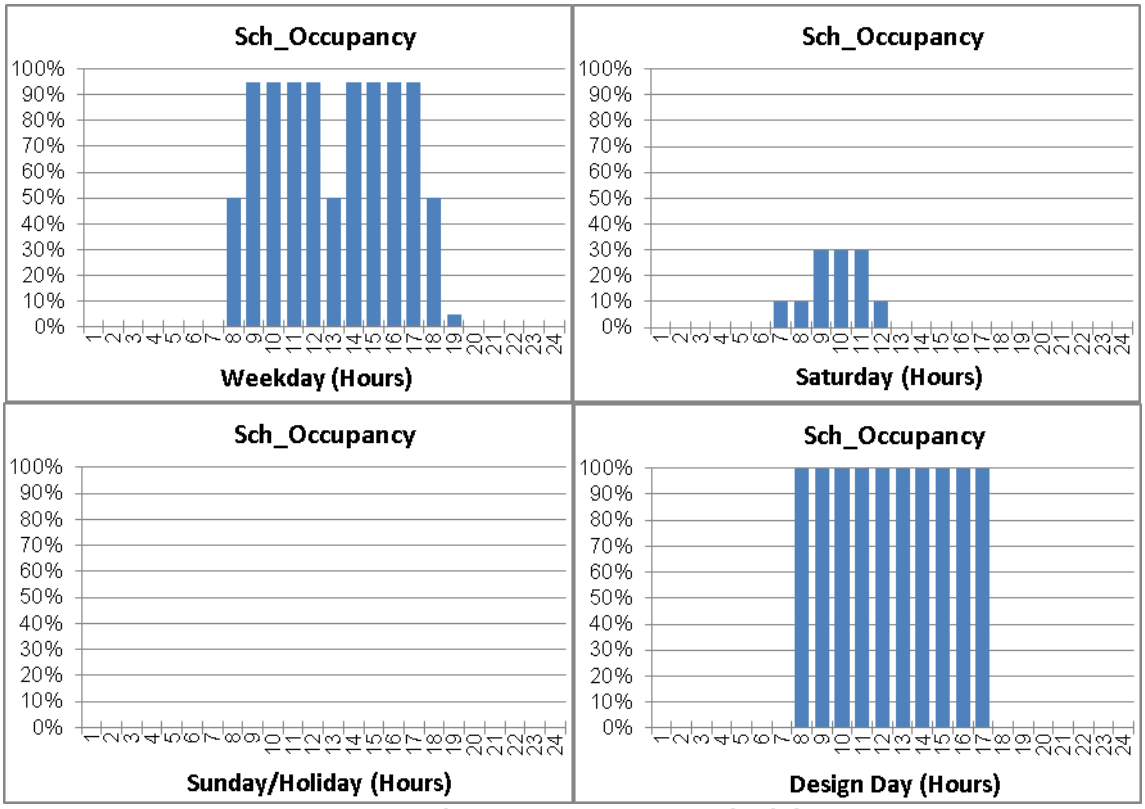

Figure 3: Occupancy Schedule

The schedules below show the operation hours for the carpark lighting:

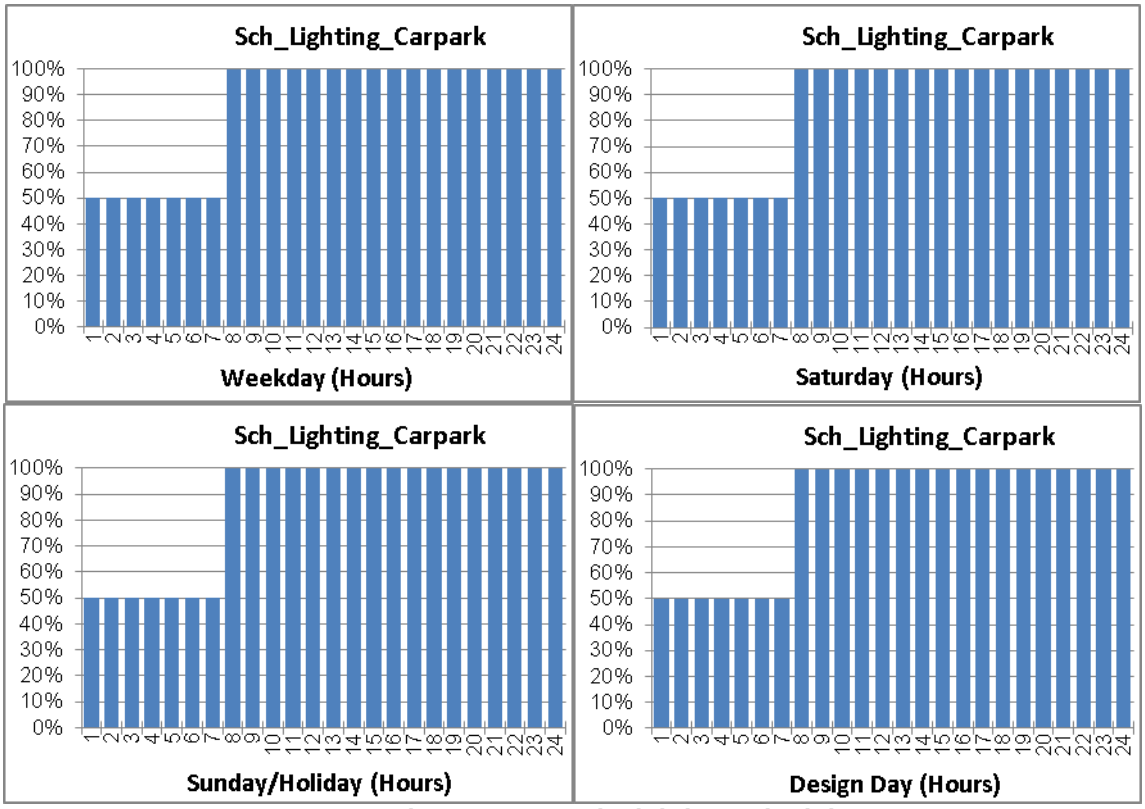

Figure 4: Carpark Lighting Schedule

The schedule below shows the operation hours for the staircase lighting:

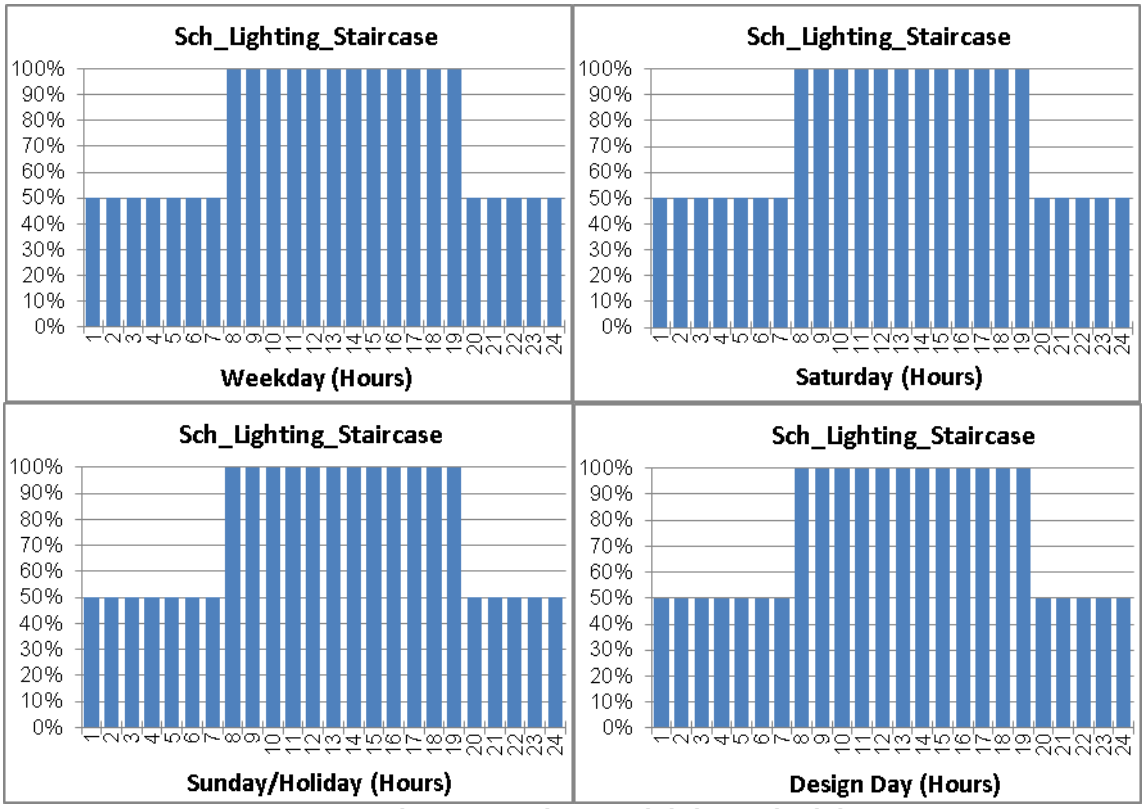

Figure 5: Staircase Lighting Schedule

The schedules below show the operation hours for the office and toilet lighting:

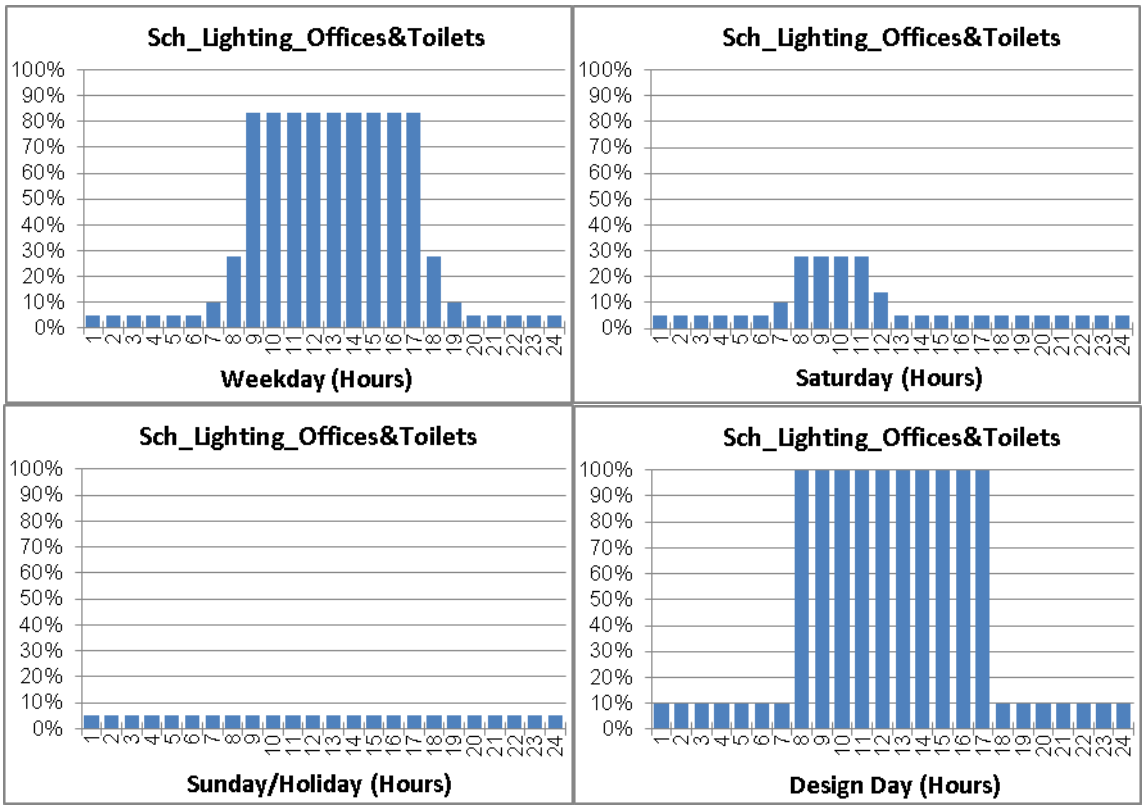

Figure 6: Office & Toilet Lighting Schedule

The schedules below show the equipment operating hours for the office zones. As there were insufficient data on the typical off-peak plug load for Singapore, the off-peak plug load was assumed to be 5% of the peak load.

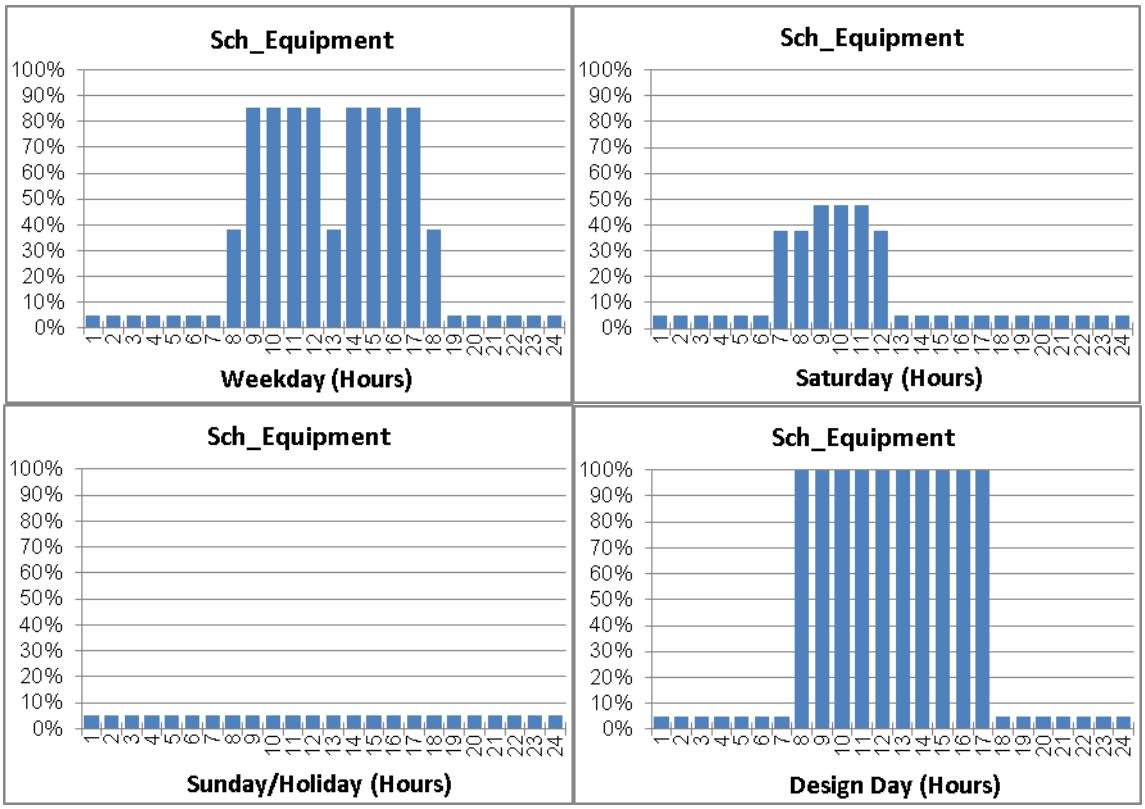

Figure 7: Equipment Schedule

The schedules below show the infiltration schedules for the office perimeter zones:

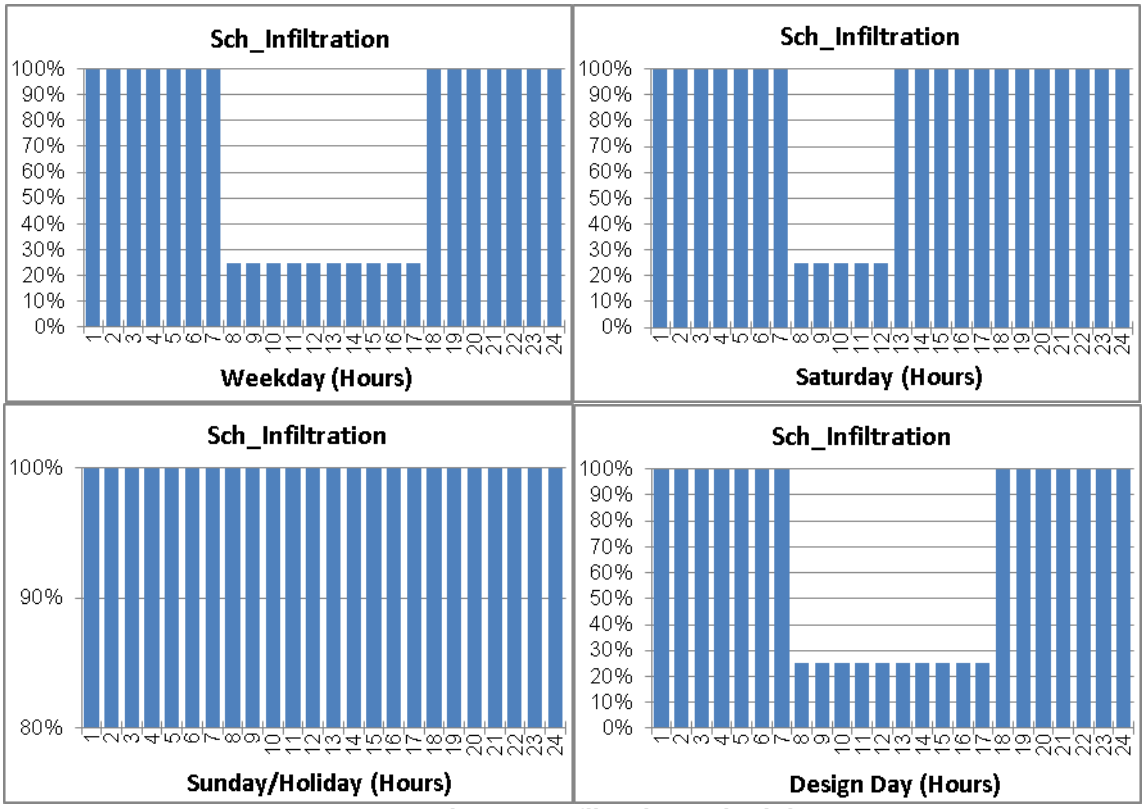

Figure 8: Infiltration Schedule

The schedules below show the lift operatiing hours for the building:

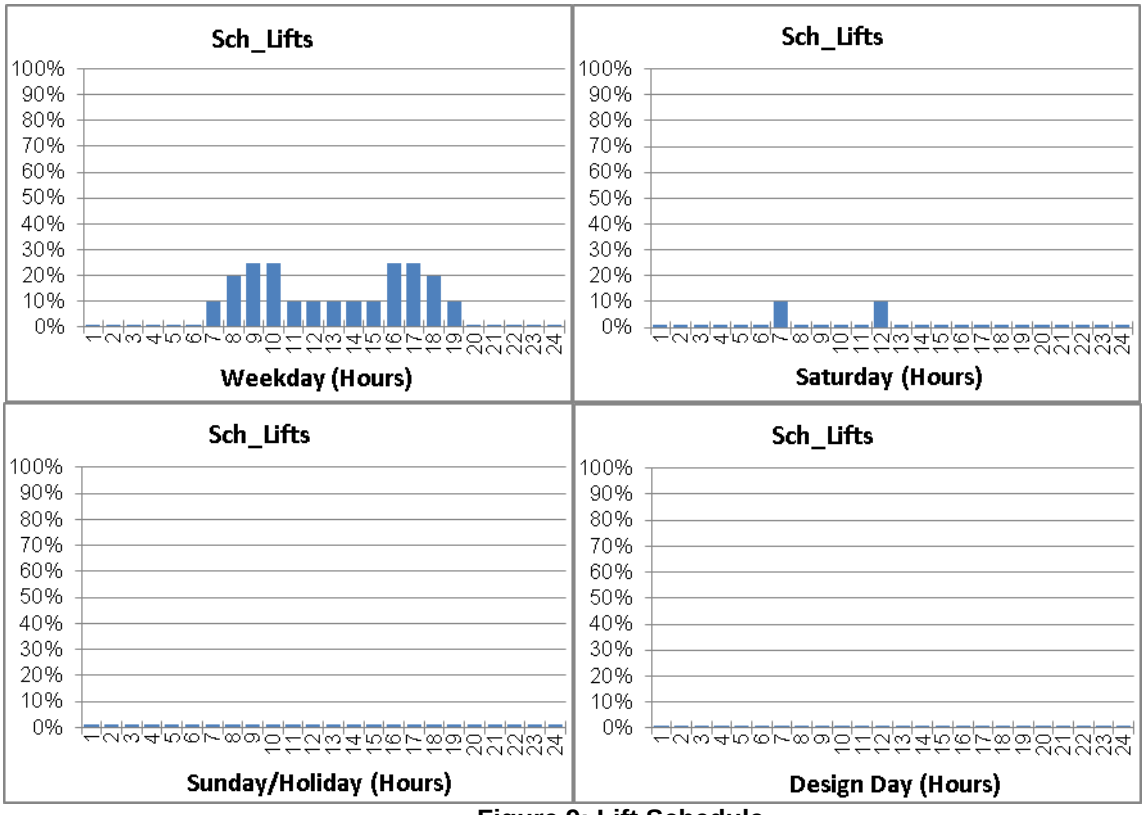

Figure 9: Lift Schedule

2.8 Air Conditioning & Mechanical Ventilation (ACMV)

2.8.1 Weather Data and Design Day

The EP weather file "SINGAPORE - SGP IWEC Data WMO#=486980" was used by BEARS for the energy modeling. It is based on 18 years of hourly weather data collected by the weather station in Changi and is an approved weather data for Green Mark energy modeling.

Beca initially recommended weather data from NEA weather station data (1) as it will be a more reliable source and a better representation of Singapore's weather. While the historical data was available, the Typical Meteorological Year (TMY) data was not available from this source. This TMY data is commonly used to assess long-term energy performance of buildings, as suggested by BCA's Green Mark rating system. As BCA Green Mark certification permits the use of ASHRAE standard weather data, IWEC Singapore weather data was therefore agreed to be used.

The design day maximum dry bulb temperature of 33.3°C, with corresponding 27.8°C wet bulb, and minimum 25.5°C dry bulb temperature were input into the model. The 21st day of months February, April, June, August, October and December, total of 6 days, were selected to be the design days by BEARS. Although design days are typically auto-generated by the Carrier E-20 software (as per Beca's practice), BEARS noted that these 6 design days were selected for the solar variation.

2.8.2 Zone Level

The air-conditioning system at the office zone comprised of variable air volume (VAV) terminal boxes without reheat and with a minimum air flow of 20% to provide minimum cooling when the building is in operation. VAV system was assumed for the office spaces as each office floor is divided into 5 independent air conditioned control zones (4 perimeters and 1 core) served by a central AHU. In typical large offices, VAV system is implemented to control air distribution at core zones, perimeter zones and partitioned spaces such as the meeting rooms and pantries etc. separately.

Zone cooling setpoint was fixed at dry bulb temperature of 24°C and a sizing factor of 10% was applied, as a cooling load safety factor for the entire system. However, the perimeter zones cooling setpoint was set to a lower dry bulb temperature of 23°C as these areas will not meet the operative temperatures of 24^{o}C to 26°C, if the dry bulb temperature is set at 24^{o}C.

The following assumptions were made for occupancy loads:

1. Occupancy load of 10 m^2/person
2. Occupancy activity load of 130 W/person obtained from *ASHRAE Handbook – Fundamentals*, assuming a "moderately active office work" activity
3. Summer clothing is assumed with a clothing insulation factor of 0.5

2.8.3 System Level

It was assumed that each office floor (core and perimeter zones) is served by 1 no. AHU c/w Variable Speed Drives (VSD). These AHUs are assumed to have return air / fresh air mixing, no economizer and no exhaust air provision. The zone pressure will be maintained through excess air being exhausted through the toilets and also through exfiltration from the building. Fresh air is assumed to be drawn directly from the exterior to the individual AHUs and there is no centralized pre-cooled air handling units (PAHU).

The AHU fans were assumed to be a draw-through variable speed fan with the motor in the air stream. The fan motor efficiency was extracted from the minimum nominal motor efficiency table in *SS530: Code of Practice for Energy efficiency standard for building services and equipment*. The fan and coil properties of the AHUs are tabulated below:

AHU Properties	Values
Fan total efficiency	61%
Fan motor efficiency	91%
Fan pressure rise	1,000 Pa
Minimum fan air flow ratio	0.25
Fixed static fan pressure setpoint	175 Pa
Fixed coil temperature setpoint	12.8°C

Table 9: Properties of AHU Fan and Coil

Beca advised that typically in Singapore, equipment installed with VSD are set to run above 30 Hz. Therefore, applying the fan affinity laws, BEARS calculated a minimum flow fraction of 0.5 to prevent the fan speed from dropping below 30 Hz as advised by Beca.

The fan power coefficients used in the model, of 0.047182815, 0.130541742, -0.117286942, 0.940313747, 0 were obtained from the Advanced VAV Design Guide based on a typical VSD fan system curve (Plenum airfoil fan static pressure drop of 0.7"). The fan power vs. flow fraction curve of the selected fan performance is plotted below.

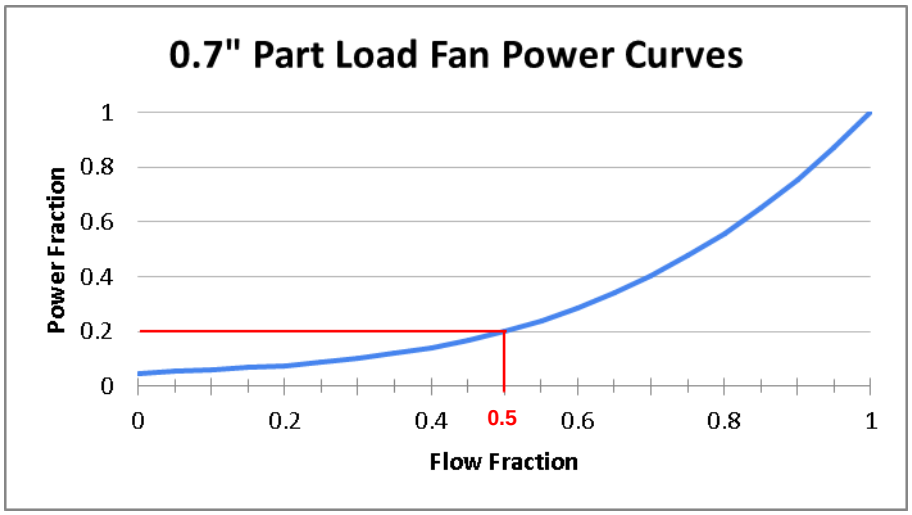

Figure 10: AHU Fan Power to Flow Fraction Curve

2.8.4 Plant Level

The simulated peak cooling load was 794.31 RT or 127 W/m^2 and this was consistent with Beca's initial cooling load assumption of 120 W/m^2 for typical office spaces.

Based on this cooling load, the chillers selected were 2 nos. single stage water-cooled centrifugal chillers with total capacity of 796 RT and full load Coefficient of Performance (COP) of 6.1 (in compliance with *SS530: Code of Practice for Energy efficiency standard for building services and equipment*). Chiller 2 (lag chiller) will operate once Chiller 1 (lead chiller) achieves full load (398 RT). The chilled water and condenser water temperatures specified for the chillers are as follows:

Chiller Properties	Values
Leaving CHW temperature	6.7°C
Entering CHW temperature	12.2°C
Entering CW temperature	29.5°C
Leaving CW temperature	35°C
Design Range	5.5°C

Table 10: CHW and CW Entering & Leaving Temperatures

The performance curves used to model the chillers in EP were WC_CENT_2010_PB_CAPFT, WC_CENT_2010_PB_EIRFT and WC_CENT_GT600_2010_PB_EIRFPLR, which were based on generic chiller sizes > 600 RT from the DOE benchmark models.

The following graph shows the performance comparison of the 398 RT modeled chiller based on the performance curves in EP and a 400 RT chiller model selected by Trane (Model TCVHE 400 RT). Both part load ratio curves were within AHRI 550/590 5% tolerances and has a low coefficient of variation of 2.76%, which indicates that the chiller performance curve in EP is representative of an actual commercially available chiller.

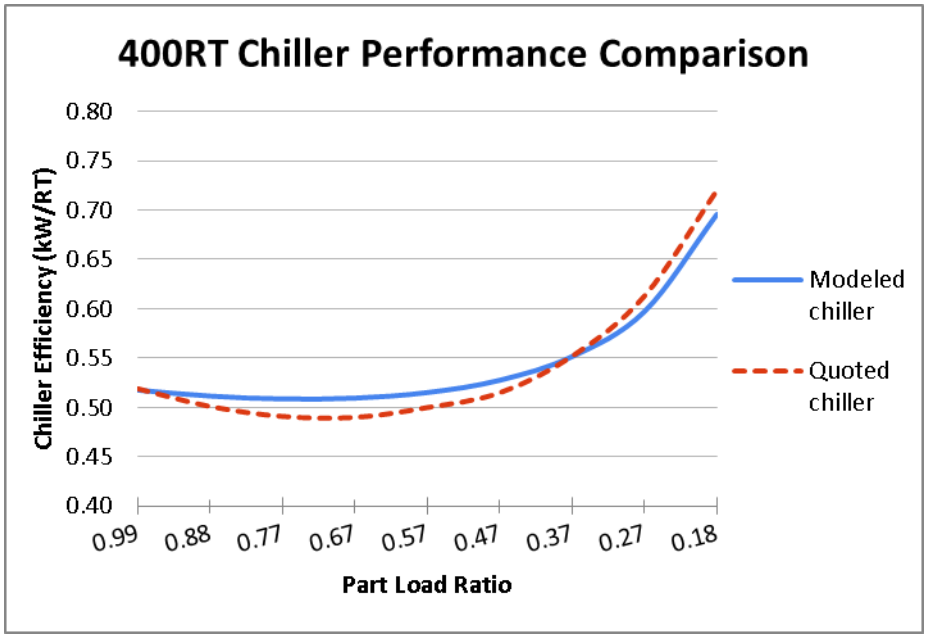

Figure 11: Chiller Performance Comparison

The following were the Chilled water pump inputs into the model:

- 2 nos. variable speed primary pumps
- Rated flow rate of 0.123 m^3/s
- Pump head of 200 kPa
- Motor efficiency of 93.2%
- Part Load Performance Curve coefficients of 0.0015303, 0.0052081, 1.1086242, -0.1163556 was selected
- Motor power auto-sized by EP

The following were the Condenser water pump inputs into the model:

- 2 nos. constant speed pumps
- Rated flow rate of 0.166 m^3/s
- Pump head of 150 kPa
- Motor efficiency of 92.6%
- Part Load Performance Curve coefficients of 0.0015303, 0.0052081, 1.1086242, -0.1163556 was selected
- Motor power auto-sized by EP

The chilled water pump flow rate was based on 2.4 USgpm/RT while the condenser water pump flow rate was based on the cooling tower selection. The pump motor efficiencies were based on *SS530: Code of Practice for Energy efficiency standard for building services and equipment*.

2 nos. fixed speed, cross flow cooling towers were assumed with heat rejection capacities of 500 RT each. The cooling towers were sized based on applying 1.25 times of the chiller plant capacity. The table below summarizes the properties of the cooling towers. The cooling tower model SKB-645 was selected based on the selection chart from Kuken as a reference for the cooling tower properties. Other properties were auto-sized by EP and the cooling tower efficiencies were reviewed and observed to be within the range stipulated by the local Singapore Standards.

Cooling Tower Properties	Values
Design water flow rate	0.0829 m^3/s
Design air flow rate	62.5 m^3/s
Design fan power	16.5 kW
Design inlet air wet bulb	27.7°C
Design approach	1.7°C
Design range	5.5°C
Minimum air flow ratio	0.2
Free convection capacity fraction	0.125
Fixed CW temperature setpoint	29.5°C

Table 11: Properties of Cooling Tower

The chiller plant was designed to meet 0.70kW/RT efficiency as per Green Mark v4.0 Certified requirement.

3 ANALYSIS OF ENERGY MODELING OUTPUT

3.1 Component Summary

The energy modeling output from BEARS extracted on 23rd June 2015 was analyzed (refer to Appendix 2 for the extracted result). The breakdown summary of the energy consumption from the energy modeling is tabulated below:

Component	Energy Consumption (kWh)
AHUs	232,883
Air System Fans (Total):	232,883
Chillers	878,852
Chilled & Condenser Water Pumps	142,661
Cooling Towers	53,971
Chiller Plant (Chiller, CHWP, CWP and CT):	1,075,484
MV Fans	194,828
HVAC Total (Chiller Plant, Air Side - AHU and MV Fans):	**1,503,194**
Lights (General)	846,450
Lights (Carpark)	157,133
Lights (Exterior & Facade)	50,096
Total Lighting:	1,053,679
Electric Equipment	741,588
Total Electric:	741,588
Lifts	159,154
Plumbing & Sanitary Systems	25,696
Non-HVAC Total:	**1,980,117**
Total Energy Consumption	**3,483,312**
EUI (kWh/m²/year)	**146**

Table 12: Energy Model Summary

The EUI/ EEI for the modelled benchmark building was 146 kWh/m^2/year which could be representative of a Green Mark Office Building at Certified Level assuming no off-peak operations to simplify the benchmark model.

BCA's shared data on the EEI (from energy model submissions) for Green Mark Gold^{Plus} and Platinum office buildings, based on a limited number of buildings in Singapore of various sizes, is tabulated in the table below. As these buildings are of higher certification, their EEIs are expected to be lower than a benchmark model representing a certified building.

Summary of Surveyed Buildings	Average EEI (kWh/m^2/year)	No. of Buildings
GM Gold^{Plus} & Platinum office	146.61	31
GM Gold^{Plus} & Platinum office since 2010	137.55	19
GM Gold^{Plus} & Platinum office since 2010 (>20,000m^2)	132.9	15

Table 13: Summary of Surveyed GM Gold^{Plus} and Platinum Office Buildings

A more relevant comparison with this benchmark building model should refer to office buildings > 20,000 m^2, which is of similar size as the benchmark building model (this size is relevant as larger buildings are required to have more efficient cooling systems). For this group of buildings, the average EEI was 132.9 kWh/m^2/year, which works out to be 10% more energy efficient than the benchmark building currently modeled.

Therefore, this shows that the EEI of 146 kWh/m^2/year could be a reasonable estimate of a typical Green Mark Certified office building in Singapore.

The following figures show the HVAC and non-HVAC energy consumption breakdown and component breakdown percentages in the benchmark building:

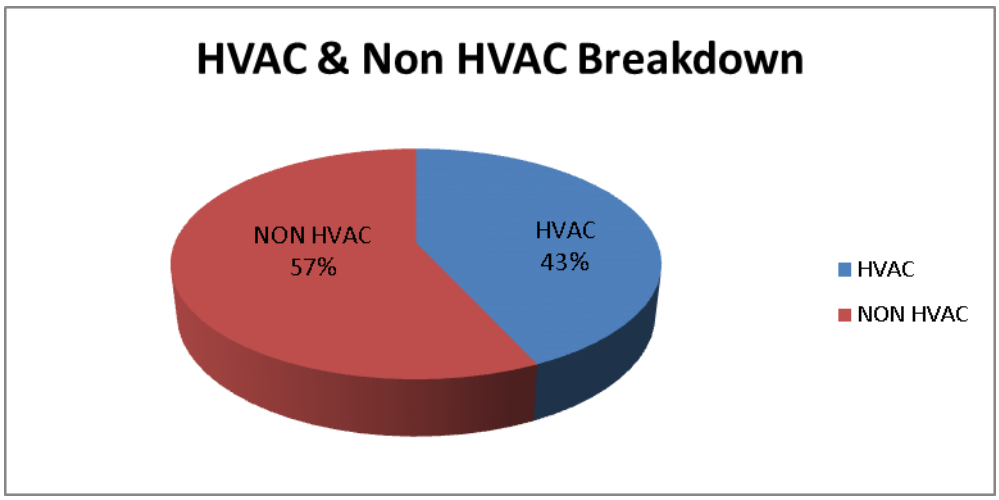

Figure 12: HVAC and Non-HVAC Energy Consumption Breakdown

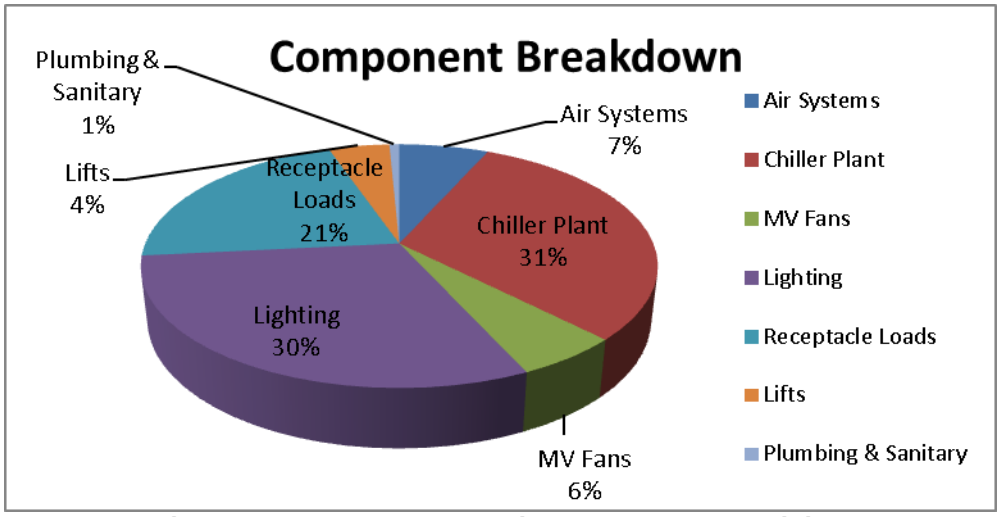

Figure 13: Energy Consumption Component Breakdown

The energy model outputs were assessed to be reasonable and representative of a typical Green Mark Certified office building and the major component equipment efficiencies met the Green Mark and Singapore Standard requirements.

3.2 Component Efficiencies

The simulated parameters and computed efficiencies of individual equipment for the chiller plant and air systems are tabulated below and compared with the Singapore Standards requirements. The baseline efficiencies based on Green Mark and Singapore Standards (*SS553: Code of Practice for Air-conditioning and mechanical ventilation in buildings* and *SS530: Code of Practice for Energy efficiency standard for building services and equipment)* requirements. The operating efficiency was computed using the annual total energy consumed, divided by the annual total building cooling load.

Chiller	Capacity		Efficiency		Operating Efficiency	Baseline Efficiency
	kW	RT	COP	kW/RT	kW/RT	kW/RT
Chiller 1 & 2	2,800	796	6.1	0.577	0.574	0.577

Table 14: Chiller Efficiencies

Chiller Plant Pump	Water Flow Rate	Power	Efficiency		Operating Efficiency	Baseline Efficiency
	m^3/s	kW	$kW/m^3/s$	kW/RT	kW/RT	$kW/m^3/s$
CHW Pumps 1 & 2	0.123	33.8	275.07	0.0425	0.0303	349
CW Pumps 1 & 2	0.166	34.4	207.63	0.0432	0.0629	301

Table 15: Chiller Pump Efficiencies

Cooling Tower	Water Flow Rate	Fan Power at Design Air Flow	Efficiency		Operating Efficiency	Baseline Efficiency
	m^3/s	kW	l/s.kW	kW/RT	kW/RT	l/s.kW
CT 1 & 2	0.1658	33.0	5.02	0.0415	0.0353	3.23

Table 16: Cooling Tower Efficiencies

AHU VAV Fan	Max Air Flow Rate	Power	Efficiency		Baseline Efficiency
	m^3/s	kW	$kW/m^3/s$	W/cmh	$kW/m^3/s$
AHU (Bottom)	7.22	11.8	1.639	0.455	2.4
AHU (Mid) x15	94.46	154.9	1.639	0.455	2.4
AHU (Top)	6.79	11.1	1.639	0.455	2.4

Table 17: AHU Overall Efficiencies

Toilet Exhaust Fan	Air Flow Rate	Power	Efficiency		Baseline Efficiency
	m^3/s	kW	$kW/m^3/s$	W/cmh	$kW/m^3/s$
TEF (Bottom)	0.39	0.48	1.23	0.341	1.7
TEF (Mid) x15	5.85	7.18	1.23	0.341	1.7
TEF (Top)	0.39	0.48	1.23	0.341	1.7

Table 18: Toilet Exhaust Fan Efficiencies

Carpark Fan	Air Flow Rate	Power	Efficiency		Baseline Efficiency
	m^3/s	kW	$kW/m^3/s$	W/cmh	$kW/m^3/s$
Carpark (Bottom)	0.234	0.29	1.23	0.342	1.7
Carpark (Mid)	0.234	0.29	1.23	0.342	1.7
Carpark (Top)	0.234	0.29	1.23	0.342	1.7

Table 19: Carpark MV Fan Efficiencies

Staircase Fan	Air Flow Rate	Power	Efficiency		Baseline Efficiency
	m^3/s	kW	$kW/m^3/s$	W/cmh	$kW/m^3/s$
Stairs (Bottom)	0.26	0.24	0.923	0.256	1.7
Stairs (Mid) x15	3.90	3.60	0.923	0.256	1.7
Stairs (Top)	0.26	0.24	0.923	0.256	1.7

Table 20: Staircase MV Fan Efficiencies

The chiller plant annual operating system efficiency (consisting of the chillers, cooling towers, CHW and CW pumps) was computed as 0.70 kW/RT and complies with the Singapore Standards and Green Mark Certified requirements.

4 CONCLUSION

Beca has provided inputs for the energy model based on a typical Singapore office building that meets the baseline Green Mark Certified building with operating hours of 55 hours a week. Beca also ensured that the inputs for the energy model complied with the Singapore Standards and Codes of Practice for Singapore.

The benchmark model EEI was 146 kWh/m^2/year and this was considered reasonable as it was around 10% higher than the average EEI for Green Mark $Gold^{Plus}$ and Platinum office buildings > 20,000m^2, based on data shared by BCA. The building model energy consumption breakdown was also typical of a Green Mark Certified office building.

During the building modeling process, there was often limited information available to base many of the decisions needed to define a benchmark building. For example, there was no published plug load study available for Singapore, and no published measured data on energy end uses for office buildings in Singapore. In such cases where no published information was available, the combined best judgment of BEARS, Beca and BCA was used to specify reasonable values.

All in all, the simulated office model can be used as a benchmark comparison model to determine the impact of SinBerBEST's new technologies developments on the energy consumption of a typical office building. As there are many variations to office building designs which are plausible in Singapore (such as smaller buildings with completely different cooling systems - air cooled, etc.), this benchmark building model is intended to give a representation of one possible benchmark building that is realistic for Singapore, for the purposes of comparison. Hence variations may need to be applied to suit the application of the new technology, when necessary.

5 REFERENCES

5.1 Singapore Code References

1. **Building Construction Authority** – Code on Envelope Thermal Performance for Buildings
2. **Singapore Standard SS 530:2006** – Code of Practice for Energy efficiency standard for building services and equipment
3. **Singapore Standard SS 553:2009** – Code of Practice for Air-conditioning and mechanical ventilation in buildings
4. **BCA Green Mark** – Certification Standard for New Buildings, GM NRB Version 4.1

5.2 Other References

1. **National Environment Agency.** Singapore's Climate Information & Data. *National Environment Agency.* [Online] [Cited: April 2015, 29] (1)

   http://www.nea.gov.sg/weather-climate/climate-information/singapore's-climate-information-data
2. **California Energy Commission.** *Advanced Variable Air Volume System Design Guide.* California : s.n., 2003.